SPECTROSCOPIC STUDY OF COBALT II SUBSTITUTED IN SOME COPPER AND ZINC ENZYMES

by

A. DESIDERI

A Thesis submitted for the Degree of

Doctor of Philosophy

in the

Faculty of Science

of the

University of Leicester

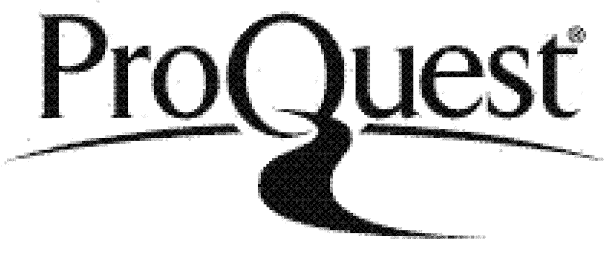

ProQuest LLC
789 East Eisenhower Parkway
P.O. Box 1346
Ann Arbor, MI 48106-1346

SPECTROSCOPIC STUDY OF COBALT II SUBSTITUTED IN SOME COPPER AND ZINC ENZYMES

by

A. DESIDERI

A Thesis submitted for the Degree of

Doctor of Philosophy

in the

Faculty of Science

of the

University of Leicester

To Nadia

STATEMENT

The work described in this thesis was carried out by the author in the Department of Chemistry of the University of Leicester and in the Department of Biological Chemistry in the University of Rome during the period January 1977 to November 1981. The work has not been presented and is not being concurrently presented for any other degree. In the case of joint work a substantial part was the original work of the author.

Signed: .....

A. Desideri

SPECTROSCOPIC STUDY OF COBALT II SUBSTITUTED IN SOME COPPER AND ZINC ENZYMES

by A. DESIDERI

ABSTRACT

The substitution of the cobalt atom into the active site of zinc metalloenzymes is becoming a useful and common practice. The zinc atom, in fact, is magnetically and optically silent, whilst the cobalt has a characteristic optical and E.P.R. spectrum, so that it can be followed spectroscopically to obtain structural and functional information on the enzyme.

In this thesis a spectroscopic study of the cobalt substituted into two metalloenzymes, namely copper-zinc-Superoxide Dismutase and Zinc-Carbonic Anhydrase, and of some low molecular weight cobalt complexes has been performed.

In Superoxide Dismutase the cobalt has been selectively substituted either into the zinc or into the copper site, so that all the possible derivatives [Co-Cu], [Co-•••], [Co-Co] and [Zn-Co], have been investigated.

The [Co-•••]SOD derivative is characterized by an axial E.P.R. spectrum and by an absorption spectrum in the visible region of intermediate intensity $\varepsilon_{530}=315$, $\varepsilon_{560}=425$, $\varepsilon_{588}=450$ and a near infrared band at 1000 nm ($\varepsilon=90$), indicating a tetrahedral coordination with a quite strong crystal field around the Co(II) centre. The [Co-Cu]SOD derivative does not show any E.P.R. signal and a magnetic susceptibility study, carried out between 30-210 K indicates that this is due to the strong antiferromagnetic coupling ($2J \geqslant 600$ cm^{-1}) occurring between the two metal centres. The [Zn-Co]SOD derivative shows an interesting phosphate buffer spectral dependence. In particular, the electronic spectrum, carried out in the presence of phosphate buffer, has three quite intense bands in the visible region ($\varepsilon_{540}=225$, $\varepsilon_{580}=330$, $\varepsilon_{605}=330$) and a band in the near infrared at 1050 nm ($\varepsilon=40$). When the same spectrum is carried out in the absence of phosphate buffer the bands in the visible region are much less intense and the near infrared band is shifted toward lower wavelengths. This behaviour indicates a change in symmetry around the Co(II) centre, from tetrahedral to pentacoordinate in the presence and in the absence of phosphate respectively. The E.P.R. spectra also support this hypothesis.

The reaction of cyanide and H_2O_2 with the [Zn-Co] and [Co-Co]SOD derivatives have also been investigated. The binding of CN^- to the cobalt is temperature or freezing dependent. The E.P.R. spectra carried out at

77 K shows, in fact, that the CN^- easily binds to the cobalt which is transformed into a low spin form, whilst the electronic room temperature spectra show that a very large CN^-:Co ratio is needed to decrease the d-d bands of the unreacted high spin cobalt. The E.P.R. spectrum is rhombic with $g_z = 2.027$ and $A_z = 115 \times 10^{-4} cm^{-1}$, suggesting a distorted pentacoordinate structure around the metal. The reaction with H_2O_2 shows a decrease of the electronic absorption spectrum of the cobalt and the appearance of a radical at $g \simeq 2$ in the E.P.R. spectrum. Oxidation of the Co(II) to Co(III) can probably be excluded because addition of sodium dithionite does not restore back the original spectrum.

A comparative study of the K-absorption edge of several cobalt derivatives has allowed several structural correlations to be done. In particular, the [Co(II)-····] and the [Co(II)-Cu(I)]SOD derivatives have a completely identical K-edge spectrum, which is slightly different from that of the [Co(II)-Cu(II)] derivative, indicating that a conformational change and/or a different charge on the imidazole bridging the two metal sites occurs coincidentally with the change of copper valence.

An E.P.R. study on low molecular weight model compounds suggests that the zero field splitting value δ between the two Kramers doublets in a high spin cobalt(II) ion can be used diagnostically to assign the geometry around the metal centre. The zero field splitting value is, in fact, greater in the pentacoordinate case than in the tetrahedral one. By comparison with the model compounds a pentacoordinate structure is assigned to the high pH and the iodide form of the cobalt carbonic anhydrase derivative.

The study of the reaction of the native and the copper and cobalt substituted Carbonic Anhydrase shows that Cu(II) is easily extracted from the enzyme, Co(II) with some difficulty and Zn(II) is unaffected in any condition. Before the depletion, a stable pentacoordinate species and two stable and different intermediates in the case of cobalt and copper respectively are observed.

A γ-irradiation investigation of the native Carbonic Anhydrase and Superoxide Dismutase has allowed detection of the E.P.R. signal of the Zn^+ ion with a configuration $3d^{10}4s^1$. In both cases, the electron seems to be in an approximately sp hybrid orbital so explaining the lack of magnetic interaction in the native SOD. In fact, the σ hybrid orbital of the zinc is in a wrong symmetry to couple with the π electron system of the imidazole and with the ground state of the copper.

CONTENTS

ACKNOWLEDGEMENTS

The author wishes to thank the following:

Dr. J. B. Raynor for his constant guidance during the course of this work.

Professor G. Rotilio for the continuous encouragement and discussions.

Dr. L. Morpurgo for the pleasure to work and to discuss with her.

Professor L. Calabrese for her helpful advice on matters concerning Chapter 4 of this thesis.

Dr. A. A. G. Tomlinson for his helpful discussion on Chapter 5 of this thesis.

All the members of the Biological Chemistry Department and, in particular, Dr. D. Cocco, for their freely given advice and friendship.

A particular thanks to my parents for their continuous encouragement to study and to work in scientific fields.

LIST OF ABBREVIATIONS

SOD	Superoxide dismutase
[Zn- •••] SOD	Derivative where the native copper has been removed
[Zn-Co] SOD	Derivative where the native copper has been replaced by cobalt
[Co- •••] SOD	Derivative where the native zinc has been replaced by cobalt and the copper has been removed
[Co-Co] SOD	Derivative where both the native zinc and copper have been replaced by cobalt
[Co-Cu] SOD	Derivative where the native zinc has been replaced by cobalt
BCA	Bovine carbonic anhydrase
CD	Circular dichroism
M.C.D.	Magnetic circular dichroism
XANES	X-ray absorption near edge spectroscopy
E.P.R.	Electron Paramagnetic Resonance

CHAPTER 1

INTRODUCTION

A. Enzymes and Metalloenzymes

Enzymes are biological catalysts that modify the rate of chemical reactions without changing the course of the reaction. Their main aim is to lower the activation energy, that means the energy required to bring the molecules into the reactive state and so to increase the number of molecules able to react.

As shown in Fig. 1.1 the initial and final states of the catalysed and not catalysed reaction do not change, and that means that the catalyst has not affected the equilibrium of the reaction but only the rate. A peculiar feature of enzymes is also their high specificity, i.e. they act only on a specific class of substrates. This characteristic feature allows the logical order of the metabolic reactions to proceed, and has its reason in the fact that enzymes must bind to the substrate for a short period of time. The enzymatic specificity will be greater or lower depending on the number of binding atoms occurring between the enzyme and the substrate. There must exist on the surface of this large molecule a specific region able to bind to the substrate; this region is called "the active site". The molecular mechanisms of enzymatic reaction are still not clear. Fische in 1894 proposed the famous model commonly referred to as "the key in the lock". In this model the surface of the enzyme has a pre-formed conformation where the substrate can exactly fit as a key in the lock, and even slight molecular modifications of the substrate prevent the fit with the enzyme. This view ascribes a static rôle to the active site that does not now agree any more with experimental data. The idea now is that the active site is something that is capable of modification by several factors (like pH, inhibitors, temperature, etc.) or by the substrate itself which could produce some modification in order to obtain a better fit. This hypothesis has been confirmed by the

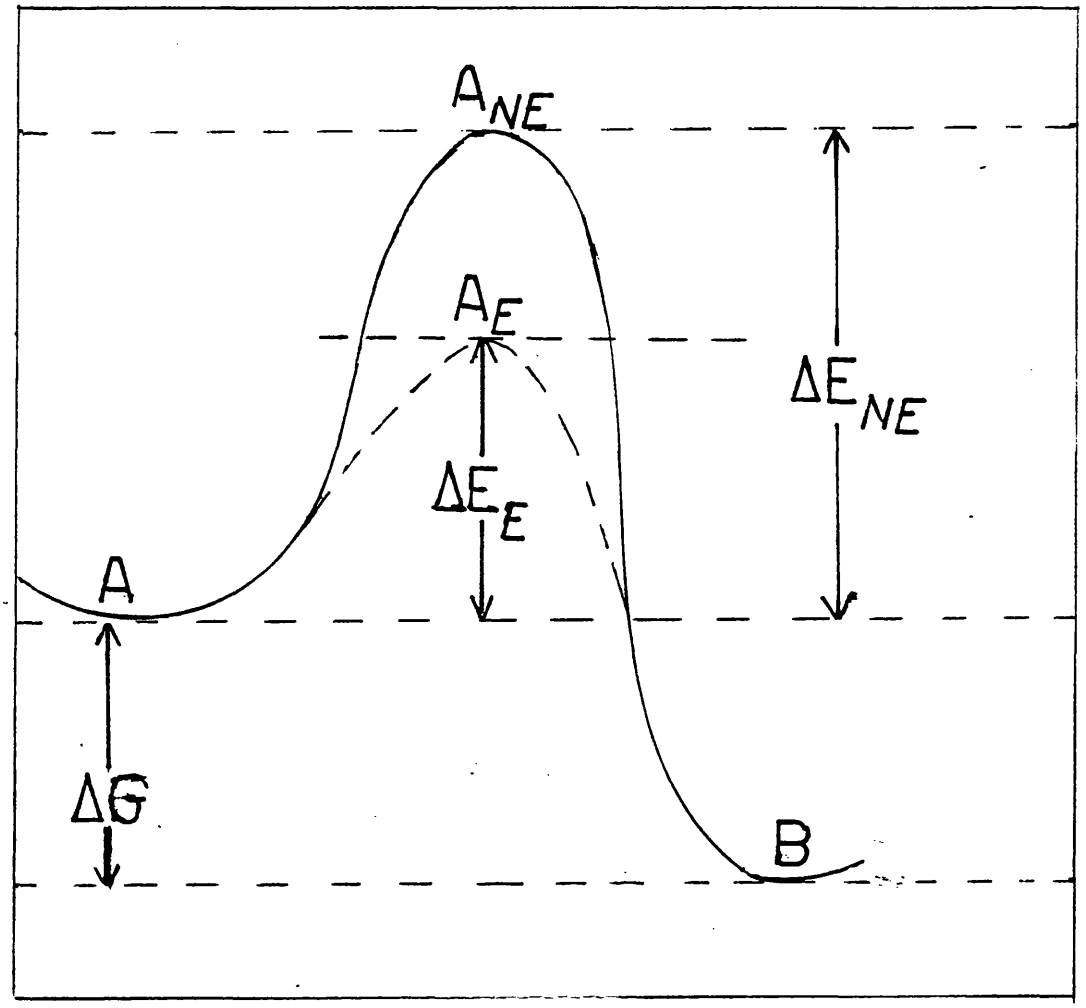

FIG. 1.1 The diagram indicates the energetic gap between the reaction A → B. A_{NE} indicates the activated state of a non-enzymatic reaction, A_E indicates the activated state of a reaction catalyzed by an enzyme.

difference observed in the enzymatic conformation after the binding of the substrate, and it allows one to consider the enzyme as something dynamic and not tightly pre-formed.

One class of enzymes consist of simple proteins whilst another class are conjugate proteins. That means they have also a prosthetic group so firmly bound to the proteic group that the usual procedures for the purification and the extraction of the enzyme do not produce the dissociation of the two different groups. The prosthetic part is usually called coenzyme, the proteic part is called apoenzyme, and both together is called holoenzyme. The activity is due only to the holoenzyme even if the actual transformation of the substrate is due to the coenzyme which is the active site of the complex.

A particular class of conjugate proteins is the metalloproteins, characterized by enzymes with a tightly bound metal. The most usual metals found in metalloproteins are transition metal ions of the first row and in particular Cu, Zn and Fe; the metal usually occupies the active site of the protein and is an efficient catalyst of the enzymatic reaction. The presence of metals as active sites in the proteins allows one to study the characteristics of the enzymes by following the metals using spectroscopic techniques. In particular, copper has been widely studied due to its wide occurrence as a prosthetic group in various functional classes of metalloproteins. This metal is usually present in the proteins in the oxidized state so that it is possible to follow it by different spectroscopic techniques such as E.P.R., electronic absorption, circular dichroism, magnetic circular dichroism. Proton N.M.R. has been used to investigate any coordinated water that may be bonded to the metal. The E.P.R. technique is particularly useful as it immediately gives different kinds of information. For example, it quantifies how

much of the copper that is present in the protein is in the oxidized state. This is usually done by comparing the integrated intensity of the E.P.R. signal with the total copper as determined by chemical reaction or atomic absorption spectroscopy. In many cases, copper is not seen by E.P.R., or is seen only in part. In these cases, it is not straightforward to establish the valence state of the invisible copper on the sole basis of absence of E.P.R. signals which may be due to copper (I) or to copper (II) dimers (or polymers). In this situation, optical spectroscopy and magnetic susceptibility of the system supply additional information for the correct establishment of the valence state. Moreover, the spectroscopic behaviour of copper (II) is quite well known, due to the many studies done on low molecular weight inorganic compounds of known structure, so that a rough idea of the nature and the symmetry of the ligands around the metal can be obtained.

Not all the metals in the proteins are like copper. Zinc, for instance, is magnetically and optically silent so that no information can be obtained through spectroscopic techniques. In this case, it is possible to replace the native silent metal atom in the active site by another metal which has identical charge, closely similar size and parallel stereochemical demands, but which is optically and magnetically active. The substitution of zinc by cobalt and of magnesium by manganese is of this kind. In Table 1.1 are reported the properties of some metals with respect to the replacements that are usually done in biological systems.

Once this substitution has been done it is possible to monitor the chemical properties of the moiety constituted by the donor atoms and the metal ion, perturbing the system by changing the pH, by adding inhibitors, by adding artificial or natural substrates, and by comparing with the

TABLE 1.1

Metals which usually may replace the native metal in enzymes

Native Metal	Replacement Metal	Size	Charge	Stereochemistry	Chemical Properties
Zn^{2+}	Co^{2+}	Exact	Exact	Very Good	Very Good
Mg^{2+}	Mn^{2+}	Good	Exact	Very Good	Good
Fe^{3+}	Gd^{3+}	Exact	Exact	Good	Poor (in redox)
Cu^{2+}	Co^{2+}	Good	Exact	Moderate	Poor (in redox)

physico-chemical properties of simple inorganic compounds. The study of the actual physico-chemical properties at molecular and sub-molecular level by spectroscopic techniques is probably the most useful and less perturbative method and constitutes an important resource to supplement X-ray crystallographic structure analysis and to extend its potential to the study of conformation and structure of enzymes in solution.

B. Molecular Spectroscopic and Catalytic Properties of Superoxide Dismutase (SOD)

Superoxide dismutase is a copper-zinc protein purified from eucariotic organisms which has activity towards the superoxide ion O_2^-. The molecular weight of SOD has been determined by different research workers [1,2,3]. It varies between 31,000 and 33,000 independently of the source of the red cells. SOD has two Cu^{2+} and two Zn^{2+} ions for each molecule and can be divided into two sub-units equal in molecular weight (16,000) by treatment with denaturing agents such as sodium dodecylsulphate [2,3]. The need to use reducing agents to separate the two sub-units suggested that there must be at least one disulphide bridge between the two sub-units [4,5]. Later Beauchamp and Fridovich demonstrated that the disulphide bridges were present within each of the sub-units [6]. The difficulty of dissociating the enzyme is then explained by the stabilising effect of these disulphide bridges on the conformation of the sub-units that are then tightly associated in their native state. These properties have been definitely demonstrated by X-ray structural investigations at 3 Å resolution [7] which have also shown the identity of the two sub-units, each containing one copper and one zinc atom.

The spectroscopic properties of the Cu(II) have been widely investigated by optical, C.D., N.M.R. and E.P.R. techniques. The optical spectrum of the Cu(II) is characterized by an intense band in the U.V. region at 350 nm assigned to a charge transfer transition together with a shoulder at 450 nm (22,000 cm^{-1}), probably again due to charge transfer and two bands at 600 nm (16,700 cm^{-1}) and at 750 nm (13,300 cm^{-1}) which are assigned to d-d transitions [8]. The E.P.R. spectrum of the enzyme is due to the copper and double integration of the signal indicates that all the copper is in a divalent state. The E.P.R. signal [9] has three g-values

(2.265, 2.11, 2.03) which accords with the distorted penta-coordinate structure shown by the X-ray analysis (Fig. 1.2).

The E.P.R. spectrum of the native enzyme is a very sensitive probe for changes in the environment of the Cu^{2+} and has been extensively used in probing the catalytic site of the Zn/Cu superoxide dismutase in a wide variety of experiments. E.P.R. [9], N.M.R. [10,11] and other [12] techniques have shown that the copper is bonded to four imidazole nitrogen atoms from histidines and one water (Fig. 1.2). The water molecule may be replaced by inhibitors suggesting that the substrate behaves in the same way. In particular, kinetic measurements [13] have shown that inhibition of the enzyme by OH^- and CN^-, which coordinate to the copper in place of the water [9,10,11,14], is competitive with the substrate. The redox properties of the enzyme have been investigated by reaction with reductants such as sulphide, ferrocyanide and H_2O_2 [15]. The exchange of electrons is quite efficient, whilst addition of cyanide (which changes the shape of the E.P.R. spectrum [9] from rhombic to axial symmetry) stabilises the oxidized form of the enzyme in the reaction with ferrocyanide and H_2O_2 [15]. Acidification of the native protein in the range of pH 3-4 brings some alteration in the spectral properties of the Cu^{2+} [5,16] and, in particular, the E.P.R. spectrum loses its rhombic shape and the A_z value increases from 130 to 150 G.

The meaning of these spectral changes is now better understood as a result of experiments in which the zinc has been replaced by cobalt [17]. This substitution has been particularly useful because it has allowed the investigation of the zinc site which is optically and magnetically silent. In the Co(II)-Cu(II) protein, the cobalt chromophore is characterized by a visible absorption with a maximum at 600 nm and is E.P.R. silent because of the magnetic coupling occurring between the two metal systems [17,18].

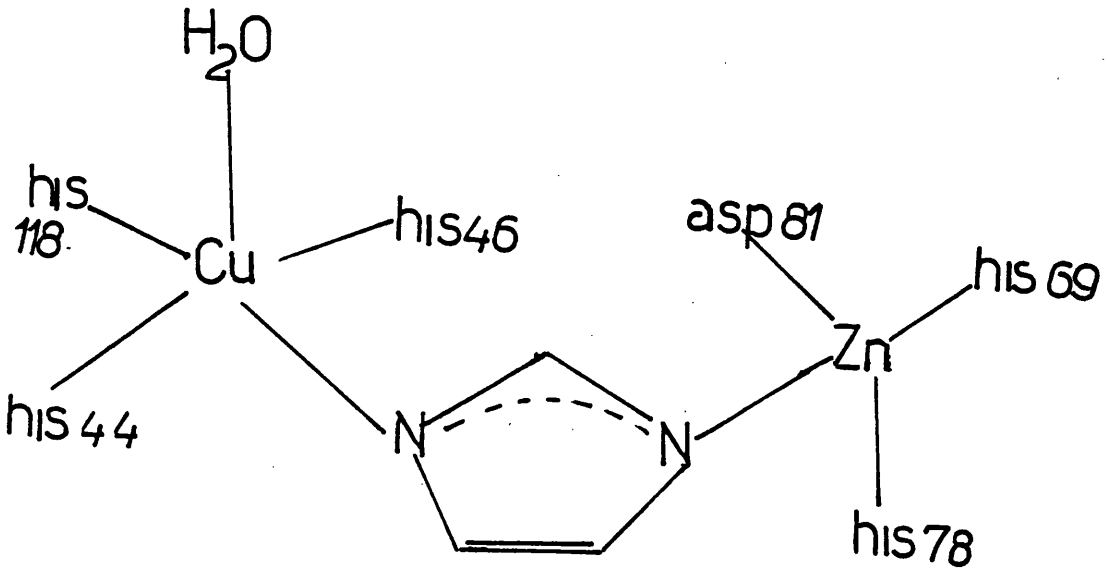

FIG. 1.2 Schematic representation of the active site of native superoxide dismutase.

When the copper is either reduced [18] or removed [19], the E.P.R. signal of the cobalt is observed and its optical spectrum exhibits a shift towards a shorter wavelength. From the identity of the E.P.R. and optical spectra of these two derivatives, it has been suggested that in the reduction, the copper bond to the imidazole bridge has been broken [19]. The E.P.R. signal of the cobalt is also detected when the protein is brought to a low pH, whereupon, at the same time, the E.P.R. signal of the copper becomes axial as in the native protein. Under these conditions the optical spectrum of the cobalt disappears while the broad band due to the copper is practically unchanged [20].

These facts have suggested that the uncoupling of the Co(II)-Cu(II) spin systems is again due to the breaking of the imidazole bridge but, this time, the bond which is broken is the Co-imidazole bond. It is important to remember that in these conditions the copper is not reduced by ferrocyanide [15] and that the imidazole bridge plays an essential rôle in the activity of the enzyme, constraining the copper in a structural arrangement suitable for reduction. In fact, when the enzyme is in the pH range 5-10 it shows full enzymatic activity and the copper displays a rhombic E.P.R. spectrum due to its distorted penta-coordinate structure which allows a fast reduction because the tetrahedral arrangement preferred by the Cu(I) can be easily obtained from the release of one of the five-coordinate groups. The group released is likely to be the imidazole bridge because the lack of pH dependence of the enzyme in the region pH 5-10 [21] is in agreement with the pK of free ($\geqslant$14) and metal-bound ($\geqslant$11.7) imidazole [22]. The clearest evidence for the implication of the imidazole group comes from the similarity of the electronic and E.P.R. spectra of the [Co(II)-Cu(I)] and [Co(II)- ...] protein which strongly suggests that copper reduction leads to the release of Cu(I)

from the imidazole, which subsequently becomes protonated. (The [Co(II)- ...] protein is one in which the Zn(II) has been replaced by Co(II) and the Cu(II) completely removed.) Protonation and deprotonation of the bridging imidazole followed by the valence change of the copper seems then to be an important mechanism for the activity of the protein. The functional rôle of the superoxide dismutase seems, in fact, to be the reaction with the superoxide anion in the following way:-

$$Cu(II) + O_2^- \rightleftharpoons Cu(I) + O_2$$

$$Cu(I) + O_2^- + 2H^+ \rightleftharpoons Cu(II) + H_2O_2$$

The first kinetic study was done by producing O_2^- enzymatically or chemically which was then used to reduce the cytochrome C [1]. Upon addition of superoxide dismutase the reaction is inhibited but it is impossible to measure the rate constant of the reaction as the concentration of O_2^- and the rate of reaction with the cytochrome C are unknown. Using a pulse radiolysis apparatus, Fielden et al. have measured the rate constant which was found to be 2×10^9 mol^{-1} s^{-1} [23] which was unaffected in the pH range 5-10. A recent study in a pulse radiolysis apparatus of the Co(II)-Cu(II) SOD derivative has also demonstrated that the cobalt environment undergoes chemical changes while copper is reduced and re-oxidized catalytically [24].

C. Molecular Spectroscopic and Catalytic Properties of Carbonic Anhydrase

Carbonic anhydrase is a metalloprotein very widespread in nature [25]. In mammalian red cells the enzyme is constituted by a monomeric polypeptide of molecular weight around 30,000 and contains a single zinc(II) ion per molecule which is essential for the catalytic activity [26]. Three different types of isoenzymes are present in human erythrocytes, designated A, B and C in relative abundance 5, 83 and 12% respectively [27,28], whilst two isoenzymes A and B in relative abundance 20 and 80% respectively are present in bovine erythrocytes [29]. Despite the difference in the amino acid composition between the different isoenzymes [30,31], the secondary and tertiary structure is almost the same for all isoenzymes [32], as shown by their similar chemical behaviour. High resolution X-ray data [32,33] has shown that the zinc ion is bound to three histidines and a water molecule, in a structure that may be consistent with a pseudo-tetrahedral one (see Fig. 1.3). There is some evidence that the metal-bound water molecule participates in the catalytic reaction that consists of the reversible hydration of CO_2 to H_2CO_3:

$$CO_2 + H_2O \rightleftharpoons HCO_3^- + H^+$$

The enzyme is able to enhance the hydration rate by a factor of 10^7 [34] and its catalytic activity is pH dependent, i.e. the hydration activity increases with increasing pH [35,36]. The pH dependence of the activity is of sigmoidal type which suggests that the activity is controlled by an ionizing group with pK = 7. This group has been hypothesised to be the zinc-bound water molecule [37], one of the coordinated histidines [38,39], or a glutamate residue [40].

The active site of carbonic anhydrase has been shown to be very

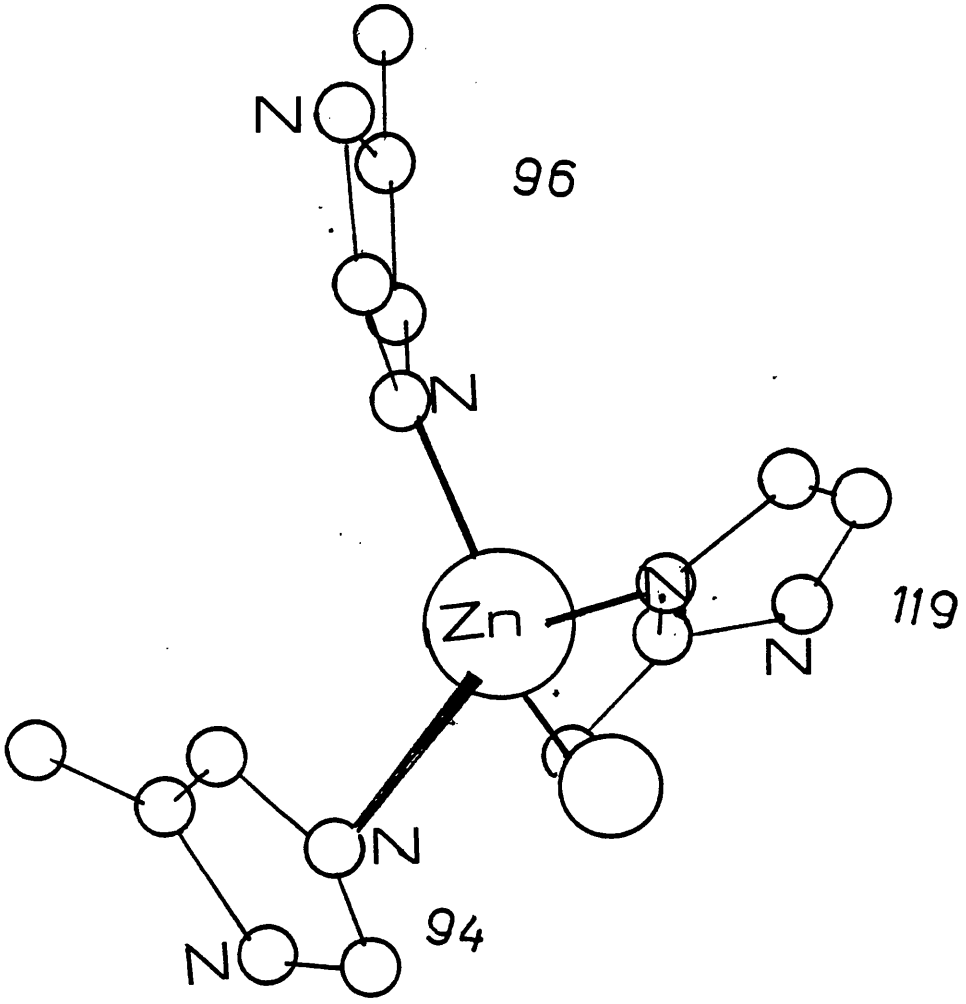

FIG. 1.3 Coordination of the zinc site in carbonic anhydrase.

flexible as the native zinc can be replaced by several metal ions, such as VO^{2+}, Fe^{2+}, Co^{2+}, Ni^{2+}, Cu^{2+}, Cd^{2+} and Hg^{2+} [41-44]. These substitutions have been very useful because in these conditions it has been possible to test the properties of the active site by spectroscopic techniques. In particular, the copper and cobalt derivatives have been widely studied, the former because it has allowed a comparison between other copper proteins [45], the latter because it is the only derivative with activity comparable to that of the native enzyme [42].

The electronic absorption spectrum of the bovine carbonic anhydrase derivative CuBCA shows a single broad band at 13,000 cm^{-1}, whilst the E.P.R. spectrum shows an axial shape with $g_{\parallel} = 2.31$, $g_{\perp} = 2.06$, $A_{\parallel} = 131 \times 10^{-4}$ cm^{-1}. This axial copper site seems to be unsuited for redox reactions but appears to be rather unique in stabilizing binding of external ligands in a distorted environment [46]. In fact, contrary to the superoxide dismutase, binding of anion inhibitors changes the E.P.R. spectrum from axial to rhombic, and the stability constant of the resulting complexes is much higher than that of the analogous derivatives of superoxide dismutase [46].

Optical spectra of the derivatives of each inhibitor are again characterized by a broad band between 12,000 and 14,000 cm^{-1}. In particular, the iodide and azide derivatives show also charge transfer absorption bands, indicating a direct binding of the inhibitor to the copper [46,47]. Moreover, most of the inhibitors (N_3^-, I^-, acetate) do not remove the water molecule from coordination since they bind without affecting the ^1H N.M.R. relaxation rate of the water solution [47]. In this case, the inhibitor either binds by replacing a bound histidine residue in the first coordination sphere of the metal or it binds at a further coordination position. In principle, both hypotheses are possible

but, since the overall shapes of the electronic absorption and of the E.P.R. spectra are strictly similar along the series of the inhibitor derivatives, it is more probable that the three nitrogens from the histidines and the oxygen atom of water remains constant and the inhibitor binds at a further position.

In the case of the cyanide ion, two adducts have been characterized [48,49]. At room temperature independent of the cyanide:enzyme ratio only the 1:1 cyanide complex is formed. Upon lowering the temperature, a new species appears characterized by an E.P.R. spectrum with $g_{||} = 2.20$, $g_{\perp} = 2.05$, $A_{||} = 185 \times 10^{-4}$ cm^{-1}. Ligand superhyperfine structure due to two magnetically equivalent nitrogen ligands and to two magnetically equivalent carbon ligands of the bound cyanide are also evident in measurements using enriched ^{13}CN [48]. Cyanide is the only inhibitor capable of binding two ions to the metal but only at low temperature. Whereas the 1:1 adduct, by analogy to the other derivatives with anionic inhibitors, is presumably five-coordinate, the electronic and E.P.R. parameters of the dicyanide derivative suggest an essential planar tetragonal chromophore, with one or two loosely bound axial ligands [47,49]. In the presence of HCO_3^- and some sulphonamides, the natural substrate and the strongest inhibitor respectively, water is removed from the first coordination sphere because of a decrease of the ^1H N.M.R. relaxation rate [47]. In particular, addition of p-toluene sulphonamide quenches the ^1H N.M.R. relaxation rate and shows an E.P.R. spectrum with $A_{||} = 70 \times 10^{-4}$ cm^{-1} suggesting a pseudo-tetrahedral geometry for this derivative [47].

The spectroscopic properties of the cobalt derivative have been extensively studied, its electronic spectrum is well-defined and is strongly pH dependent [50]. It has been demonstrated that the low and

high pH electronic spectra, as well as those of the inhibitor derivatives, are due to a high-spin cobalt with three unpaired electrons [51,52]. In every case the electronic spectrum shows at least one absorption with $\varepsilon > 100$ mol^{-1} cm^{-1} so that the possibility that the chromophores are six-coordinated can be excluded [53]. The only stereochemistries consistent with these data are the pseudo-tetrahedral and the five-coordinated [54]. From electronic and magnetic circular dichroic spectra, a pseudo-tetrahedral structure has been suggested for the acid form, whilst both four- and five-coordination have been proposed for the alkaline form [55,56]. Recently a classification of the electronic spectra of several inhibitor derivatives of cobalt carbonic anhydrase has been done [57]; in particular, the presence of a weak band around 12,000-14,000 cm^{-1} assigned to the ^4F-^4F transitions has been taken as diagnostic for a pentacoordinate coordination. Also in the cobalt derivative, the cyanide is the only inhibitor able to give rise to two different adducts depending upon the temperature. The first has only one cyanide bound and is high spin Co(II), the second has two cyanides bound and the resulting five-coordinate chromophore is low spin Co(II) [49,58-60]. An accurate E.P.R. investigation by Cockle with ^{13}C and ^{15}N labelled cyanide ions has allowed detection of ligand superhyperfine splitting due to two magnetically equivalent carbon atoms of cyanide [49,60]. Since a ligand superhyperfine splitting due to a single nitrogen of histidine is also observed [59], a square pyramidal geometry with the unpaired electron residing in the d_{z^2} orbital has been proposed [60].

The affinity constants of the inhibitors for the cobalt enzyme are often of the same order of magnitude as for the native enzyme whilst for the copper derivative they are larger, suggesting a different way of coordination of the copper ion relative to the cobalt and zinc. The pH

dependent affinity constant of the anionic inhibitor for the enzyme has the same trend for all the three derivatives [46,61,62], indicating the presence, in all cases, of at least one acid-base equilibrium in the active site responsible for the binding of inhibitors. These pH dependent properties of the enzyme are probably the key to understanding the catalytic mechanism. As a matter of fact, several theories have been proposed [37,40]. In principle, it could be possible that different ionizing groups are governing different properties of the enzyme, and this seems confirmed by the profile of the absorption at 15,600 cm^{-1} against pH of the cobalt derivative that shows that more than one acid-base equilibrium seems capable of affecting the electronic spectra [63].

REFERENCES

1. J. M. McCord and I. Fridovich, J. Biol. Chem. 244, 6049 (1969).

2. R. A. Weisiger and I. Fridovich, J. Biol. Chem. 248, 3582 (1973).

3. K. Azada, M. Urano and M. Takahashi, Europ. J. Bioch. 36, 257 (1973).

4. B. B. Keele, J. M. McCord and I. Fridovich, J. Biol. Chem. 246, 2875 (1971).

5. G. Rotilio, L. Calabrese, F. Bossa, A. Finazzi-Agro and B. Mondovi, Biochemistry 11, 2182 (1972).

6. C. O. Beauchamp and I. Fridovich, Biochim. Biophys. Acta 317, 50 (1973).

7. J. Richardson, K. A. Thomas, B. H. Rubin and D. C. Richardson, Proc. Nat. Acad. Sci. USA 72, 1349 (1975).

8. J. A. Fee in 'Superoxide and Superoxide Dismutase', (ed. by A. M. Michelson, J. M. McCord and I. Fridovich) Academic Press, p.173 (1977).

9. G. Rotilio, L. Morpurgo, C. Giovagnoli, L. Calabrese and B. Mondovi, Biochemistry 11, 2187 (1972).

10. J. A. Fee and P. B. Gaber, J. Biol. Chem. 247, 60 (1972).

11. M. Terenzi, A. Rigo, C. Franconi, B. Mondovi, L. Calabrese and G. Rotilio, Biochim. Biophys. Acta 351, 230 (1974).

12. G. Rotilio, R. C. Bray and E. M. Fielden, Biochim. Biophys. Acta 268, 605 (1972).

13. A. Rigo, P. Viglino and G. Rotilio, Biochem. Biophys. Res. Comm. 63, 1013 (1975).

14. G. Rotilio, A. Finazzi-Agro, L. Calabrese, F. Bossa, P. Guerrieri and B. Mondovi, Biochemistry 10, 616 (1971).

15. G. Rotilio, L. Morpurgo, L. Calabrese and B. Mondovi, Biochim. Biophys. Acta 302, 229 (1973).

16. J. A. Fee and W. D. Phillips, Biochim. Biophys. Acta 412, 26 (1975).

17. L. Calabrese, G. Rotilio and B. Mondovi, Biochim. Biophys. Acta 263, 827 (1972).

18. G. Rotilio, L. Calabrese, B. Mondovi and W. E. Blumberg, J. Biol. Chem. 249, 3157 (1974).

19. L. Calabrese, D. Cocco, L. Morpurgo, B. Mondovi and G. Rotilio, Eur. J. Biochem. 64, 465 (1976).

20. L. Calabrese, D. Cocco, L. Morpurgo, B. Mondovi and G. Rotilio, FEBS Letters 59, 29 (1975).

21. J. A. Fee and P. E. Di Corleto, Biochemistry 12, 4893 (1973).

22. R. T. Sundberg and R. B. Martin, Chem. Rev. 74, 471 (1974).

23. E. M. Fielden, P. B. Roberts, R. C. Bray, C. N. Mautner, G. Rotilio and L. Calabrese, Biochem. J. 199, 49 (1974).

24. M. E. McAdam, E. M. Fielden, F. Lavelle, L. Calabrese, D. Cocco and G. Rotilio, Biochem. J. 167, 271 (1977).

25. Y. Focker and S. Sarkanen, Adv. Enzymol. 47, 149 (1978).

26. D. Keilin and R. Mann, Nature 144, 442 (1939).

27. P. O. Nyman, Biochim. Biophys. Acta 52, 1 (1961).

28. E. E. Rickli and J. T. Edsall, J. Biol. Chem. 237, 258 (1962).

29. S. Lindskog, Biochim. Biophys. Acta 39, 218 (1960).

30. M. M. Gulian, N. Limozin, B. Malet, J. Di Costanzo and M. Carrel, Biochimie 59, 293 (1977).

31. M. M. Giulian, D. Faure, J. Buc and M. Charrel, Biochimie 60, 473 (1978).

32. K. K. Kannan in 'Biophysics and Physiology of Carbon Dioxide', (ed. by C. Bauer, G. Gros and H. Bartels) Springer-Verlag, Berlin, p.184 (1980).

33. K. K. Kannan, B. Nostrand, K. Fridborg, S. Lövgren, A. Ohlsson and M. Petef, Proc. Nat. Acad. Sci. USA 72, 51 (1975).

34. B. M. Gibbons and J. T. Edsall, J. Biol. Chem. 239, 2539 (1964).

35. R. G. Khalifah, J. Biol. Chem. 246, 2561 (1971).

36. S. H. Koenig, R. D. Brown, R. E. London, T. E. Needham and N. A. Matwiyoff, Pure Appl. Chem. 40, 103 (1974).

37. I. D. Campbell, S. Lindskog and A. I. White, J. Mol. Biol. 98, 597 (1975).

38. J. M. Pesando and A. P. Grollman, Biochemistry 14, 689 (1975).

39. R. K. Gupta and J. M. Pesando, J. Biol. Chem. 250, 630 (1975).

40. K. K. Kannan, M. Petef, K. Fridborg, H. Ciddresdner and S. Lövgren, FEBS Letters 73, 115 (1977).

41. S. Lindskog and P. O. Nyman, Biochim. Biophys. Acta 85, 462 (1964).

42. S. Lindskog and B. G. Malmstrom, J. Biol. Chem. 237, 1129 (1962).

43. J. J. Fitzgerald and N. D. Chasteen, Biochemistry 13, 4338 (1974).

44. H. Shinar and G. Navon, Biochim. Biophys. Acta 334, 471 (1974).

45. G. Rotilio, L. Morpurgo, L. Calabrese, A. Finazzi-Agro and B. Mondovi in 'Metal-Ligand Interactions in Organic Chemistry and Biochemistry' (ed. by B. Pullman and N. Goldblum) D. Reidel Publishing Company, Dordrecht, Holland, p.243 (1978).

46. L. Morpurgo, G. Rotilio, A. Finazzi-Agro and B. Mondovi, Arch. Biochem. Biophys. 170, 360 (1975).

47. I. Bertini, G. Canti, C. Luchinat and A. Scozzafava, J.C.S. Dalton 1269 (1978).

48. P. H. Haffner and J. E. Coleman, J. Biol. Chem. 248, 6628 (1973).

49. P. H. Haffner and J. E. Coleman, J. Biol. Chem. 250, 996 (1975).

50. S. Lindskog, J. Biol. Chem. 238, 945 (1963).

51. S. Lindskog and A. Ehrenberg, J. Mol. Biol. 24, 133 (1967).

52. R. Aasa, M. Hanson and S. Lindskog, Biochim. Biophys. Acta 453, 211 (1976).

53. R. C. Carlin in 'Transition Metal Chemistry' (ed. by R. C. Carlin) Marcel Dekker Inc., New York, p.1 (1966).

54. A. F. Dennard and R. J. P. Williams in 'Transition Metal Chemistry, Vol. 2' (ed. by R. C. Carlin) Marcel Dekker Inc., New York, p.115.

55. J. E. Coleman and R. V. Coleman, J. Biol. Chem. 247, 4718 (1972).

56. B. Holmquist, T. A. Kaden and B. L. Vallee, Biochemistry 14, 1454 (1975).

57. I. Bertini, G. Canti, C. Luchinat and A. Scozzafava, J. Am. Chem. Soc. 100, 4873 (1978).

58. E. Grell and R. C. Bray, Biochim. Biophys. Acta 236, 503 (1971).

59. J. S. Taylor and J. E. Coleman, J. Biol. Chem. 246, 7058 (1971).

60. S. A. Cockle, Biochem. J. 137, 587 (1974).

61. A. Lanir and G. Navon, Biochim. Biophys. Acta 341, 75 (1974).

62. S. Lindskog, Biochemistry 5, 2641 (1966).

63. I. Bertini, C. Luchinat and A. Scozzafava in 'Biophysics and Physiology of Carbon Dioxide' (ed. by C. Baver, C. Gros and H. Bartels) Springer-Verlag, Berlin, p.151 (1980).

CHAPTER 2

EXPERIMENTAL TECHNIQUES

A. E.P.R.

X-band E.P.R. spectra were recorded with an E-9 Varian spectrometer. Room temperature studies were performed using flat cells to maximize the intensity of the paramagnetic centre. The cells were of pure quartz glass to avoid any signal coming from paramagnetic impurities present in any other glass.

E.P.R. studies at 77 K were performed by using a Varian V4540 liquid nitrogen accessory. In this device the temperature can be controlled between room temperature to 77 K through a thermo-resistor. In this case, cylindrical quartz tubes with diameter as large as possible were used as cells.

Liquid helium temperature was obtained with an Air Products and Chemical CT-3-110 liquid transfer Cryo-Tip refrigerator with automatic temperature controller. This accessory has been used to detect the signal of the Co(II) high spin that has a short relaxation time and which shows a signal only at temperatures near to that of liquid helium. In some experiments an E.P.R. tube sealed to a Thunberg apparatus were used for work in anaerobic conditions.

The protein concentration of the samples used ranged between 2×10^{-4} and 2×10^{-3} molar.

B. Magnetic Susceptibility

The outline of the instrument used is shown in Fig. 2.1. The instrument measures the changes in magnetic flux when the sample oscillates perpendicularly to the plane of a pair of astatic pick-up coils and parallel to the applied magnetic field. The magnet is superconducting and is operated in the persistent mode of typically a field of a few tens of oersteds. The pick-up coil is the primary of a superconducting d.c. transformer; the secondary of the transformer is coupled

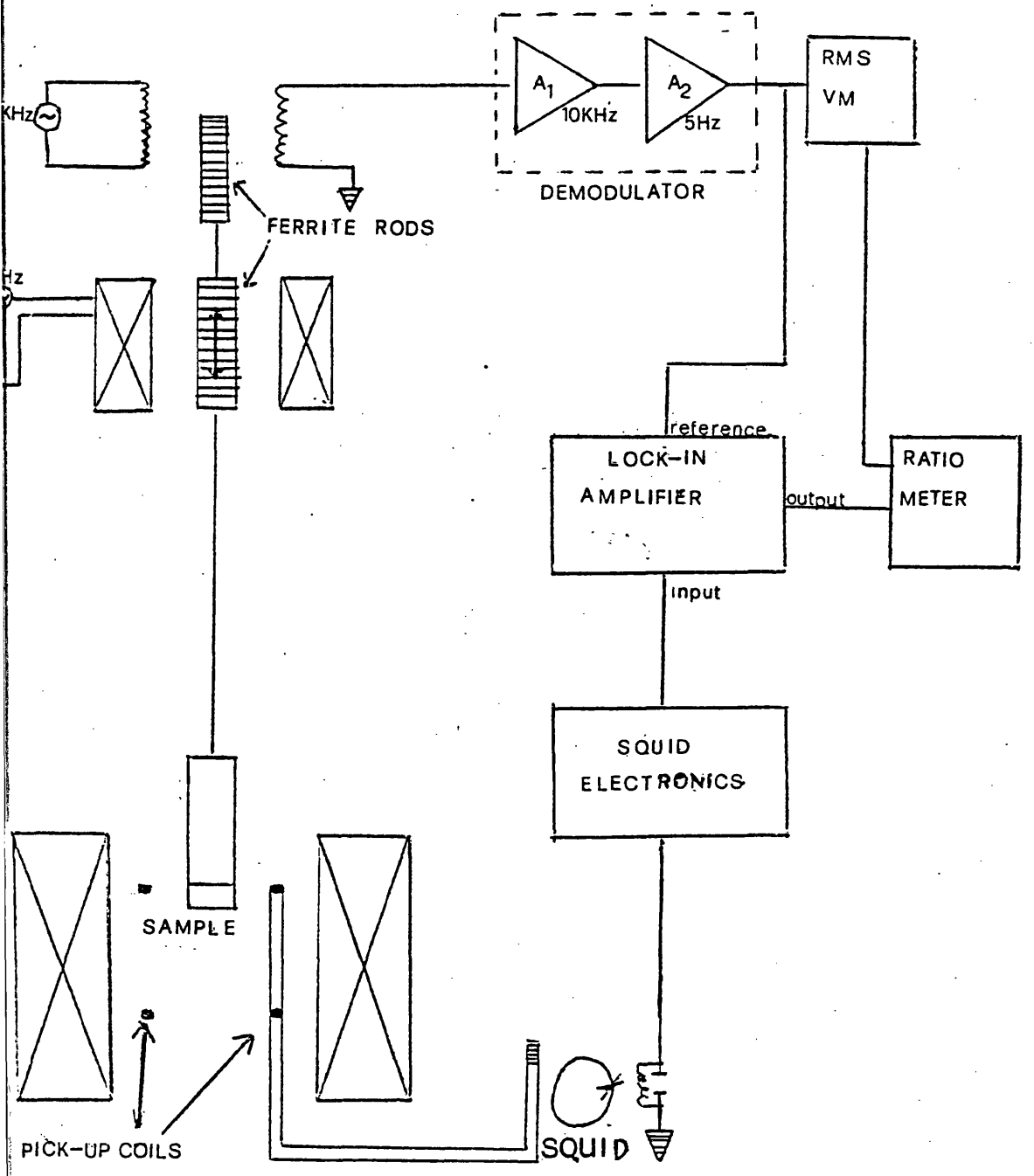

FIG. 2.1 Scheme of the detection set-up of the superconducting magnetometer.

to a SQUID superconducting magnetometer which is sensitive to a fraction of the flux quantum $\phi_o = 2 \times 10^{-15}$ Wb. The whole assembly is immersed in liquid helium at 4.2 K. The pick-up coils are a few turns of 50 μm o.d. niobium wire. The sample fills the bottom of a quartz tube of 6.0 mm o.d. and 5.2 mm i.d., to a height close to the tube diameter. The sample is suspended in a stainless steel Dewar: the tip of this Dewar, made of high purity silver, extends through the pick-up coils; the sample temperature can be regulated at any desired value between 4.2 and 350 K with the aid of platinum thermometers and manganin heaters.

The sample is supported by a ferrite rod at room temperature and this rod is caused to oscillate at about 5 Hz by a co-axial magnet. A second ferrite rod is used to generate a reference signal proportional to the oscillation amplitude. This rod modulates the mutual inductance between two coils, one of which is fed with a stable 10 KHz signal. The 5 Hz amplitude-modulated 10 KHz carrier from the other coils is amplified and demodulated to give a d.c. signal proportional to the root mean square amplitude of oscillation of the sample. The signal from the SQUID magnetometer is fed to a lock-in amplifier, which uses as reference signal the 5 Hz oscillation amplitude signal, and yields a d.c. signal proportional to the root mean square change in flux. Finally, a ratiometer gives the ratio D of the root mean square magnetic flux change to the root mean square oscillation amplitude.

The value D is taken as a measure of the susceptibility of the sample. The relation that binds the value D to the susceptibility is:

$$D = \kappa H \sum_i n_i \chi_{iM}$$

where H is the external applied field, n_i is the total number of moles

of the i component of the sample of molar susceptibility χ_{iM}, and κ is an instrumental constant independent of the amount of sample and its density. This instrument allows one to detect changes in susceptibility as small as 0.3% of the diamagnetism of water and it is particularly suited for measurements of very weakly magnetic samples, like biochemical compounds.

C. Optical and Atomic Absorption

Optical spectra were recorded on a Cary 14 spectrophotometer. Cells with a pathlength of 1 cm were usually used. Anaerobic experiments were carried out in an optical cell sealed to a Thunberg-type apparatus. Metal analyses were performed with a Hilger & Watts Atomspek Model H 1170 atomic absorption spectrometer.

D. X-Ray Absorption

X-ray absorption data were taken at the Adone storage ring, at the Synchrotron Radiation Facility P.U.L.S. of the Frascati National Laboratory. Fig. 2.2 shows the basic feature of an electronic storage ring. A closed continuous high vacuum system threads through various elements such as:

(a) an inflector which permits electrons from a separate machine to be injected into the ring,

(b) bending magnets which bend the electrons in a circle,

(c) R.F. cavities which replace the synchrotron radiation energy loss,

(d) vacuum pumps which provide the high vacuum necessary to permit electrons to continue in orbit for hours.

In this way electrons can be accelerated up to extremely high energies and, when constrained by a magnetic field to a curved path, emit radiation

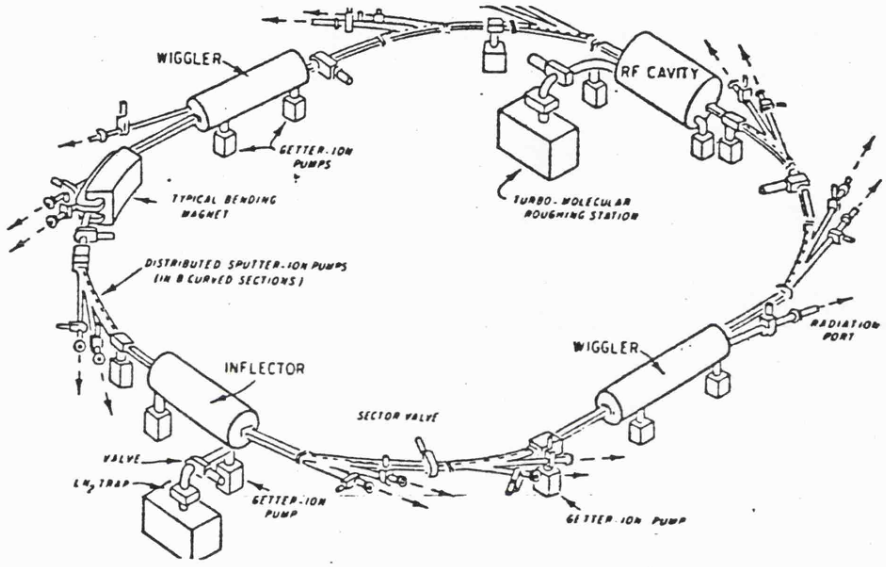

FIG. 2.2 View of a high current storage ring as utilized for synchrotron radiation.

FIG. 2.3 Radiation emission pattern by electrons in circular motion. Case I, $v \ll c$; case 2, $v \approx c$.

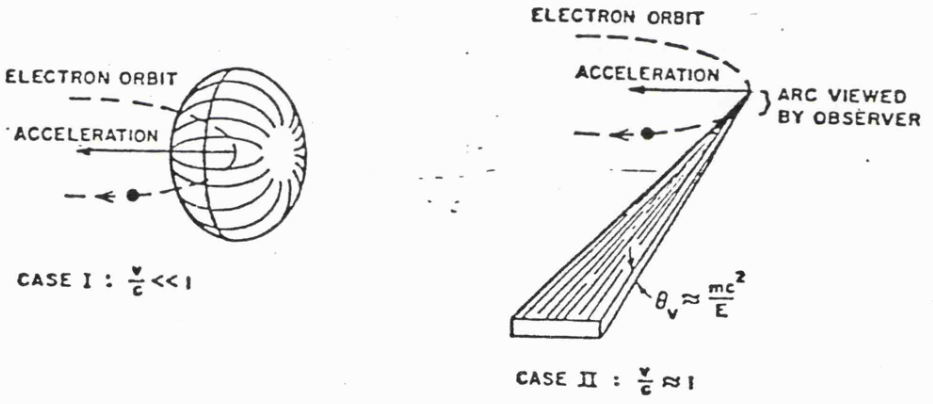

whose directional pattern and frequencies are very different from those associated with classical accelerating changes. Fig. 2.3 shows schematically the radiation emission pattern of electrons in circular motion. At low energy the radiation is emitted in a rather non-directional dipole pattern. At high energy when the velocity, v, of the electron is close to the velocity of light, c, and when the electron energy, E, is larger than its rest mass energy (0.51 MeV), relativistic effects cause a sharp forward peaking of the radiation and, at the same time, a large increase in the total energy radiated occurs. The radiation is highly polarized with the electric vector in the plane of the acceleration.

In a storage ring the injected electrons are brought up to a final energy and maintained in orbit at this energy for hours. The current, and consequently the photon beam intensities, decay slowly because of the occasional encounters with residual gas molecules even at pressure of 10^{-9} torr. Energy, lost as radiation, is restored to the electrons in passing through a radio-frequency (r.f.) cavity; to do this efficiently, one wants the electrons to be in the r.f. cavity when the r.f. is a maximum. Therefore, the electrons go around in bunches and the photon beam emitted is consequently in pulses of duration less than $\sim 10^{-9}$ second.

In Fig. 2.4 the photon spectrum emitted by Adone is shown. With the storage ring operating at 1.5 GeV and with a current of 100 mA the maximum (critical) energy, E_c, is 1.5 KeV and the photon flux at E_c is $>10^{13}$ photons sec^{-1} $mrad^{-1}$ mA^{-1}, allowing one to obtain a good photon flux up to ~10 KeV. The most important parameters of Adone as a synchrotron radiation source are shown in Table 2.1.

As seen from Fig. 2.4 and the parameters reported in Table 2.1, synchrotron radiation has characteristics unique as compared to the

FIG. 2.4 Spectral distribution of synchrotron radiation from Adone.

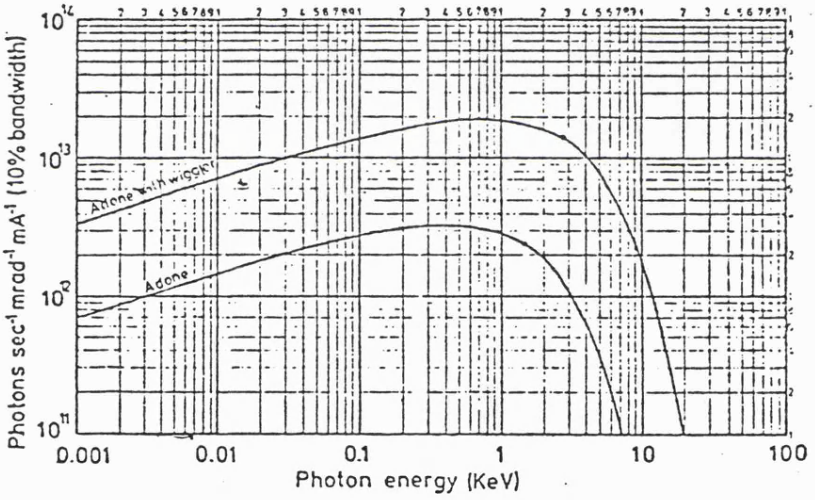

TABLE 2.1

The most important parameters of Adone as a synchrotron-radiation source

(1)	Maximum energy of the electron beam	$E_{max} = 1.5$ GeV
(2)	Critical photon energy	$E_c = 1.5$ KeV
(3)	Bending radius	$\rho = 5$ m
(4)	Maximum injected current	$I_{max} = 100$ mA
(5)	Number of bunches	$K = 3$
(6)	Number of bending magnets	$n = 12$
(7)	Emission angle	$\theta = 0.3$ mrad
(8)	Radio-frequency	$f = 8.54$ MHz
(9)	Beam life-time	$\tau \simeq 10$ h
(10)	Time structure of the beam	$\sigma_y \simeq 0.6$ ns $\tau = 117$ ns

electromagnetic radiation obtained from any other conventional source. The electromagnetic spectrum covered by synchrotron radiation goes from the visible to the X-ray region; it is characterized by a high and stable intensity, it is highly polarized and it has pulsed time structure. A comparison between synchrotron radiation and a standard X-ray tube is shown in Fig. 2.5. The availability of this intense and stable radiation has allowed researchers to begin X-ray photo-absorption studies on diluted samples such as biological materials and metalloproteins in particular.

X-rays are absorbed by matter according to the equation:

$$I = I_o e^{-\mu x}$$

where I_o is the initial intensity, I the transmitted intensity, μ the

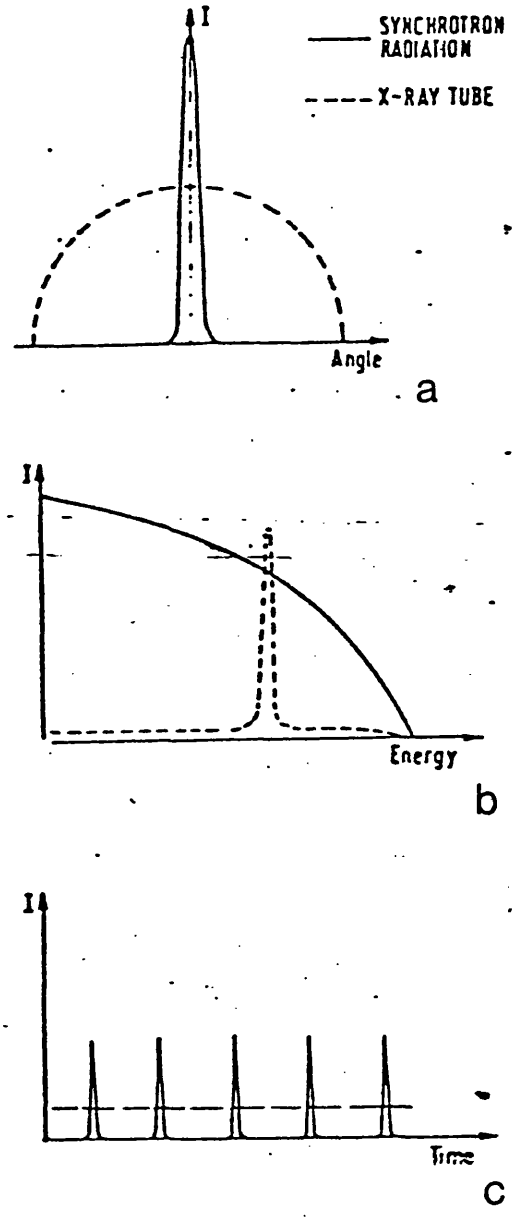

FIG. 2.5 Comparison of the intensity I, of synchrotron radiation and an X-ray tube with respect to (a) angle, (b) energy, (c) time.

absorption coefficient and x, the distance the X-rays travel through the sample.

The experimental scheme used to monochromatize the synchrotron radiation and to measure the absorption coefficients as a function of energy is shown in Fig. 2.6. It consists of a condensing mirror, a parallel crystal monochromator, and a pair of ion chambers for measuring the intensity of the incident and transmitted radiation, I_o and I respectively. The parallel crystal monochromator selects a narrow band of radiation from the continuous spectrum produced by the stored electron beam in the storage ring. By changing the Bragg angle of reflection in the monochromator, the output photon energy may be varied over a wide range allowing one to study the K-edges of elements from potassium to zinc, that is, from a photon energy of about 3 to about 10 KeV.

The absorption spectrum of an isolated atom, like krypton gas, consists of a sharp increase in the absorption (μx) at X-ray photon energies sufficient to liberate inner shell electrons. Above this threshold, called the absorption edge, the absorption gradually decreases monotonically as the X-ray photon energy increases. However, for atoms involved in chemical bonding, sinusoidal oscillations are detected in addition to the main absorption. These are the EXAFS oscillations which are due to a final-state interference effect occurring from the photo-electron wave ejected from the absorbing atoms and back-scattered from the neighbouring atoms. The study of this region gives useful information about the local environment of a specific atom and, in particular and most importantly, can give the distance between this atom and the atoms in its first coordination sphere. Also the absorption edge ($\sim$ 40-50 eV around the abrupt change in μx) can give information about the atomic energy level of the absorbing atom. For simplicity in Fig. 2.7 the

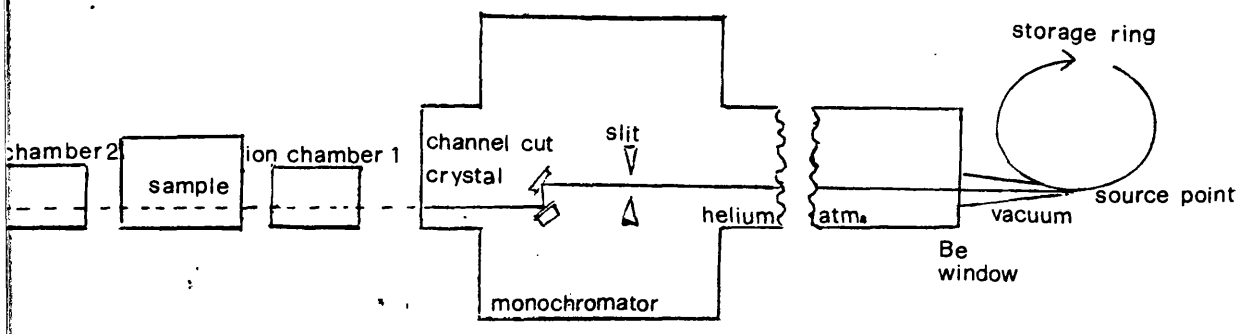

FIG. 2.6 Experimental scheme used to monochromatize the synchrotron radiation and to measure the absorption coefficient as a function of energy.

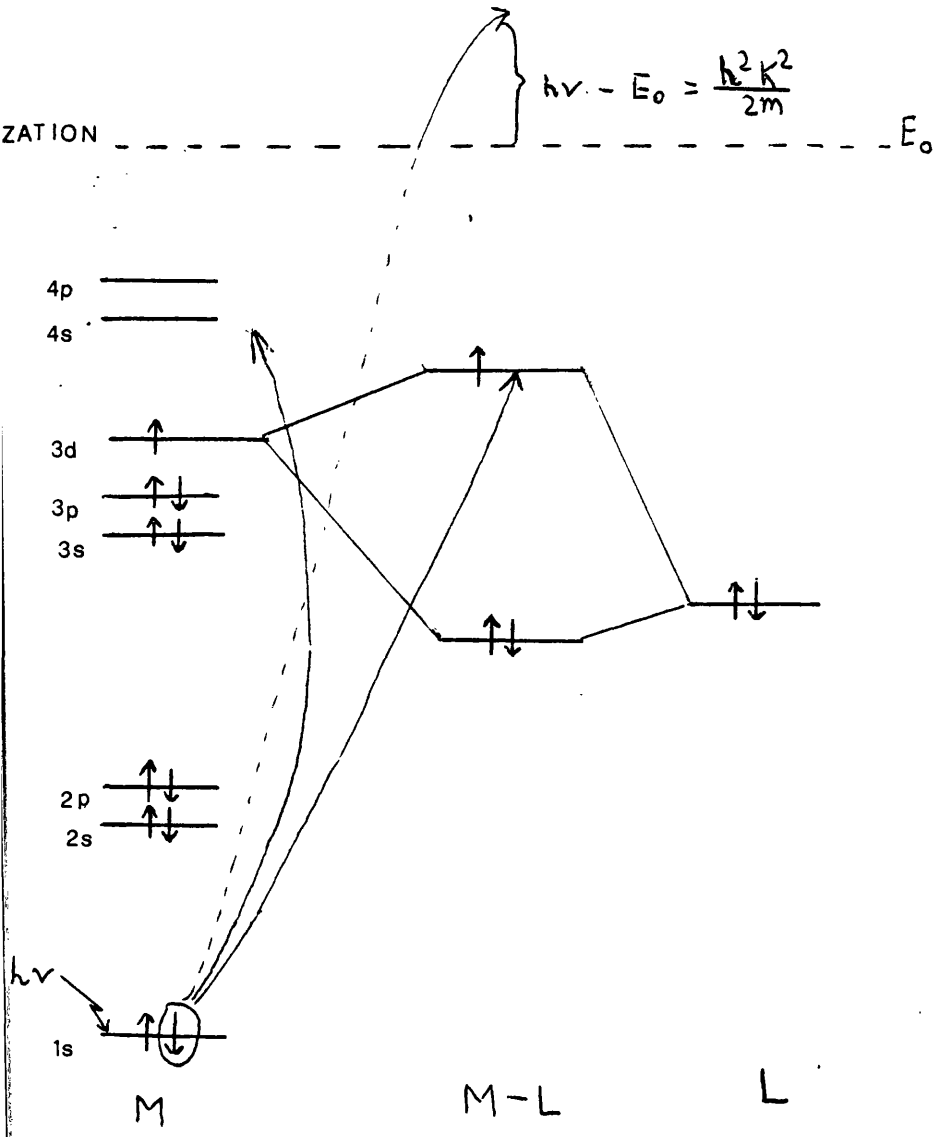

FIG. 2.7 Idealized energy level scheme showing some of the transitions induced at the K-edge by X-ray absorption.

idealized energy level scheme for a Co(II) ion is given. In this case, the K edge is in the vicinity of 7,700 eV. The edge energy is roughly the binding energy of the K-shell electrons, so the absorption of a photon can promote a 1s electron first to the lowest empty localized orbitals (such as the antibonding 3d molecular orbitals in this case) and then to the 4s and 4p orbitals before being ejected, for higher photon energies, to the free electron continuum. The absorption edge spectrum depends on the charge of the absorber, the degree of covalency of bonds, and the coordination geometry. From the relative intensity of the $1s \rightarrow 3d$, $1s \rightarrow 4s$ and $1s \rightarrow 4p$ transitions and their relative energy differences, useful information can be derived about the symmetry and the covalency of the atoms surrounding the absorbing atom.

E. Preparation of the Samples

(1) The native proteins

Superoxide dismutase and carbonic anhydrase were prepared from fresh bovine blood. Red cells were collected from approximately 10ℓ of blood by centrifugation, and then re-suspended and washed in 0.9% NaCl by centrifugation. Deionized water was added to the 4ℓ packed cells to lyse them. 25% of ethanol and 15% of chloroform was slowly added, in the cold, to the 7ℓ haemolysate to precipitate the haemoglobin. The mixture was allowed to stir for 15 minutes, during which time the mixture was very thick. The precipitate was removed by centrifugation and to the supernatant liquid, solid K_2HPO_4 (300g for each litre) was added. The two phases were then separated, the denser one was essentially aqueous and contained the salt, the lighter one was water-ethanol and contained little salt. The lighter phase was centrifuged and to the pale yellow supernatant liquid, 75% of cold acetone was slowly added with stirring. The mixture was centrifuged, and the precipitate was dissolved in water

and then dialyzed against water. The solution was concentrated and dialyzed against 5 mM potassium phosphate at pH 7.4. The solution was applied to a DE-32 resin column equilibrated with the same buffer. The column was then washed with the same buffer and from this phase the carbonic anhydrase was obtained. Elution of the column with a gradient of potassium phosphate buffer ranging from 5 to 200 mM produced the purification of the superoxide dismutase.

(2) Substituted proteins

The copper-free, i.e. [Zn - ...] SOD, was prepared by reducing the native enzyme by ferrocyanide and then by dialyzing against a mixture of 50 mM potassium phosphate at pH 6 and 50 mM KCN for ~12 hours. After addition of cyanide the pH of the sample was adjusted to 6 by adding H_3PO_4. The sample was then dialyzed against 100 mM potassium phosphate or water. From this sample the [Zn-Co] SOD was obtained by adding a stoichiometric amount of $CoCl_2$ and then by incubating for about 12 hours. The sample was again dialyzed against 100 mM potassium phosphate.

The complete metal-free apo-SOD was obtained by dialyzing the enzyme against 50 mM acetate buffer at pH 3.8 and 4-5 mM EDTA for 48 hours at room temperature. The solution was dialyzed against 100 mM perchlorate at pH 7.4 and then against water. From this completely metal depleted enzyme it was possible to obtain the [Co - ...] SOD, [Co-Co] SOD and [Co - Cu] SOD derivatives. The [Co - Co] SOD was obtained by adding stoichiometric $CoCl_2$ to the apo-protein and incubating for 12 hours. The solution was then dialyzed against 100 mM potassium phosphate at pH 7.4. The reconstitution with cobalt was followed by its optical spectrum. The [Co-Cu] SOD was obtained by adding to the apo-protein stoichiometric $CoCl_2$ to fill the zinc site and then stoichiometric $CuSO_4$ to fill the copper site. The protein was then dialyzed against 100 mM phosphate

buffer at pH 7.4. In this case, the [Co-Cu] SOD contained the same amount of cobalt and copper and no zinc at all. The [Co-Cu] SOD could also be obtained by dialysis of the native enzyme against 100 mM acetate buffer at pH 5.4 and 0.6 M $CoCl_2$ for 48 hours. The solution was then dialyzed against 100 mM acetate buffer at pH 5.4. In this case, the [Co-Cu] SOD derivative contained a ratio of 1.2/2 cobalt to copper, thus a part of the native zinc was not removed by the dialysis.

The apo-carbonic anhydrase was prepared by dialysis against 1,10-phenanthroline in 0.1 M acetate buffer at pH 5.3. The Co(II) and Cu(II) derivatives were obtained by adding a stoichiometric amount of $CoSO_4$ and $CuSO_4$ respectively. The protein was then dialyzed against 50 mM acetate buffer at pH 5.3.

(3) Preparation of inorganic model compounds

$[Co/Zn(atsz)Cl_2]$ [1] where atsz = $NH_2C(S)NHN{=}C(CH_3)_2$, $[Co/Zn(\gamma\text{-pic})_2Br_2]$ [2] where γ-pic = 4 methyl pyridine, $[Co/Zn(etu)_2(CH_3CO_2)_2]$ [3] where etu = $-S\begin{smallmatrix}\diagup NH-CH_2 \\ \diagdown NH-CH_2\end{smallmatrix}$, were prepared according to the literature method. The doped complexes were obtained by co-crystallisation from the appropriate solvents mentioned in the references. Nominal concentrations of 0.5 to 2% Co^{2+} were used for the E.P.R. measurements. As no suitable diamagnetic hosts for $[Co(im)_2(CH_3CO_2)_2]$ [4] where im = $-N\begin{smallmatrix}\diagup CH{=}CH \\ \diagdown CH{=}N\end{smallmatrix}$, $[Co(S_2PPh_2)_2.C_9H_7N]$ [5], $[Co(atsz)_2Cl]Cl.H_2O$ [6], $[Co(aptsz)_2I_2]$ [6] where aptsz = $NH_2C(S)NHN{=}C(CH_3)(C_6H_5)$ and $[Co(btsz)_2Cl_2]$ [6] where btsz = $NH_2C(S)NHN{=}CH(C_6H_5)$ were available, the E.P.R. spectra were recorded on frozen solutions because the un-doped powder gave a very broad signal. $[Co(bipy)_3](ClO_4)_2$, where bipy = bipyridyl, was prepared according to [7] and $Co(atsz)_2I_2.2H_2O$ according to [6]. Powders of the cobalt compounds were used for the K-edge X-ray spectra.

REFERENCES

1. M. Mathew and G. J. Palenik, Inorg. Chim. Acta 5, 349 (1971).

2. L. Fanfani, A. Nunri and P. F. Zanazzi, Acta Cryst. 28B, 323 (1972).

3. E. M. Holt, S. L. Holt and K. J. Watson, J. Am. Chem. Soc. 92, 2721 (1970).

4. A. Gadet, C.R. Acad. Sci. (Paris) C272, 1299 (1971).

5. A. C. Villa, C. Guastini, P. Porta and A. A. G. Tomlinson, J. Chem. Soc. Dalton 956 (1978).

6. C. Bellitto, A. A. G. Tomlinson, C. Furlani and G. De Munno, Inorg. Chim. Acta 27, 269 (1974).

7. F. H. Burstall and R. S. Nyholm, J. Chem. Soc. 3571 (1952).

CHAPTER 3

PROPERTIES OF THE Co(II) METAL ION AND ITS USE AS A PROBE IN METALLOPROTEINS

The substitution of metal atoms at the active site of metalloenzymes is one of the mildest and most selective procedures currently available for the chemical modification of enzymes. In particular, substitution for the zinc by the cobalt atom has been very useful as these atoms share a variety of chemical properties [1]. In particular, they have the same charge, similar size, and similar stereochemical demands. Carboxypeptidase A [2] and carbonic anhydrase [3] have been the first zinc enzymes where cobalt has been substituted for the zinc and, since then, this procedure has become usual for several metalloenzymes. The Co(II) metal ion has seven d-electrons that can be disposed in a high spin or low spin configuration depending on the symmetry and the crystal field strength of its environment. Tetrahedral symmetry allows only the high spin configuration whilst in an octahedral or pentacoordinate environment both the low spin and the high spin configuration are allowed. For the Co(II) in metalloproteins the interest is mainly in the high spin state as the low spin state is reached only in particular cases such as when the cobalt is substituted in a porphyrin ring. Tetrahedral and octahedral environments both give rise to bands in the visible region between 20,000 and 15,000 cm^{-1} but it is easy to discriminate the two symmetries by the intensity of the spectra [4]. In a tetrahedral field, the molar absorbance of the Co(II) is at least a factor of 10 greater than for the octahedral field. It is more difficult to discriminate between tetrahedral and pentacoordinate structure especially when some distortion is present.

In Fig. 3.1 a simplified energy level diagram for tetrahedral (a) and trigonal bipyramidal (b) chromophores of Co(II) is given. In both cases there are three main absorptions and they fall at approximately the same energy. The first careful analysis of the behaviour of the Co(II)

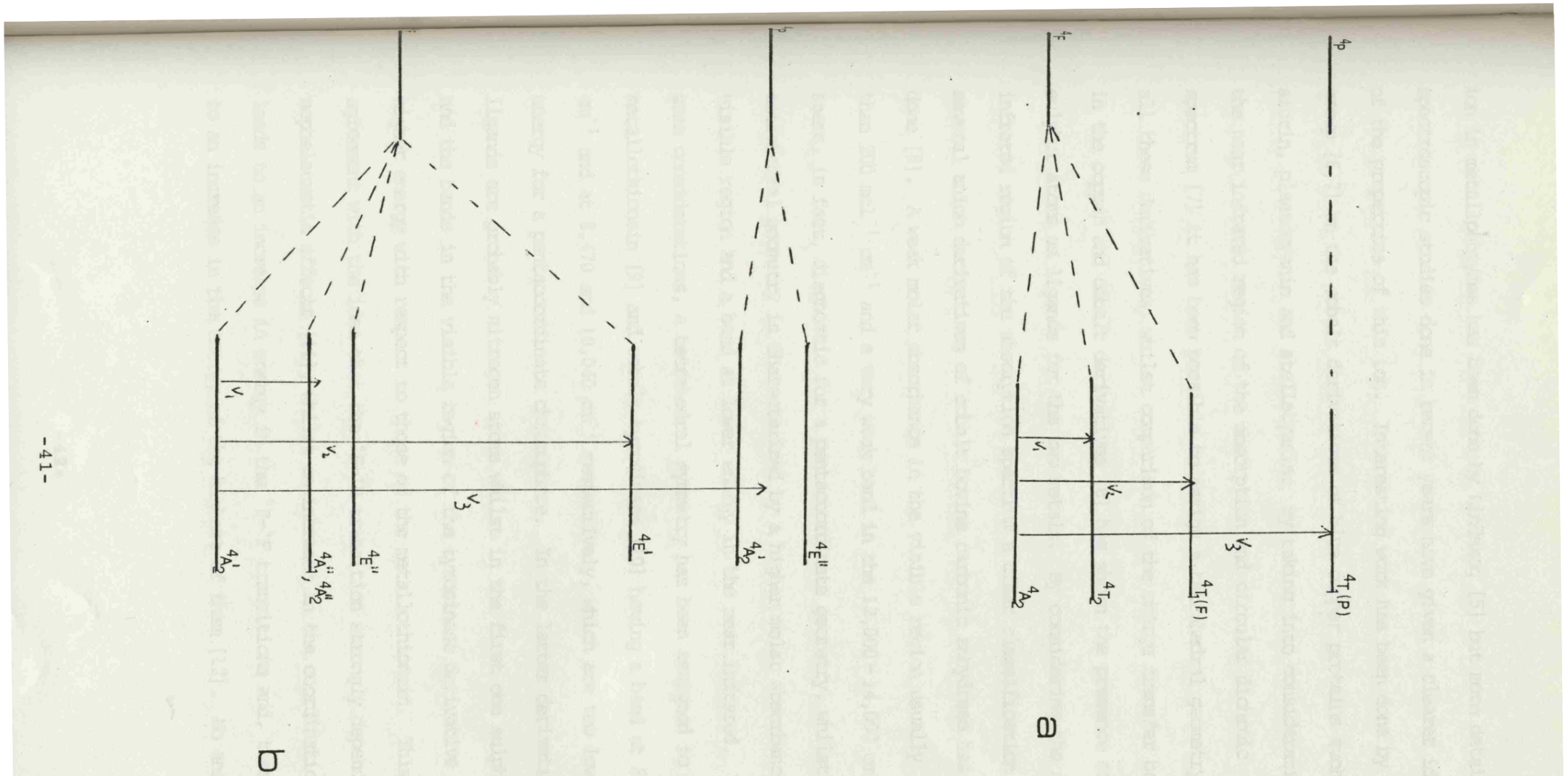

FIG. 3.1 Simplified energy level for a (a) tetrahedral and a (b) trigonal bipyramidal cobalt(II) complex.

ion in metalloenzymes has been done by Lindskog [5] but more detailed spectroscopic studies done in recent years have given a clearer idea of the properties of this ion. Interesting work has been done by Gray's group [6,7] on the cobalt derivatives of blue copper proteins such as azurin, plastocyanin and stellacyanin. By taking into consideration the near infrared region of the absorption and circular dichroic spectrum [7] it has been possible to assign a tetrahedral geometry for all these derivatives, whilst comparison of the charge transfer bands in the copper and cobalt derivatives [6] has shown the presence of sulphur atoms as ligands for the two metals. By considering the near infrared region of the absorption spectrum a clear classification of several anion derivatives of cobalt bovine carbonic anhydrase has been done [8]. A weak molar absorbance in the visible region usually lower than 200 mol^{-1} cm^{-1} and a very weak band in the 12,000 - 14,000 cm^{-1} range seems, in fact, diagnostic for a pentacoordinate geometry, whilst the tetrahedral geometry is characterized by a higher molar absorbance in the visible region and a band at lower energy in the near infrared. With the same considerations, a tetrahedral symmetry has been assigned to cobalt metallothionein [9] and cobalt tyrosinase [10] having a band at 8,100 cm^{-1} and at 8,470 and 10,040 cm^{-1} respectively, which are too low in energy for a pentacoordinate chromophore. In the latter derivative, the ligands are probably nitrogen atoms whilst in the first one sulphurs, and the bands in the visible region of the tyrosinase derivative are at higher energy with respect to those of the metallothionein. This is in agreement with the idea that the ^4F-^4P transition strongly depends on nephelauxetic effects [11], whilst an increase in the coordination number leads to an increase in energy in the ^4F-^4F transitions and, therefore, to an increase in the energy of the highest of them [12]. No analysis of

the near infrared region has been done in the case of Co(II) rubredoxin [13] and the two Co(II) derivatives of alcohol dehydrogenase [14] but from the data of the X-ray analysis of the native enzyme [15] and from a comparison with a low molecular weight model compound [16], a tetrahedral structure can be assigned. The study of inorganic model compounds has made a big contribution to the understanding of the Co(II) properties and, in fact, electronic absorption spectroscopy is now one of the most useful diagnostic tools to obtain information on the symmetry of this metal.

Information on the properties of the Co(II) ions has also been derived from the study of its M.C.D. spectra. This technique involves the measurement, as a function of frequency, of the difference induced in the absorption coefficient for left and right circularly polarized light by a longitudinal magnetic field. A classification of the M.C.D. spectra of Co(II) depending on its coordination geometry has been done by Vallee based on studies on simple Co(II) model complexes [17,18]. The octahedral complexes have been characterized by a pronounced negative band at 20,000 cm^{-1}, the tetrahedral complexes by a negative band at lower energy and one or two smaller positive bands at higher energy, and the pentacoordinate complexes by two negative bands in the 16,000 - 20,000 cm^{-1} range. A qualitative comparison of several Co(II) metalloenzymes has been done on the basis of this classification [18]. A tetrahedral symmetry has been assigned to Co(II) thermolysin and Co(II) carboxypeptidase [18,19], whilst a change from a tetrahedral to a pentacoordinate structure has been suggested for the Co(II) carbonic anhydrase on passing from acid to alkaline pH [20]. Previous M.C.D. work [21] on the active alkaline form of the Co(II) BCA and some of its anion complexes suggested an almost tetrahedral geometry for the anion derivatives

and a trigonally distorted tetrahedron for the alkaline form. Comparison of the M.C.D. spectra of the cobalt derivative of SOD [22], where the cobalt has been replaced in the native zinc, with that of the CN^- derivative of BCA suggested a tetrahedral geometry for both chromophores. Most of the analysis of the M.C.D. spectra of cobalt metalloproteins has only taken into account the visible part of the spectrum, and the lack of the spectrum of the near infrared region can result in misleading interpretations about the geometry of the metal site..

Some E.P.R. studies on the Co(II) ion in metalloenzymes have been done. Whilst the theory and the interpretation of the Co(II) low spin E.P.R. spectra is well developed [23], the situation is more complicated in the high spin case. Owing to rapid electron spin relaxation, satisfactory measurements on high spin Co(II) require temperatures below about 30 K, which in the past has impeded experimentation on molecular species in frozen solution. Moreover, the E.P.R. spectra of high spin Co(II) compounds are difficult to interpretate owing to the complexity of theory. The first report on the E.P.R. of Co(II) high spin in metalloenzymes was given by Grell and Bray [24] on some derivative of carbonic anhydrase. Since then several papers have appeared but no interpretation of the spectra has been given and always a qualitative discussion was done [25,26,27]. The most complete paper is probably that regarding some sulphonamide derivatives of cobalt carbonic anhydrase [28] where the authors calculated the effective g-values and δ, the value of the zero-field splitting. More information comes from the study of low molecular weight compounds of known structure [29,30]. A relatively recent work [31] has described a method, based on the expansion to third order of the exact eigen-value formulas, to calculate the effective g-values. Much further work is needed to identify in detail the geometry

of the Co(II) by E.P.R. spectroscopy because low symmetry components play a major rôle in determining the resonance fields.

REFERENCES

1. B. L. Vallee and R. J. P. Williams, Proc. Nat. Acad. Sci. USA 59, 498 (1968).

2. B. L. Vallee, J. A. Rupley, T. L. Coombs and H. Neurath, J. Am. Chem. Soc. 80, 4750 (1958).

3. J. E. Coleman, Biochemistry 4, 2644 (1965).

4. R. L. Carlin in "Transition Metal Chemistry" (ed. by R. L. Carlin) Vol. 1, p.1, Marcel Dekker Inc., New York (1965).

5. S. Lindskog, Structure and Bonding 8, 153 (1970).

6. D. R. McMillin, R. C. Rosenberg and H. B. Gray, Proc. Nat. Acad. Sci. USA 71, 4760 (1974).

7. E. I. Solomon, J. Rawlings, D. R. McMillin, P. J. Stephens and H. B. Gray, J. Am. Chem. Soc. 98, 8046 (1976).

8. I. Bertini, G. Canti, C. Luchinat and A. Scozzafava, J. Am. Chem. Soc. 100, 4873 (1978).

9. M. Vasak, J. Am. Chem. Soc. 80, 3953 (1980).

10. C. Ruegg and K. Lerch, Biochemistry 81, 1255 (1981).

11. R. Morassi, I. Bertini and L. Sacconi, Coord. Chem. Rev. 11, 343 (1973).

12. C. K. Jorgensen "Modern Aspect of Ligand Field Theory" North-Holland Publishing Company, Amsterdam (1971).

13. S. W. May and J. Y. Kuo, Biochemistry 78, 3333 (1978).

14. W. Maret, I. Andersson, H. Dietrich, H. Schneider Bernlohr, R. Einarsson and M. Zeppezauer, Eur. J. Biochem. 98, 501 (1979).

15. L. I. Branden, H. Jornvall, H. Eklund and B. Furugren in "The Enzymes" (ed. by P. D. Boyer) 3rd. edn., Vol. 2, p.103, Academic Press, New York/London (1975).

16. P. W. Lane, J. A. Ibers, R. B. Frankel, G. L. Papaefthymiou and R. H. Holm, J. Am. Chem. Soc. 99, 84 (1977).

17. T. A. Kaden, B. Holmquist and B. L. Vallee, Inorg. Chem. 13, 2585 (1974).

18. B. L. Vallee and B. Holmquist in "Methods for Determining Metal Ion Environments in Proteins" (ed. by D. W. Darnall and R. G. Wilkins), Elsevier North Holland, Inc., New York, p.27 (1980).

19. B. Holmquist, T. A. Kaden and B. L. Vallee, Biochemistry 14, 1454 (1975).

20. B. Holmquist, Biochemistry 16, 4591 (1977).

21. J. E. Coleman and P. V. Coleman, J. Biol. Chem. 247, 4718 (1972).

22. G. Rotilio, L. Calabrese and J. E. Coleman, J. Biol. Chem. 248, 3855 (1973).

23. B. R. McGarvey, Can. J. Chem. 53, 2498 (1975).

24. E. Grell and R. C. Bray, Biochim. Biophys. Acta 236, 503 (1971).

25. F. S. Kennedy, H. A. O. Hill, T. A. Kaden and B. L. Vallee, Biochem. Biophys. Res. Comm. 48, 1533 (1972).

26. P. H. Haffner and J. E. Coleman, J. Biol. Chem. 250, 996 (1975).

27. A. J. Sytkowski and B. L. Vallee, Biochem. 17, 2850 (1978).

28. S. A. Cockle, S. Lindskog and E. Grell, Biochemistry J. 143, 703 (1974).

29. G. E. Shankle, J. N. McElearney, R. W. Scwartz, A. R. Kampf and R. L. Carlin, J. Chem. Phys. 56, 3750 (1972).

30. V. K. Voronkova, M. M. Zaripov, Y. V. Yablokov, A. V. Ablov and M. A. Ablova, Dokl. Akad. Nauk. SSSR 214, 831 (1971).

31. J. R. Pilbrow, J. Magn. Res. 31, 479 (1978).

CHAPTER 4

EXPERIMENTAL STUDIES ON THE Co(II) DERIVATIVES OF SUPEROXIDE DISMUTASE

A. The Cobalt in the place of the Zinc: Optical and Magnetic Susceptibility Studies

It has already been shown that in the [Co(II)-Cu(II)]SOD derivative, the cobalt chromophore is characterized by a visible absorption with a maximum at 600 nm. and it is E.P.R. silent because of the magnetic coupling occurring between the two metal systems [1,2]. When the copper is either reduced [2] or removed [3] the E.P.R. signal of the cobalt is observed and its optical spectrum exhibits a shift toward a shorter wavelength. From the axial E.P.R. spectrum (Fig. 4.1) which lacks hyperfine structure, and from the molar absorbance $\varepsilon = 450$ mol^{-1} cm^{-1} at 600 nm., a tetrahedral chromophore was suggested for the cobalt site [2]. No careful analysis of the optical spectrum has been done and no attention has been paid to the near infrared region of the spectrum. The optical spectra in the range 350-1150 nm. was measured and is given in Fig. 4.2a and b and a band with $\varepsilon = 90$ mol^{-1} cm^{-1} was clearly resolved at 1000 nm. This band was in agreement with that found in $[Co(benzimidazole)_4](ClO_4)_2$ $\varepsilon_{1110} = 60$ [4], in the CN^- cobalt carbonic anhydrase (a derivative often taken as model for tetrahedral coordination), $\varepsilon_{980} = 110$ [5], and other tetrahedral cobalt compounds [6]. The earlier suggestion [1,2] of tetrahedral geometry for the [Co-...]SOD was thus confirmed. In this geometry, there are three bands that generally occur: the ν_1 an ^4F-^4F transition that occurs in the 3,000-6,000 cm^{-1} region and which is infrequently observed, the ν_2 an ^4F-^4F transition that occurs in the near infrared, and the ν_3 an intense ^4F-^4P transition that occurs in the visible region. In our case (see Fig. 4.2a) the ν_3 band is split into three components whose energy difference (1000 and 850 cm^{-1}) is too large to arise only from the spin-orbit coupling, and it may then reflect some distortions from tetrahedral symmetry. The axial E.P.R. spectrum shown

FIG. 4.1 X-Band E.P.R. spectrum of [Co- •••]SOD. Temperature 15 K, power 15 mW, modulation 10 G (from ref. 2).

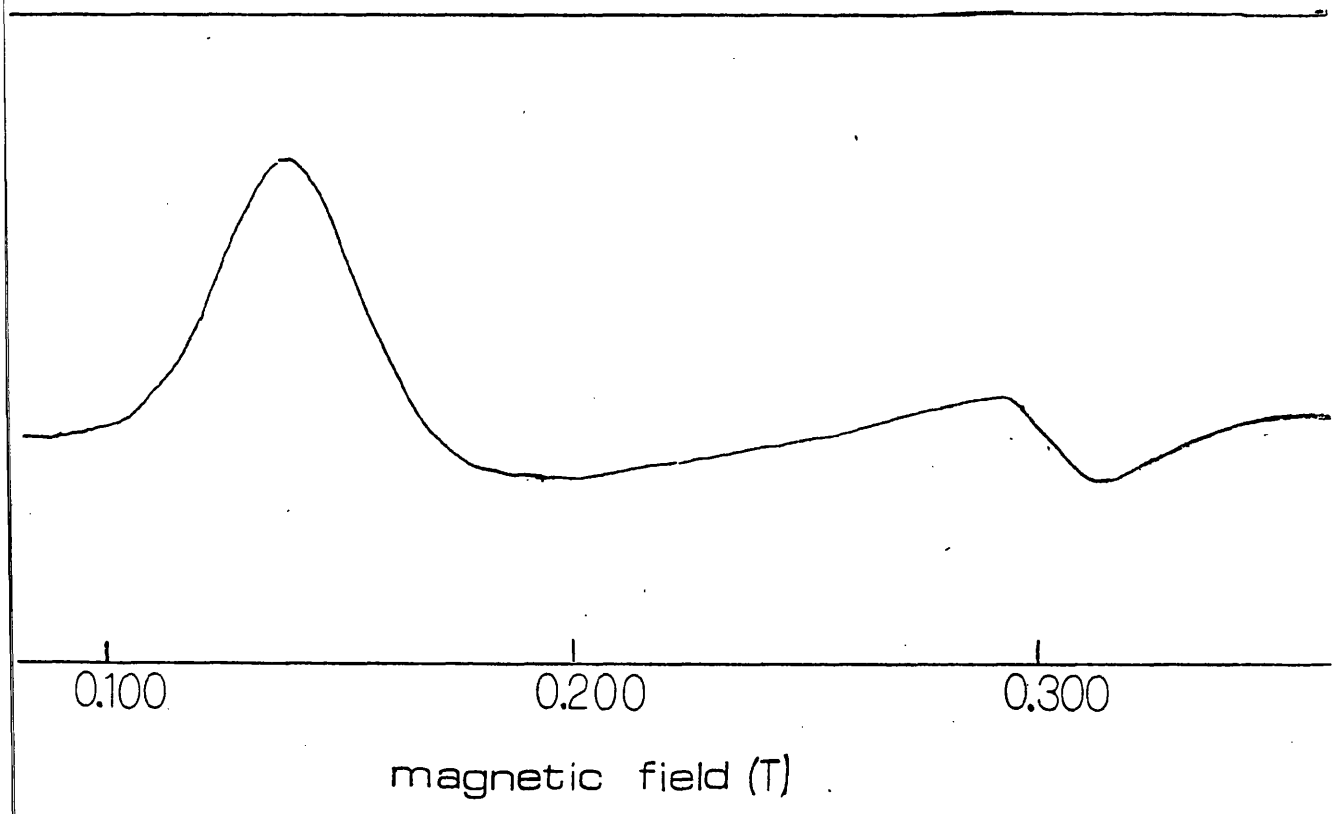

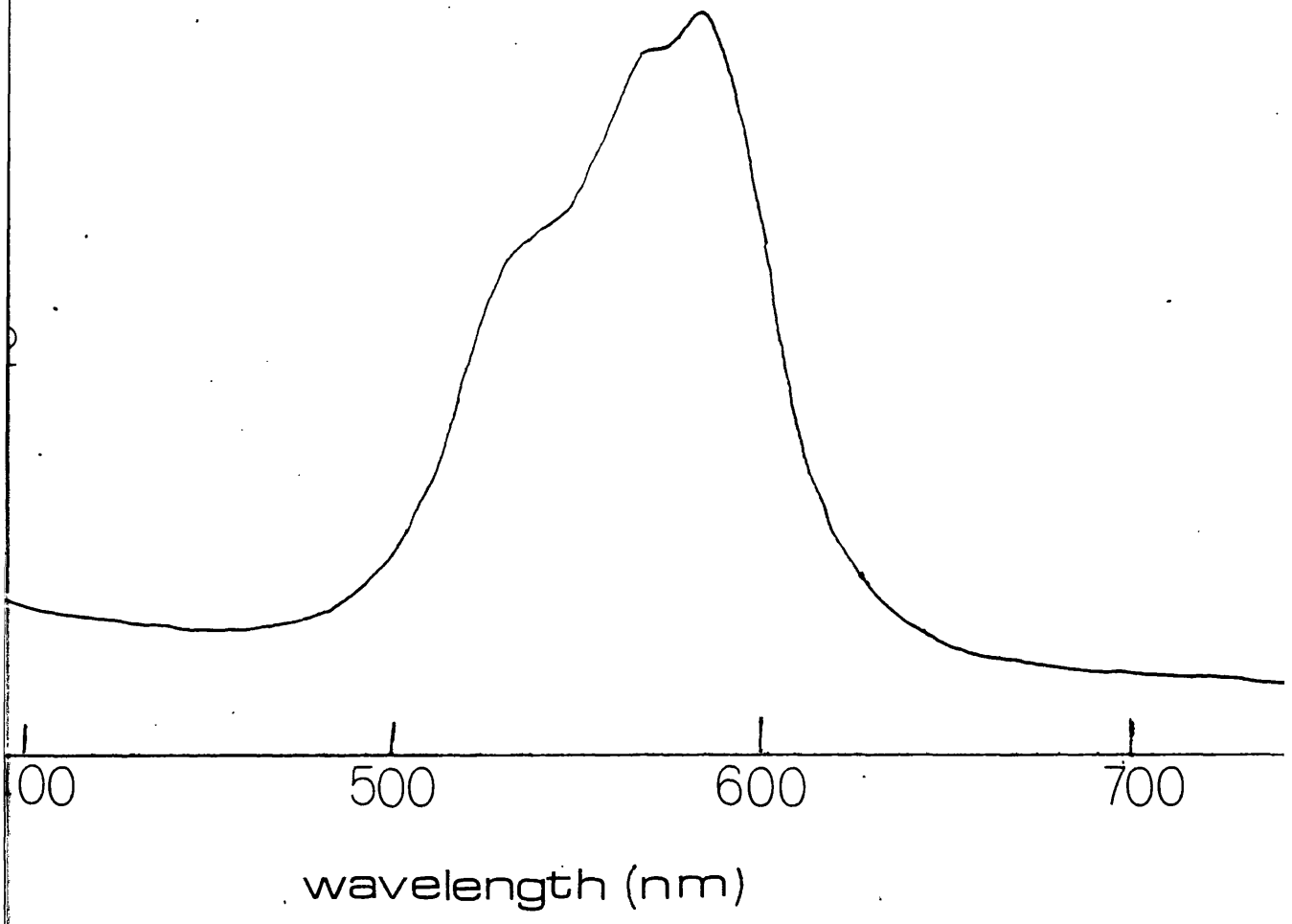

FIG. 4.2a Visible spectrum of the [Co- •••]SOD.

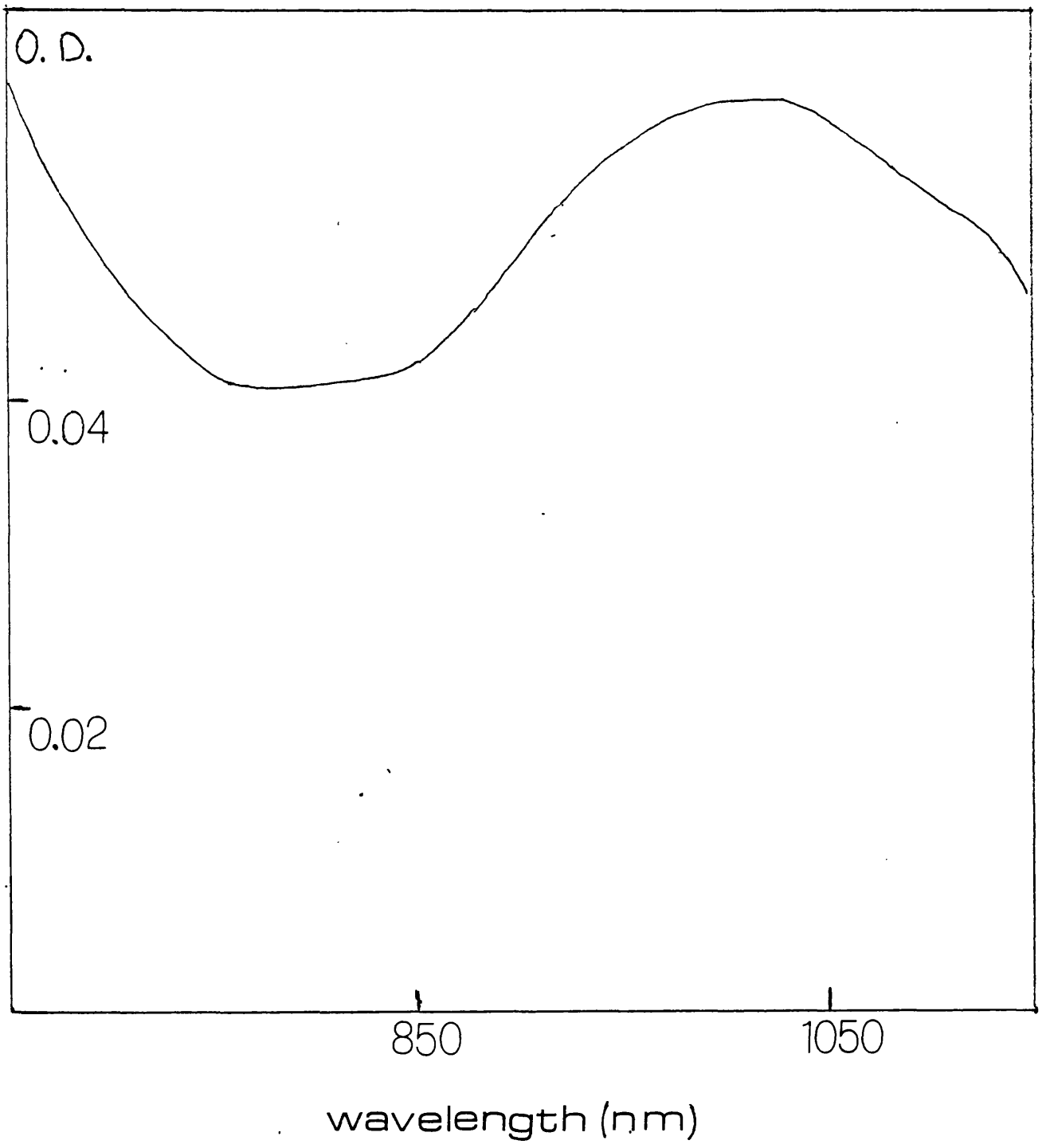

FIG. 4.2b Near infrared spectrum of the [Co- •••]SOD.
Cobalt concentration 6.5×10^{-4} M.

by the Co(II) indicates that the degree of the distortion is quite small. To have an idea of the ligand field strength around the metal, the parameter Δt, assuming a T_d microsymmetry and neglecting the spin-orbit coupling, was evaluated from

$$\Delta t^2 - 0.529\ (\nu_2 + \nu_3)\ \Delta t + 0.294\ \nu_2\ \nu_3 = 0 \qquad \ldots\ (4.1)$$

Taking $\nu_3 = 17{,}900\ cm^{-1}$, the average value of the three resolved components, and $\nu_2 = 10{,}000\ cm^{-1}$, a value of $\Delta t = 6{,}000\ cm^{-1}$ was obtained, indicating a strong ligand field around the metal. The evaluated Δt value is probably not very accurate because some other, unobserved, components may exist at lower energy so decreasing the effective value of ν_2 used in equation 4.1. Since model compounds having nitrogen ligands, mostly imidazole or benzimidazole groups, exhibit ligand fields above $5{,}000\ cm^{-1}$ [7], the Δt value of [Co(II) -...]SOD strongly supports the presence of coordinated nitrogens as found by X-ray crystallographic analysis around the native zinc site of superoxide dismutase [8]. No analysis of the near infrared spectrum was attempted in the [Co(II)-Cu(II)]SOD derivative due to the presence of the bands of the copper that obscure the cobalt absorption. In any case from the slight shift of the visible region toward lower energy of [Co(II)-Cu(II)]SOD relative to [Co(II) -...]SOD a similar geometry with a slightly decreased ligand field is suggested. In this derivative the cobalt ion has no E.P.R. signal due to its magnetic interaction with the copper ion [2].

In a magnetic susceptibility work [9] over a very narrow temperature range (4-20 K) and on a sample containing approximately 30% uncoupled Co(II) and about 50% of Cu(II) as Cu(II)-Cu(II) pair, only a lower limit for the coupling constant J of $5\ cm^{-1}$ was indicated. Measurements of the water proton relaxation time on a better characterised sample has suggested that the coupling between the Co(II) and Cu(II) system is still

present at room temperature [10]. The best method for obtaining information on the type and the strength of the magnetic interaction between the two metal ions is to measure the magnetic susceptibility over as large a temperature range as possible. In fact, for an antiferromagnetically-coupled dimer the variation of the susceptibility with temperature will not follow the Curie law $\left(\chi \propto \frac{1}{T}\right)$ for paramagnetism, but will exhibit a maximum at a position dependent on the strength of the coupling. The magnetic susceptibility was measured using an oscillating sample superconducting magnetometer [11], whose characteristics have been described in Chapter 2 of this thesis. The high sensitivity of this instrument allows changes in volume susceptibility as small as 0.3% of the diamagnetism of water, i.e. 2×10^{-9} c.g.s. to be resolved. Measurements of the volume susceptibilities of three different preparations of the [Co(II)-Cu(II)]SOD sample were carried out always with identical results in the temperature range 30-210 K.

All the samples were prepared by exchange dialysis as explained in Chapter 2. Samples prepared by this method are only able to remove 50% of the total zinc present in the native enzyme, so that the protein after the dialysis is a mixture of 50% of [Co(II)-Cu(II)] and 50% of [Zn(II)-Cu(II)] pairs. For each sample the concentration of the cobalt and the copper atoms were measured by atomic absorption and the concentration of the E.P.R. detectable copper was measured by comparing the double integration of the E.P.R. signal, recorded under non-saturating conditions, against a Cu-EDTA standard. A small part of the total cobalt exchanged, usually less than 10%, does not go to the zinc site but it binds the protein in some other place. E.P.R. spectra at liquid helium temperature showed a weak signal due to this spurious cobalt but a quantification of its amount by double integration of the signal was not

attempted as poor results are generally obtained for metal ions possessing a zero-field splitting. It was preferred to compare the intensity of the Co(II) signal with that obtained after reduction of copper with ferrocyanide. The concentration of one sample used for the magnetic susceptibility measurements is reported in Table 4.1.

TABLE 4.1

Concentrations of the copper and cobalt atoms in the [Co(II)-Cu(II)]SOD sample used for the susceptibility measurements

Method	Cu (molarity)	Co (molarity)
Atomic Absorption	6.1×10^{-3}	3.4×10^{-3}
E.P.R.	3.0×10^{-3} (a)	0.3×10^{-3} (b)

(a) obtained by double integration of the E.P.R. signal

(b) obtained by comparison of the Co(II) signal before and after reduction of Cu(II) by ferrocyanide

As seen from the Table, the sample contained 6.1×10^{-3} M copper and 3.4×10^{-3} M cobalt as evaluated from atomic absorption; moreover, from the comparison of Co(II) E.P.R. signal before and after the reduction of copper with ferrocyanide it seems that 0.3×10^{-3} M Co(II) is not coupled to the copper and, in fact, the E.P.R. detectable copper of the same sample corresponded to a concentration of 3.0×10^{-3} M.

The volume susceptibility data of this sample χ_{cc} at different temperatures is plotted in Fig. 4.3 where the paramagnetism is observed as a decrease relative to the diamagnetism of the apo-protein. The intersection of the extrapolated low temperature line with the Y axis gives

FIG. 4.3 Temperature dependence of the volume susceptibility of [Co(II)-Cu(II)] bovine superoxide dismutase. The dashed line is for the apo-protein.

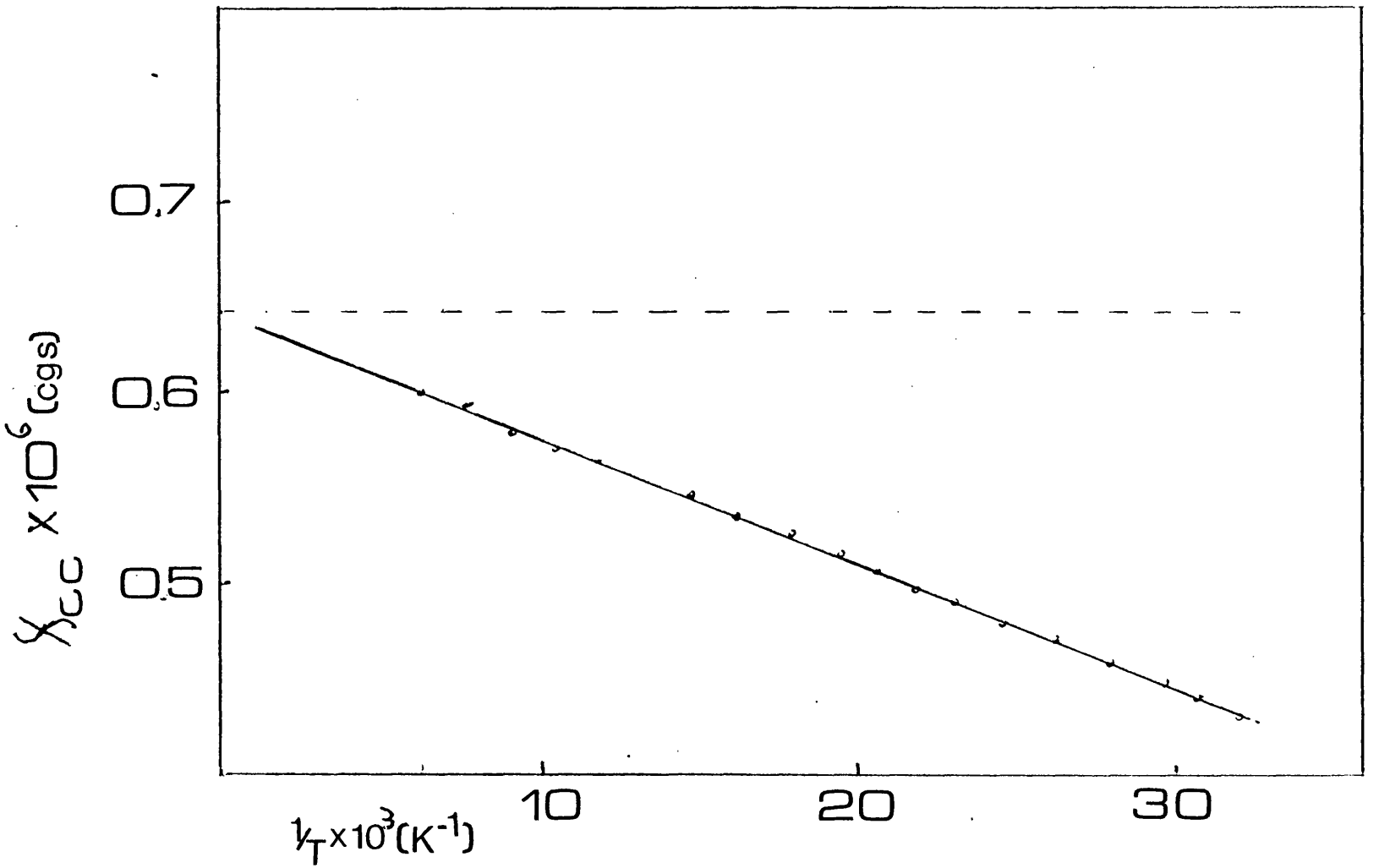

$\chi_{cc} = 0.64 \times 10^{-6}$ c.g.s. which is close to the volume susceptibility of water ($\simeq 0.68 \times 10^{-6}$ c.g.s. at 223 K). Within the accuracy of the data of Fig. 4.3 the line shows a simple linear behaviour with respect to the reciprocal temperature and the slope of the best fit line is

$$\frac{d\chi_{cc}}{dT^{-1}} = 6.0 \times 10^{-6} \text{ c.g.s. K}$$

A previous work [9] carried out in a very small temperature range 1.4-4 K gave a much lower value indicating that the system is fully coupled in that temperature region. Using the relation

$$\frac{d\chi_{cc}}{dT^{-1}} = \frac{N}{3k} \Sigma_i n_i \mu_i^2 \qquad \ldots\ (4.2)$$

where N is the Avogadro constant, k is the Boltzmann constant, n_i is the number of moles of the ith. metal and μ_i its magnetic moment, it is possible to deduce the way the two metals are coupled. If the spin system is completely uncoupled the different contributions would be that shown in Table 4.2.

TABLE 4.2

Values of μ^2 expected for the completely uncoupled system

System	Molarity	μ^2
Cu^2	6.0×10^{-3}	3.6
Co^2	3.3×10^{-3}	15.0
O_2	0.3×10^{-3}	8.0

In the Table, the magnetic moment is given for each of the components of the solution if no couplings or interactions are present at the concentrations used. The value for O_2 is for the concentration of oxygen

dissolved in the solution. Substituting the values in Table 4.2 in the equation 4.2 gives:

$$\frac{d\chi_{cc}}{dT^{-1}} = 9.2 \times 10^{-6} \text{ c.g.s. K}$$

a value much greater than the experimental one even substituting the minimum value (spin only value $\mu_B = 3.88$) for the μ_{eff} of high spin Co(II). The possibility of observing a totally uncoupled spin system must then be excluded. Another possibility is that both the zero-field splitting δ and the coupling constant 2J are of the same order of magnitude $\simeq 15$ cm^{-1}. In this case the contributions to the system are given in Table 4.3.

TABLE 4.3

Values of μ^2 expected for the system having $2J \simeq 15$ cm^{-1} and $\delta \simeq 15$ cm^{-1}

System	Molarity	μ^2
Cu^{2+}-Zn^{2+} pair	3.0×10^{-3}	3.6
Free Co^{2+}	0.3×10^{-3}	20.2
Dissolved O_2	0.3×10^{-3}	8.0
Cu^{2+}-Co^{2+} (S = 1) case 1	3.0×10^{-3}	8.0
Cu^{2+}-Co^{2+} (S = 1) case 2	3.0×10^{-3}	8.0

In this situation a contribution from 3.0×10^{-3} M uncoupled copper (effectively Cu^{2+}-Zn^{2+} pairs), 0.3×10^{-3} M uncoupled free cobalt with a $\mu = 4.5$ as expected for tetrahedral symmetry [12], 0.3×10^{-3} M molecular oxygen dissolved in the solution, 3.0×10^{-3} M Co^{2+}-Cu^{2+} pair for which there are two external configurations of S = 1. In this latter case we consider that

one electron of the cobalt is coupled with the electron of copper to give an $S = 0$ and $S = 1$ state (case 1), the other two electrons of the cobalt being uncoupled, $S = 1$ (case 2). With the hypothesis that both the δ value and the 2J coupling constant have a magnitude $\simeq 15$ cm^{-1}, all the levels are approximately equally populated at 30 K so that every level gives its contribution. Substituting the values of Table 4.3 in the equation 4.2 gives:

$$\frac{d\chi_{cc}}{dT^{-1}} = 8.4 \times 10^{-6} \text{ c.g.s. K}$$

This value is again much greater with respect to the experimental one and so also this hypothesis must be excluded. The only two alternatives, which are in principle indistinguishable, are $2J \simeq 15$ cm^{-1} and $\delta \geqslant 600$ cm^{-1} or $2J \geqslant 600$ cm^{-1} and $\delta \simeq 15$ cm^{-1}. Their respective orbital configurations are given in Fig. 4.4 (a and b respectively). In both cases the paramagnetic contribution of the system is that given in Table 4.4.

TABLE 4.4

Values of μ^2 expected for the system having $2J \simeq 15$ cm^{-1} and $\delta \geqslant 600$ cm^{-1} or $2J \geqslant 600$ cm^{-1} and $\delta \simeq 15$ cm^{-1}

System	Molarity	μ^2
Cu^{2+}-Zn^{2+} pair	3.0×10^{-3}	3.6
Free Co^{2+}	0.3×10^{-3}	20.2
Dissolved O_2	0.3×10^{-3}	8.0
Co^{2+}-Cu^{2+} pair	3.0×10^{-3}	8.0

In the former situation ($2J \simeq 15$ cm^{-1}, $\delta \geqslant 600$ cm^{-1}) the contribution of the Co-Cu pair is due to the population of the $S = 1$ state resulting from

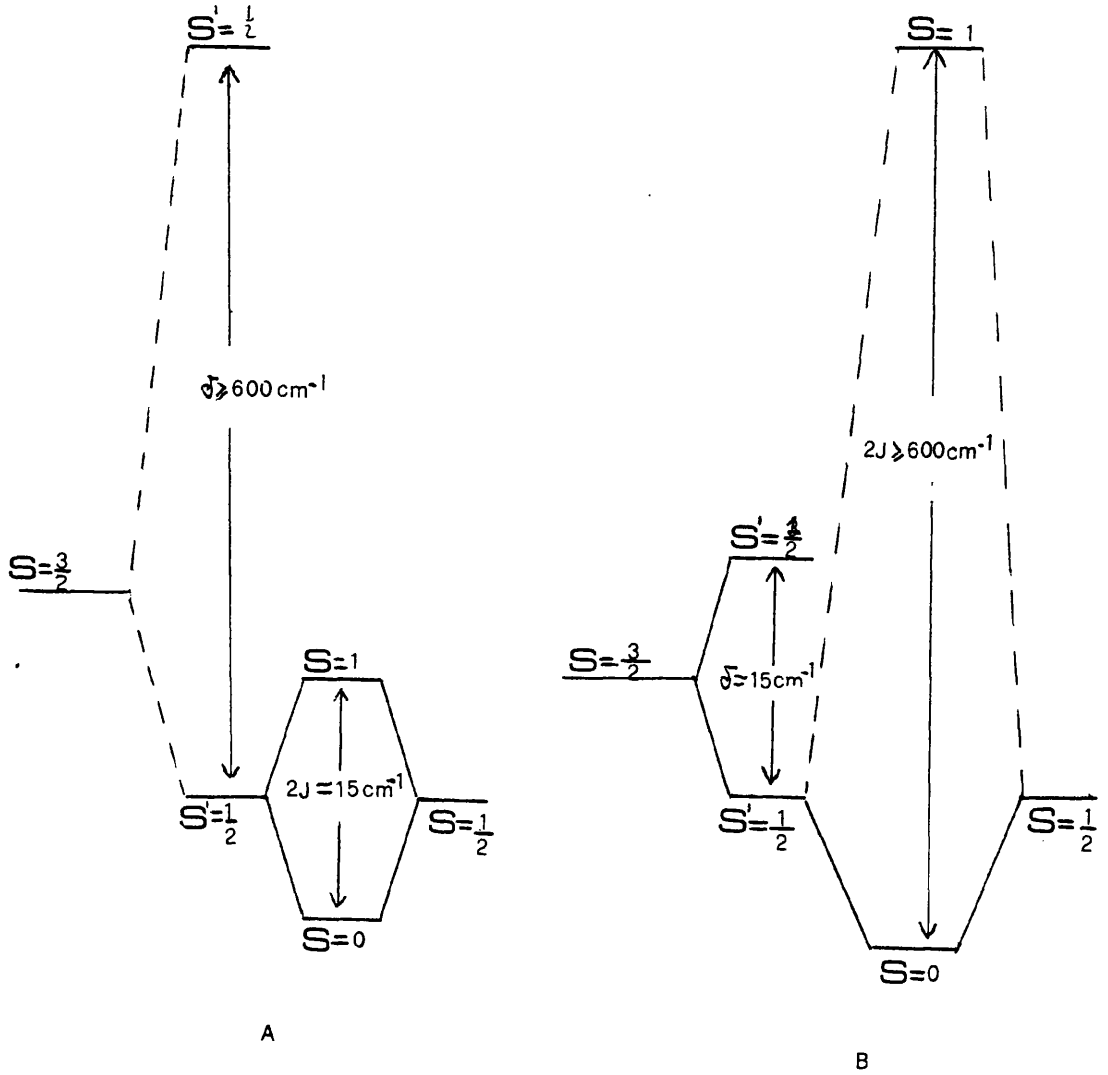

FIG. 4.4 Two possible magnetic interactions in [Co(II)-Cu(II)] superoxide dismutase based on the results presented in the text.

the interaction between the Co(II) lower doublet and Cu(II), while in the latter case ($2J \geqslant 600$ cm^{-1}, $\delta \simeq 15$ cm^{-1}) it involves the population of the higher doublet of the high spin Co(II). In both cases a value of the same

$$\frac{d\chi_{cc}}{dT^{-1}} = 6.4 \times 10^{-6} \text{ c.g.s. K}$$

order of magnitude as the experimental one is obtained. However, a value of $\delta \geqslant 100$ cm^{-1} is very unlikely as values of zero-field splitting constants have been reported for Co(II) in a variety of environments and range from -40 cm^{-1} to +80 cm^{-1} [13-15]. Moreover, in the case of reduced [Co(II)-Cu(I)]SOD $\delta = 23$ cm^{-1} has been estimated from E.P.R. measurements [2]. Therefore, $\delta \simeq 15$ cm^{-1}, that is very close to that observed for the [Co(II)-Cu(I)] protein [2], and a new lower limit for the coupling constant $2J \geqslant 600$ cm^{-1} appears to be much more likely.

There are now several examples of synthetic complexes which contain imidazole-bridged metal centres [16-18], but none of these have mixed metals. Until mixed-metal binuclear complexes with imidazolate bridge are synthesised it will be very difficult to understand the actual order of the molecular orbitals in the [Co(II)-Cu(II)]SOD system better than in the schematic diagram shown in Fig. 4.4.

B. An E.P.R. and Optical Study of the Properties of the Cobalt substituted in the Copper Site of Superoxide Dismutase

1. The binding of cobalt to the copper site: Results

Substitution of the cobalt into the zinc site of superoxide dismutase [1,19] has been very fruitful allowing a quite detailed study of the native zinc site [2,3,20] (see also the previous and the following part of this Chapter). This approach is in line with the well-known preference and fitting of cobalt(II) for four-coordinate, tetrahedrally distorted binding sites of proteins. In fact, this metal ion has been successfully substituted into the tetrahedral zinc site of carbonic anhydrase [21], carboxypeptidase [22], and alcohol dehydrogenase [23], the tetrahedral iron site of rubredoxin [24] or into the tetrahedral copper blue sites [25], but such substitution has never been attempted in a pentacoordinate native binding site. The copper site of superoxide dismutase is known to be pentacoordinate from X-ray crystallographic data [8], but it is also known to oscillate in its catalytic cycle between five and four coordination by losing a single ligand in the transition from Cu(II) to Cu(I) [26]. In view of this peculiar characteristic of the copper site, the feasibility of binding Co(II) to at least four of the original copper ligands of superoxide dismutase is an interesting object of study. Since addition of two equivalents of Co(II) to the apo-superoxide dismutase in 0.1 M acetate buffer (pH 5.4) gave rise to the [Co-•••] derivative [19], the same procedure was attempted with the copper-free protein. Addition of two equivalents of Co(II) to the copper-free protein in acetate buffer and incubation over 24 hours had no effect on the visible absorption spectrum. After dialysis against acetate buffer, only 0.1 equivalent Co(II)/mol protein were recovered. It was therefore conclusive that in 0.1 M acetate buffer (pH 5.4) the cobalt was

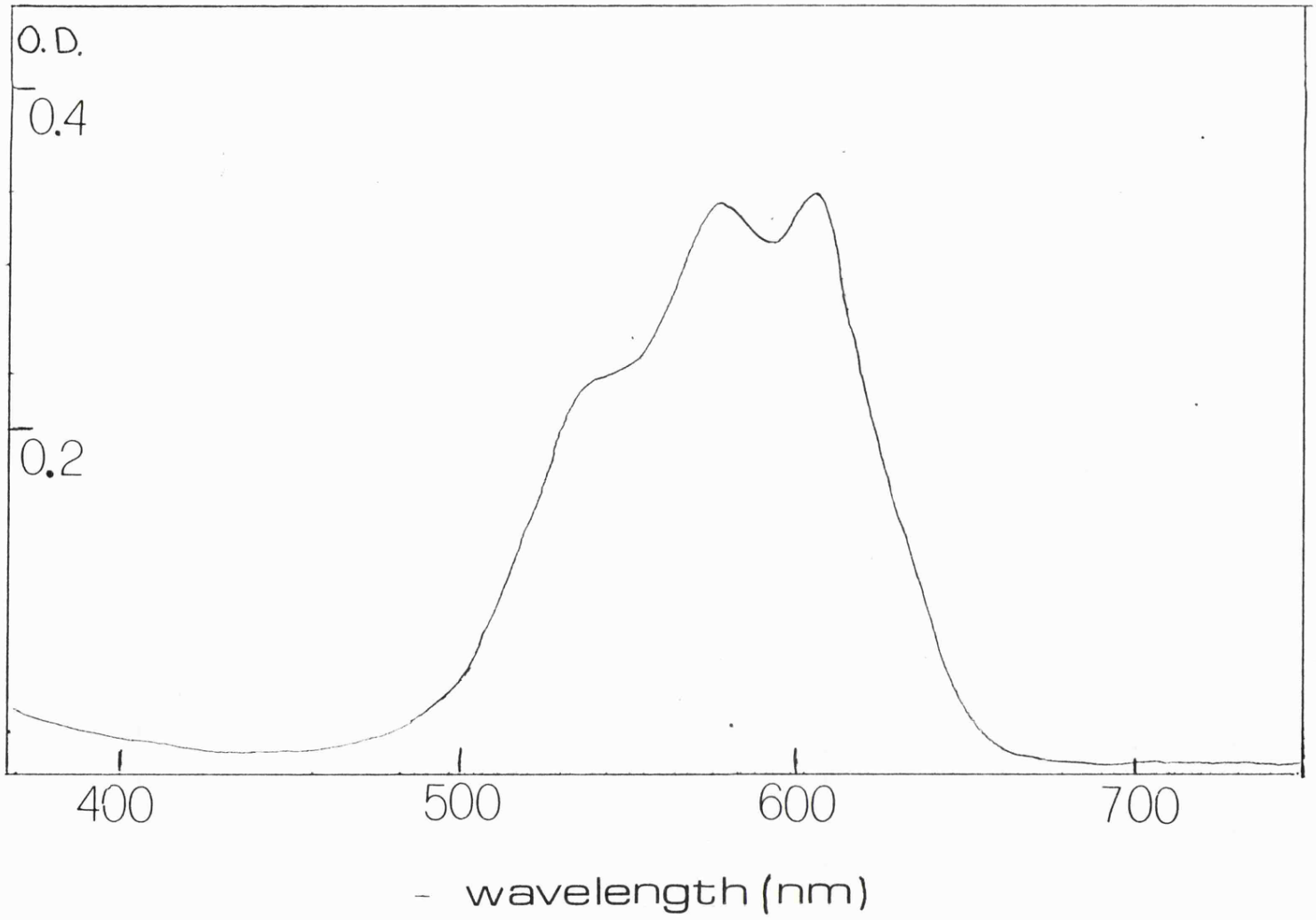

FIG. 4.5 Visible spectrum of the [Zn-Co]SOD in 0.1 M phosphate buffer; protein 0.57×10^{-3} M; Co(II) 1.04×10^{-3} M.

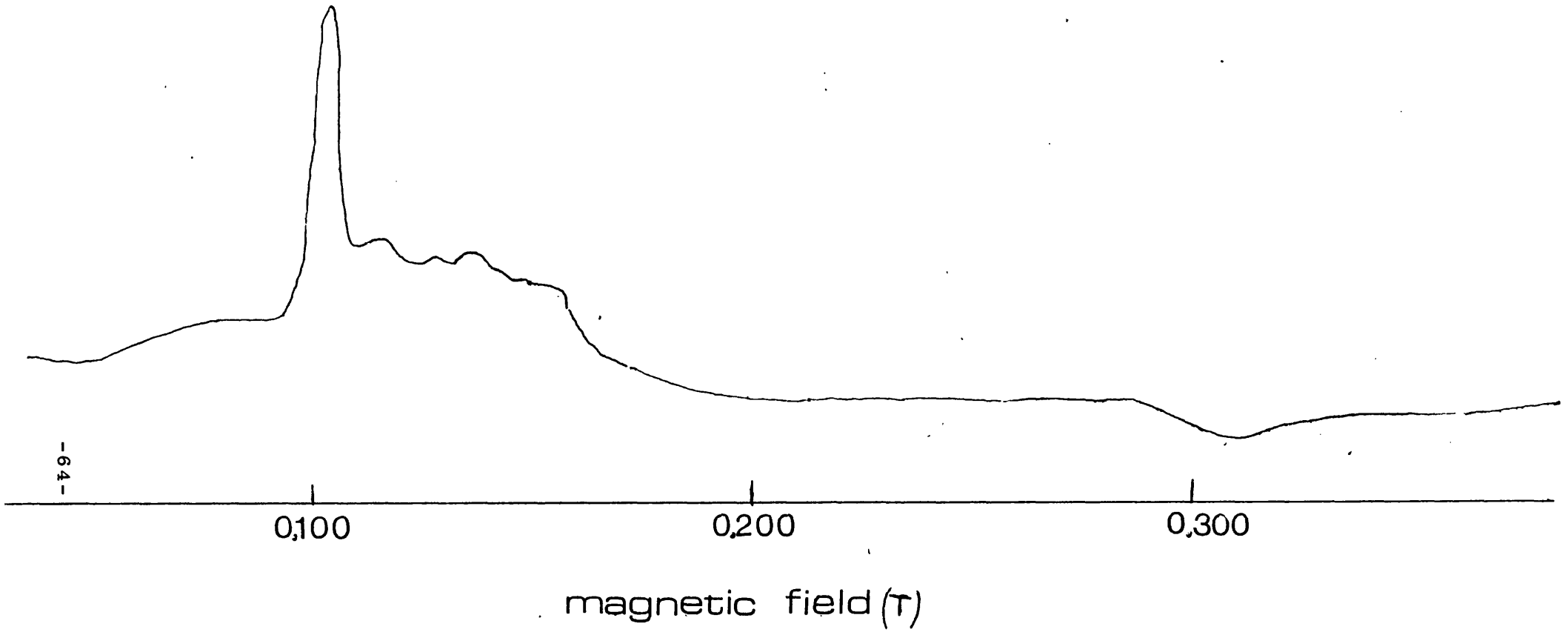

FIG. 4.6 X-Band E.P.R. spectrum of the [Zn-Co]SOD in 0.1 M phosphate buffer. Temperature 10 K; power 15 mW; modulation 10 G.

not able to bind the native copper site. A different behaviour was obtained by adding two cobalt(II) equivalents to the copper-free superoxide dismutase in 0.1 M phosphate buffer (pH 7.4) and incubating over 12 hours at room temperature. The bound cobalt was not removed by dialysis against 0.1 M phosphate buffer (pH 7.4) and gave rise to optical and E.P.R. spectra (Figs. 4.5 and 4.6 respectively) that were well distinct from those described for the cobalt at the zinc site [1,3,19]. The binding of the cobalt ion to the native copper site was also possible starting from the apo-proteins, in fact in 0.1 M phosphate buffer (pH 7.4) the apo-SOD binds $\simeq 4$ equivalents Co(II)/mol. protein. At a Co : protein ratios <2 the cobalt goes only into the zinc site as shown by the spectra in Fig. 4.7 (curves a and b) but when >2 equivalents Co(II) are added, a different line shape was obtained (Fig. 4.7, curve c). The difference optical spectrum (Fig. 4.7), shows that the species formed at higher Co : protein ratios has different absorption maxima indicating a new binding site that corresponds to that of the [Zn-Co] derivatives shown in Fig. 4.5. Spectra 4.7 (curves a and b) were recorded immediately after the metal addition, whilst curve c was recorded after 4 hours incubation at room temperature.

The same titration carried out in the E.P.R. spectrometer gave some interesting results. On addition of 0.5 : 1 Co(II)/protein, the axial E.P.R. high spin signal at $g \simeq 4$, typical of the cobalt bound at the zinc site [2,3], appeared (a in Fig. 4.8). Increasing the Co(II)/protein ratio up to 1 produced an increase in the signal without affecting the shape of the line (b in Fig. 4.8). On the other hand, when the ratio is >1, the signal centred at $g \simeq 4$ decreased and a broad line appeared at lower fields (c in Fig. 4.8). This behaviour suggests the presence of a magnetic interaction between the Co(II) ions in two different sites such

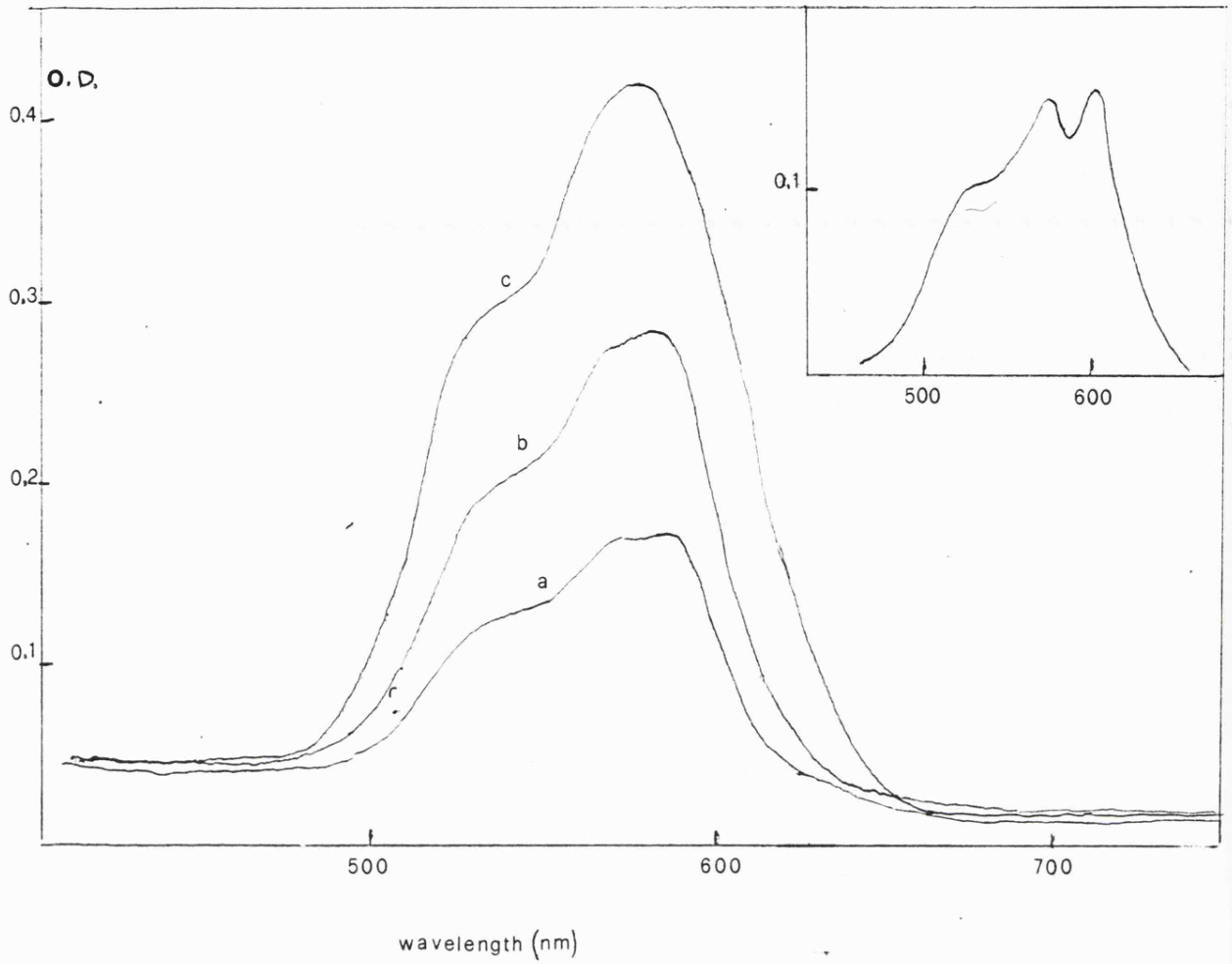

FIG. 4.7 Optical titration of 0.33×10^{-3} M apo-SOD in 0.1 M phosphate buffer (pH 7.4). Co(II):subunit ratios (a) 0.5, (b) 1, (c) 1.7. [Insert: calculated difference optical spectrum (spectrum c) minus spectrum (b).]

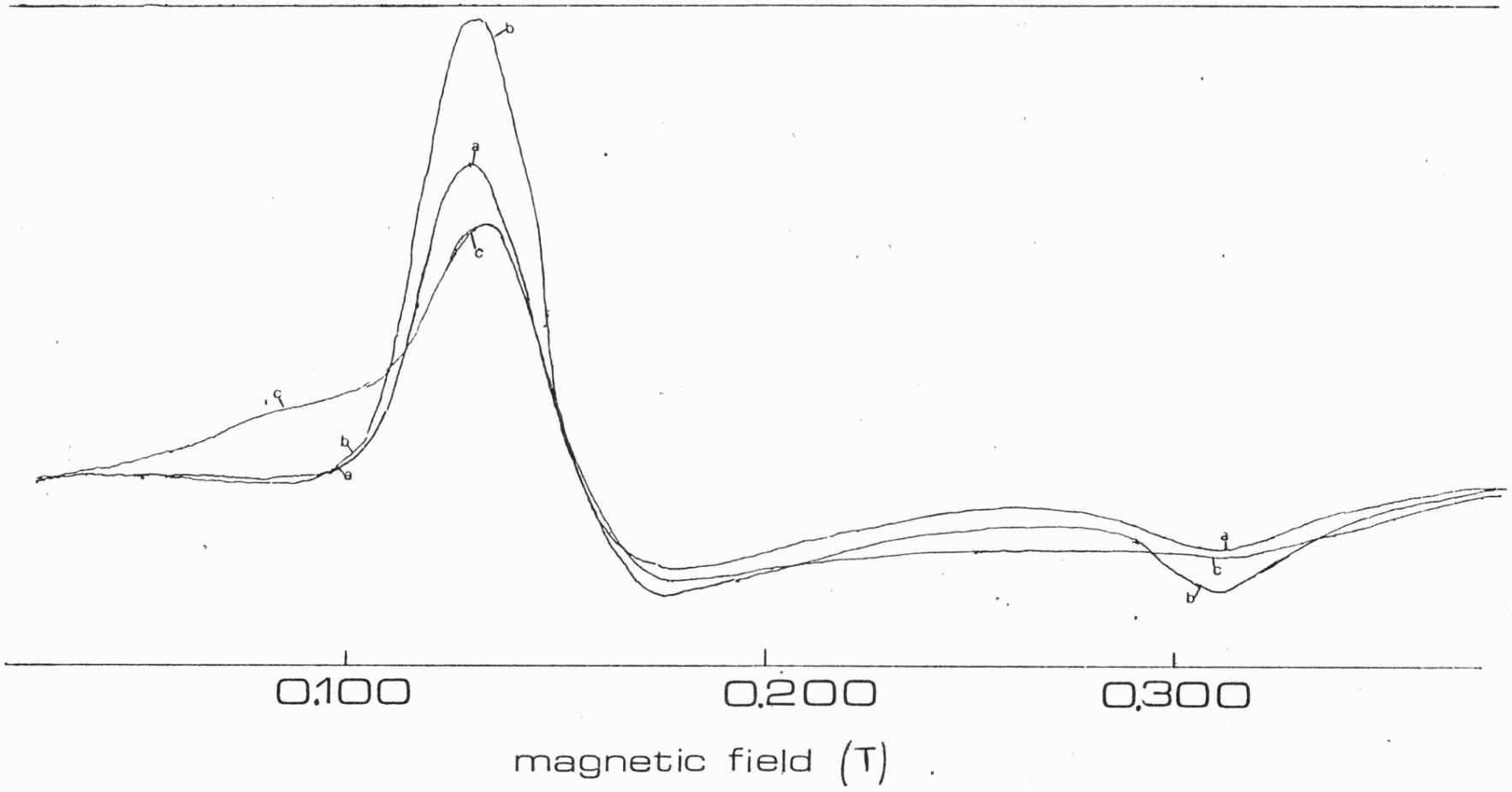

FIG. 4.8 E.P.R. titration of 0.33×10^{-3} M apo-SOD in 0.1 M phosphate buffer (pH 7.4). Co(II):protein ratios (a) 0.5, (b) 1, (c) 1.7. Temperature 10 K; power 10 mW; modulation 10 G.

as expected if the binding site occupied at Co(II) protein ratios >1 is that occupied by the copper in the native enzyme.

2. Dependence of phosphate on the symmetry of the cobalt chromophore in the vacant copper binding region of the protein: Results

The E.P.R. spectrum of the [Zn-Co] protein in 0.1 M phosphate buffer (pH 7.4), shown in Fig. 4.6, shows the presence of two different high spin cobalt signals, that are clearly resolved only at lower field. One of them displays a broad signal with poorly resolved hyperfine structure, of about 100 gauss splitting, centred at $g \simeq 6$. The other is characterized by a much sharper line at $g \simeq 6.9$. This behaviour suggests a temperature dependent equilibrium between two species as the room temperature optical spectrum seems characteristic of only one species. In fact, removal of phosphate by dialysis against water caused drastic changes in the E.P.R. and optical spectra as shown in Fig. 4.9 and Fig. 4.10 respectively. In particular in the E.P.R. spectrum the broad signal with $g \simeq 6$ and hyperfine structure was still present, although with some modifications, confirming that the heterogeneity observed in the spectrum of Fig. 4.6 was due to a mixture of two cobalt signals, that are likely to reflect different coordinations in the presence of water or phosphate. To test this hypothesis the titration of the [Zn-Co] protein in water with increasing amount of phosphate buffer (pH 7.4) was carried out. Fig. 4.11 shows this titration; two clear isosbestic points at 510 and 650 nm., reflecting the disappearance of two bands centred at 450 and 780 nm. going from the "water" to the "phosphate" form, was detected. A plot of the percentage change of the 450 and 780 nm. bands against increasing amount of phosphate buffer is reported in the insert of Fig. 4.11. The parallel trend of the two lines strongly suggests that both the 450 and 780 nm. bands belong to

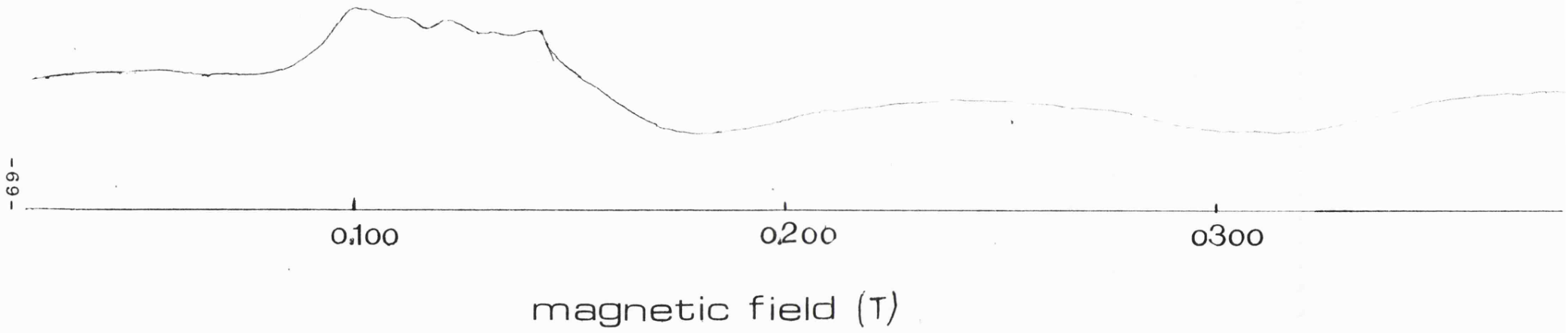

FIG. 4.9 X-Band E.P.R. spectrum of [Zn-Co]SOD in water. Temperature 10 K; power 10 mW; modulation 10 G.

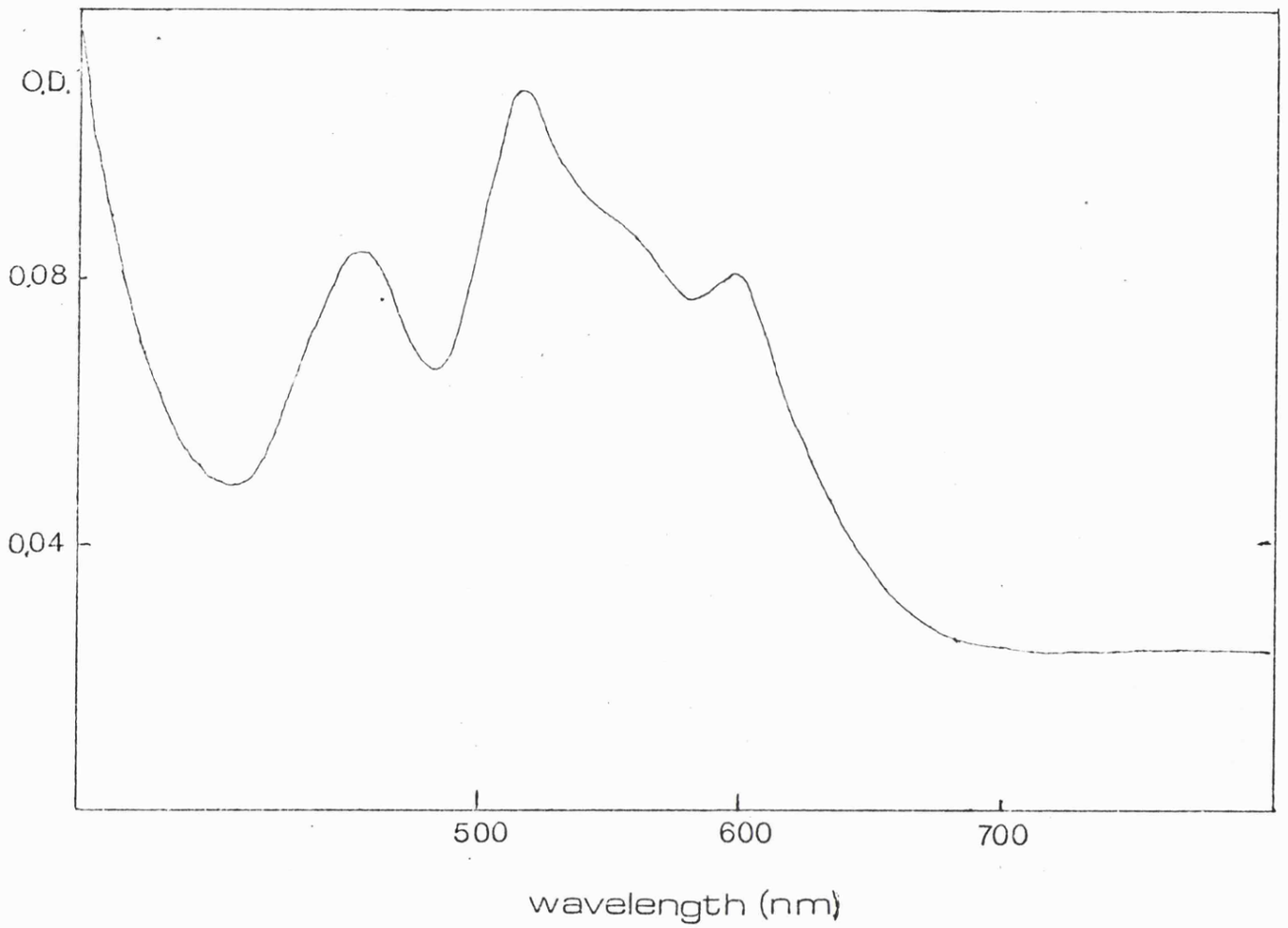

FIG. 4.10 Visible spectrum of [Zn-Co]SOD in Water. Cobalt concentration 1.2×10^{-3} M.

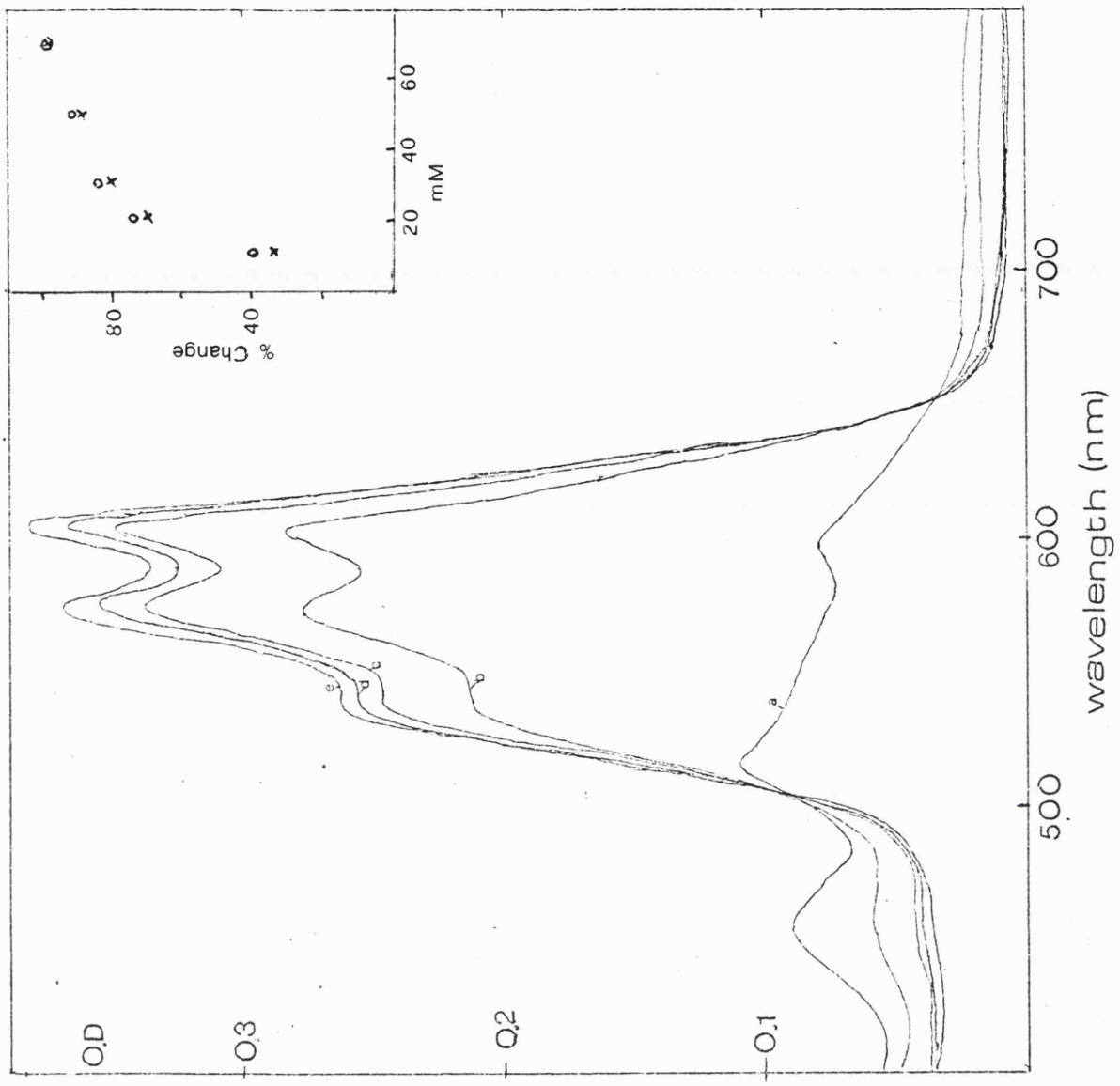

FIG. 4.11 Optical spectra of [Zn-Co]SOD in water as a function of phosphate buffer. In the insert is reported the percentage change of the 450 (x) and 780 (o) nm bands in respect to the phosphate buffer concentration.

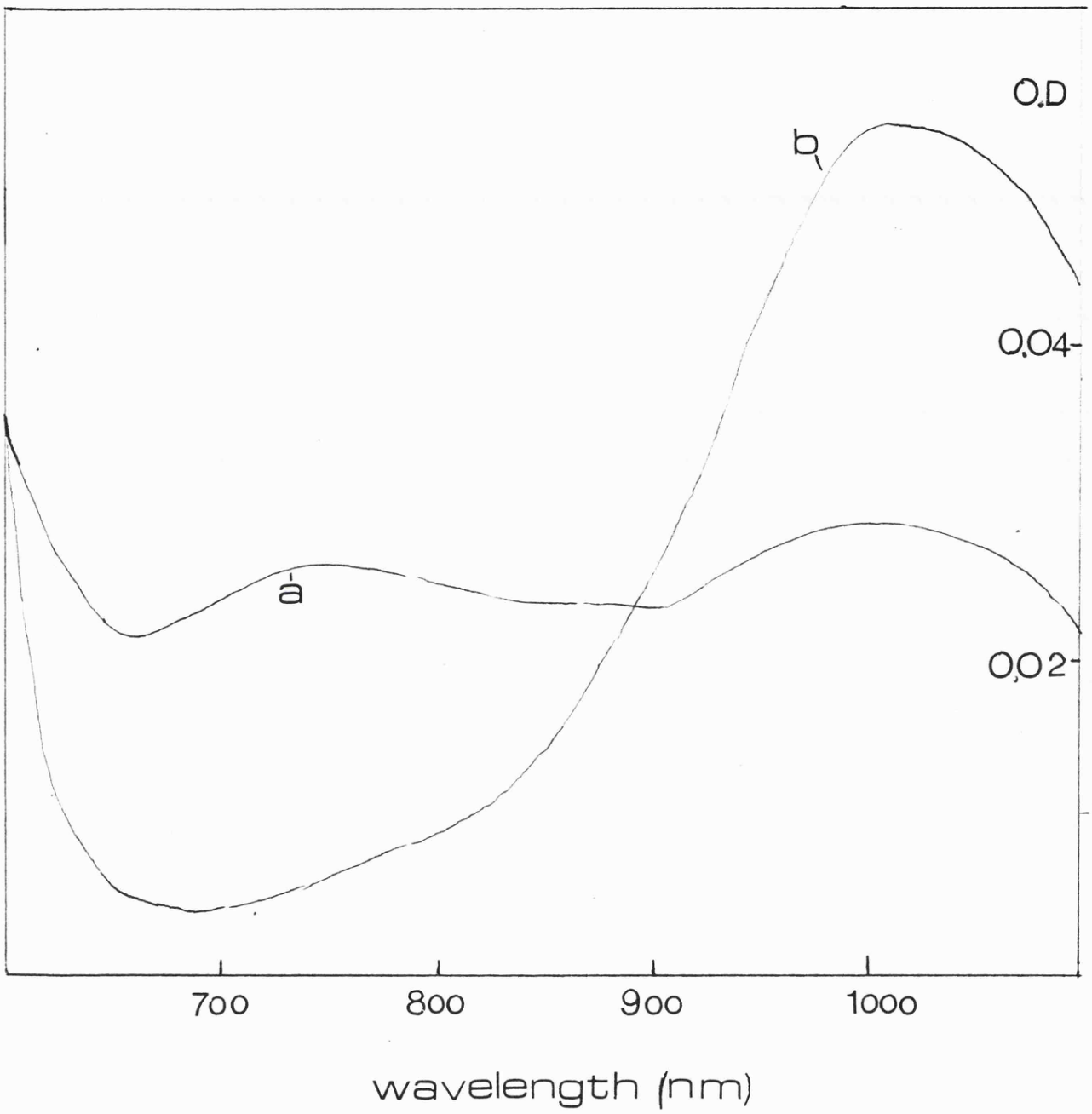

FIG. 4.12 Near infrared spectrum of [Zn-Co]SOD: Co(II) 1.4×10^{-3} M; (a) in water, (b) in 0.1 M phosphate buffer.

the "water" form. In Fig. 4.12 the near infrared region of the "water" (curve a) and "phosphate" (curve b) form is reported; curve b has a band at 1000 nm. $\varepsilon = 50\ mol^{-1}\ cm^{-1}$, which is less evident in the "water" form, characterized by a very weak band at 780 nm. The presence or the absence of phosphate is then able to induce a different coordination geometry on the cobalt site.

A spectroscopic change similar to that observed in Fig. 4.11 was obtained by titrating the [Zn-Co] protein in 0.1 M phosphate buffer by small aliquots of NaOH. This is reported in Fig. 4.13, which shows the disappearance of the spectrum typical of the "phosphate" form as pH is raised by one unit above pH 7.4, and that the process follows the simple titration of a single protonation equilibrium with apparent pK = 8.2 (see insert of Fig. 4.13). The effect was perfectly reversible as lowering the pH back to pH 7.4 immediately restored the spectrum of the "phosphate" form. To have some more information on the mechanism which controls the change of geometry of the cobalt environment, periodate was added to the [Zn-Co] protein. In fact, periodate is known to bind in the phosphate domain of phosphate-binding enzymes, such as 6-phosphogluconate dehydrogenase [27] by predominant interaction with basic side chains. This addition is shown in Fig. 4.14 where periodate is able to transform the "water" form into a transient "phosphate" form before the oxidative breakdown of the protein, suggesting that the cobalt can be affected by a binding of periodate to a nearby positively charged side chain.

3. Titration with CN^- and H_2O_2 of the [Zn-Co] and [Co-Co] protein: Results

It has already been shown [3] that in the [Co-Cu] or [Co-•••] derivatives addition of a large CN^- excess lead to detachment of cobalt from its site with the formation of $[Co(CN)_5]^{3-}$. No intermediate CN^-

FIG. 4.13 Optical spectra of [Zn-Co]SOD as a function of pH 0.6×10^{-3} M protein, 1.1×10^{-3} M Co(II), in 0.1 M phosphate buffer was titrated by small aliquots of NaOH. Curve (a) pH 7.4, (b) 8, (c) 8.6, (d) 9.6. In the insert is reported the percentage of disappearance of the 450 nm band as function of pH.

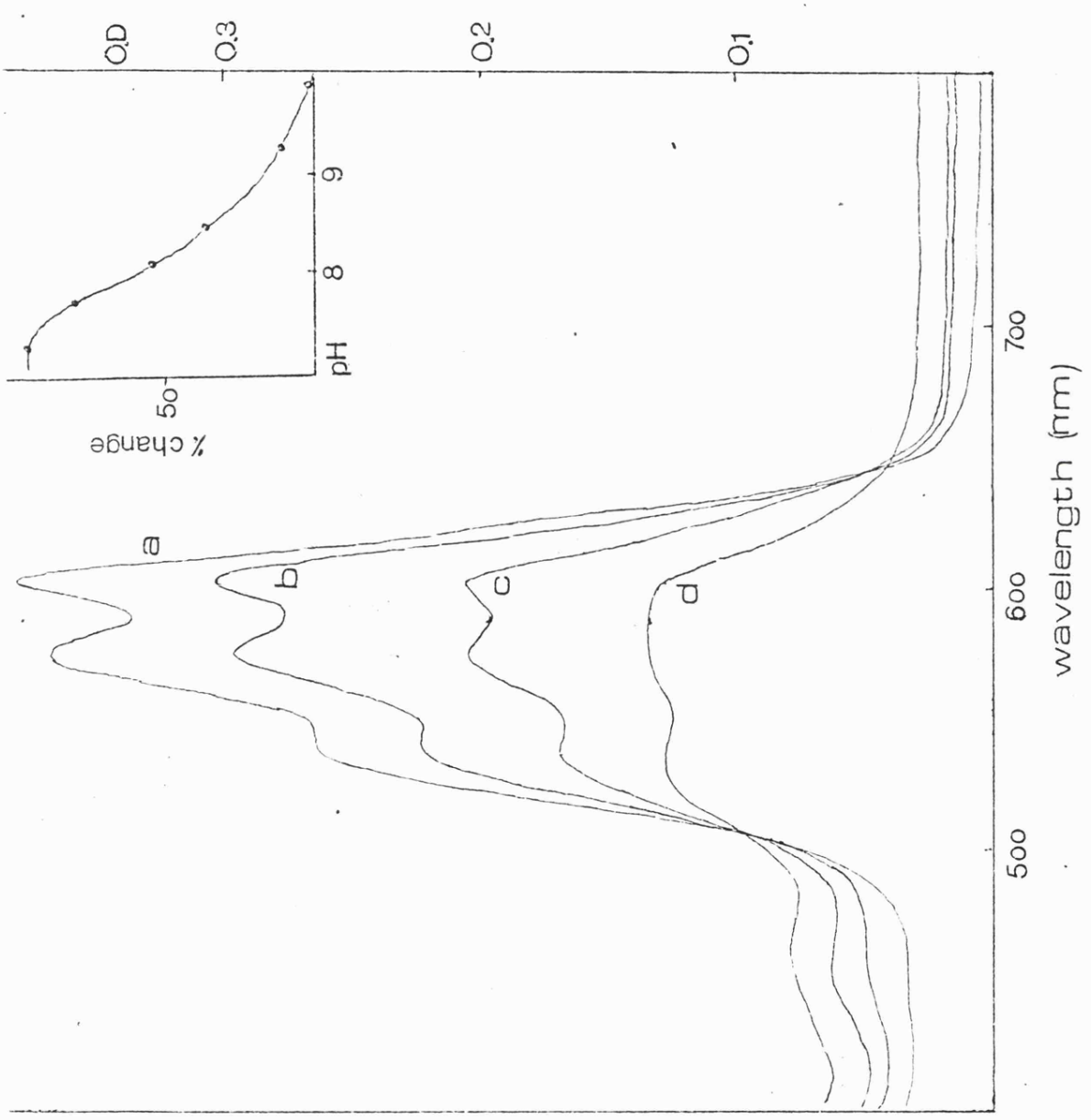

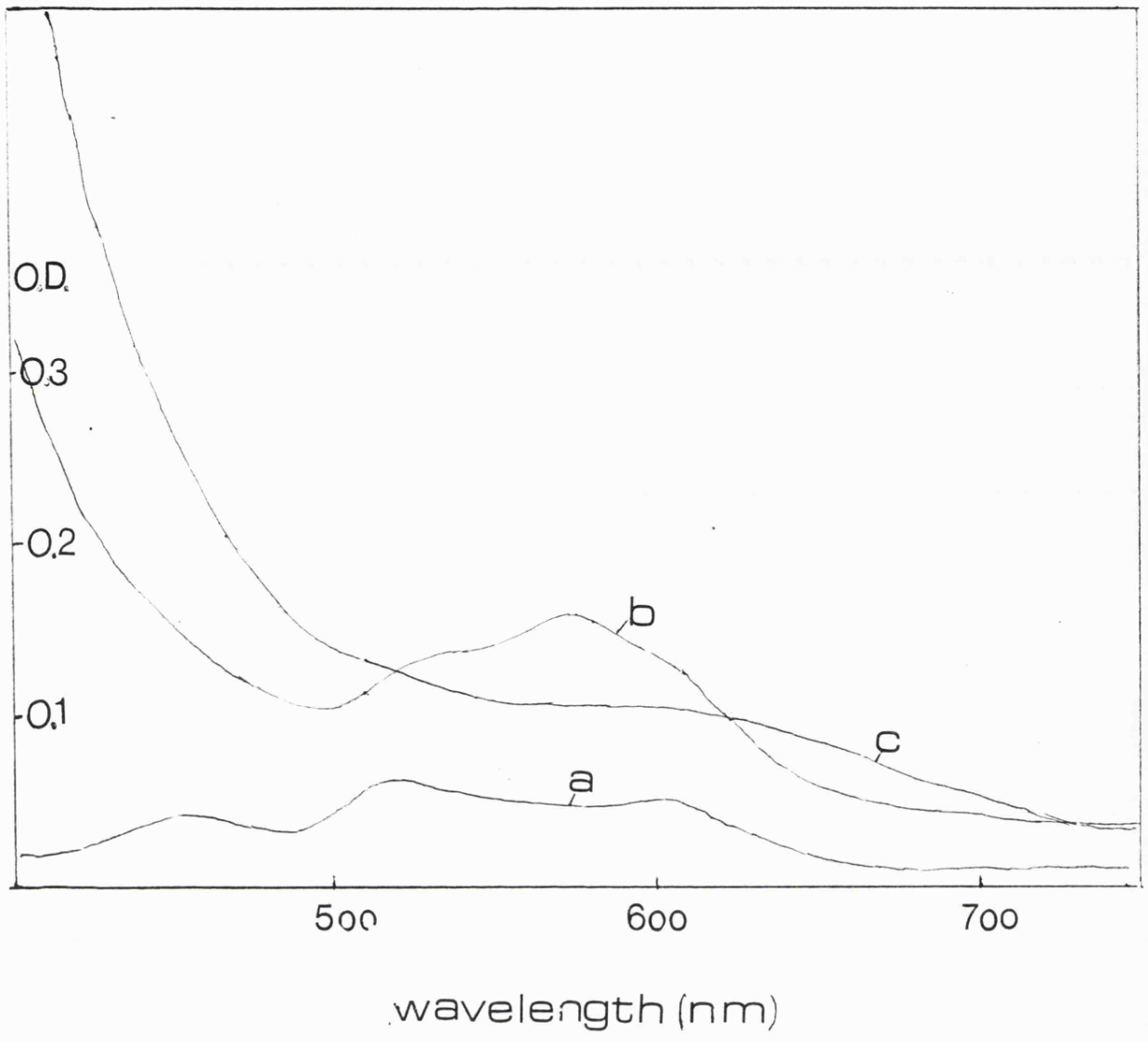

FIG. 4.14 Reaction of [Zn-Co]SOD in water with periodate; (a) the protein in water, (b) immediately after addition of 0.1 M sodium periodate, (c) after 2 hours incubation in the presence of periodate.

adduct of the native bound cobalt could be observed.

On the other hand in the [Zn-Co] protein such an intermediate at least at low temperature was formed. In Fig. 4.15 the E.P.R. spectra of the [Zn-Co] protein titrated with increasing amount of CN^- is shown. It is evident that the high spin cobalt complex typical of the unreacted [Zn-Co] protein was transformed into a low spin cobalt complex. The spectrum has a rhombic shape but only the high field region with $A_{//} = 115 \times 10^{-4}$ cm^{-1} and $g_{//} = 2.027$ is clearly resolved. At high CN^-/Co(II) ratios the cobalt begins to be released from its site and another E.P.R. signal characterized by $A_{//} = 82 \times 10^{-4}$ cm^{-1}, due to the $[Co(CN)_5]^{3-}$ complex was formed. It is interesting to notice that both the "phosphate" and the "water" form behaved in the same way, giving rise to the same low spin cobalt spectrum from their respective and specific high spin spectra, upon reaction with CN^- in the same conditions. This shows that CN^- was able to bind in the first coordination sphere of the metal, irrespective of its original coordination environment, with a consequent increase in the ligand field strength. The titration has the same trend in presence and in absence of air, indicating that the low spin intermediate species is unable to bind oxygen. The experiments were usually carried out in anaerobic conditions to avoid, at high CN^-/Co(II) ratios the formation of intermediate such as $[Co(CN)_5O_2]^{3-}$ from the $[Co(CN)_5]^{3-}$ complex. Fig. 4.16 reports a titration of [Zn-Co] superoxide dismutase, as followed by optical spectra, in 0.1M phosphate buffer at room temperature. The titration produces a decrease of the d-d bands and the appearance of a new band around 390 nm., but the disappearance of the high spin form is much slower at room than at low temperature. This behaviour clearly indicates that binding of CN^- was temperature or freezing dependent and that the low spin intermediate form was more easily formed at low temperature. The same titration was carried out

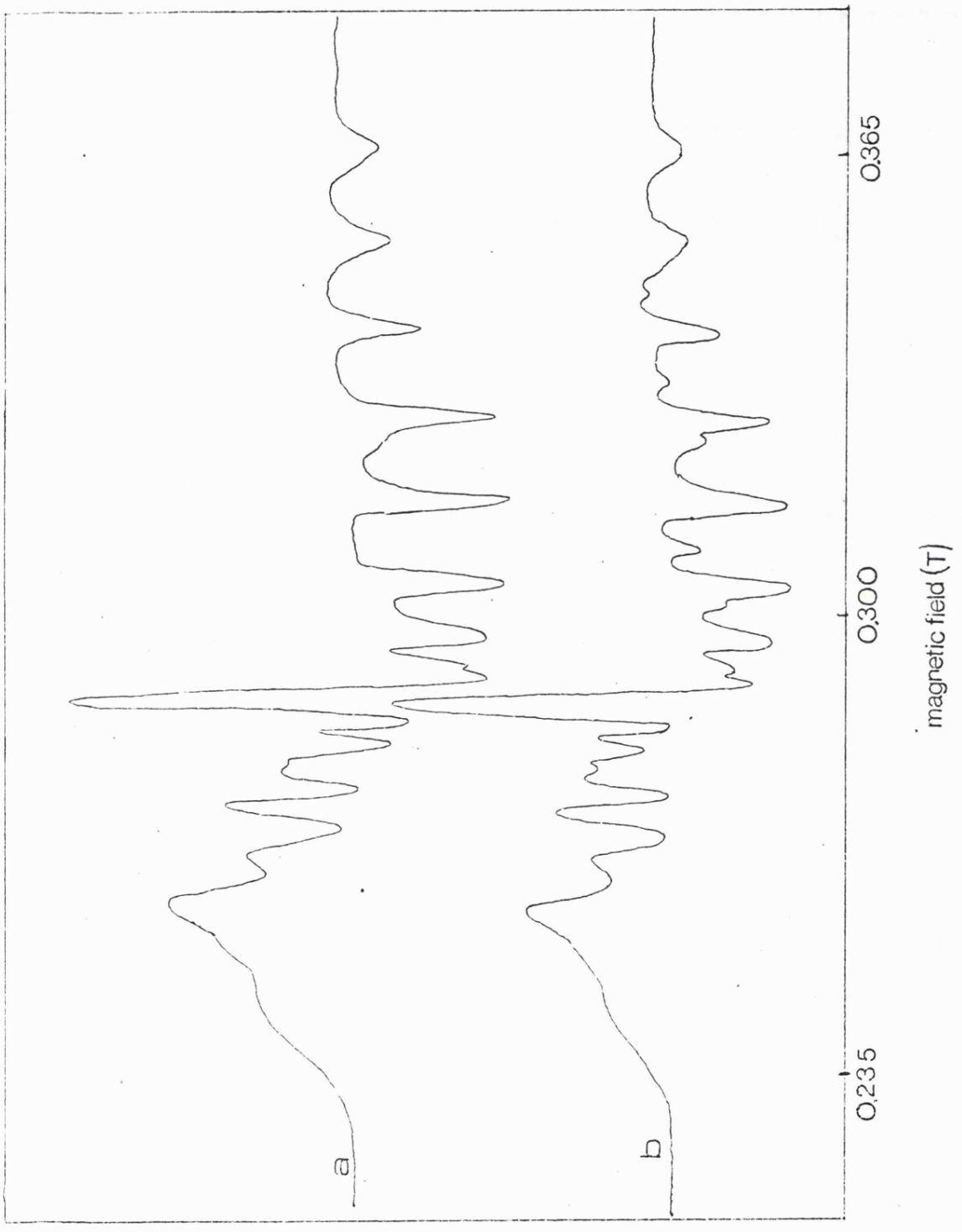

FIG. 4.15 X-Band E.P.R. spectrum of the [Zn-Co]SOD after addition of CN^-; CN^-:Co ratios (a) 8, (b) 50; temperature 77 K; power 20 mW; modulation 10 G.

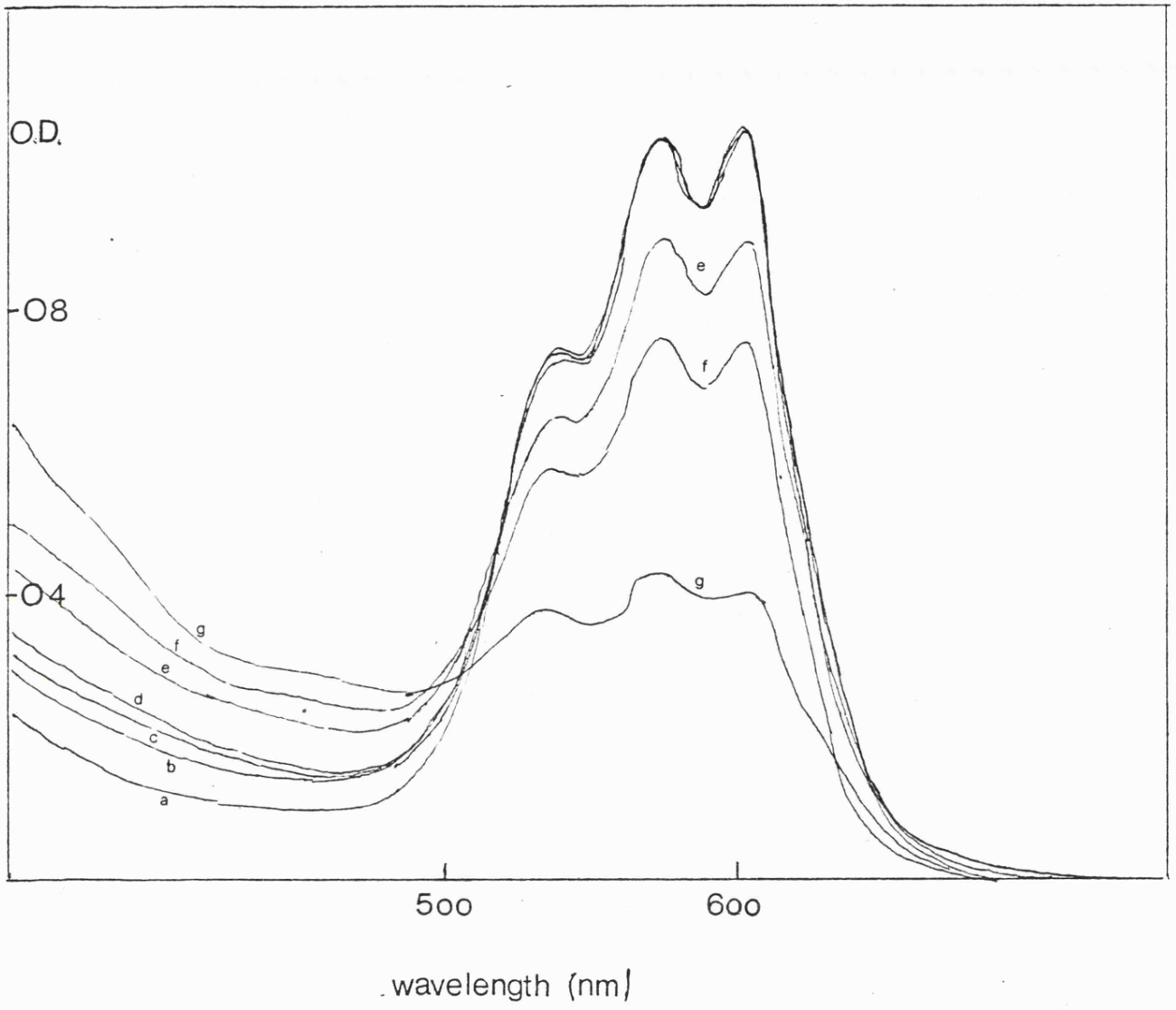

FIG. 4.16 Optical titration of the [Zn-Co]SOD in 0.1 M phosphate buffer with CN^-; protein 1.8×10^{-4}; Co 3.5×10^{-4} M; CN^-:Co ratios (b) 1, (c) 2, (d) 4, (e) 8, (f) 16, (g) 32.

in the [Co-Co] derivative, in a sample where the concentration of the cobalt at the zinc site exceeded that in the copper site by approximately 25%. No evidence for the formation of the low spin intermediate was obtained. At the lower CN^-/protein ratios, a decrease of the Co(II) high spin signals in the $g \simeq 6$ region, characteristic of the cobalt at the copper site, and in the $g \simeq 4$ region, characteristic of the cobalt at the zinc site, was observed (see Fig. 4.17). Further addition of cyanide increases the high spin signal at $g \simeq 4$ whilst at very high CN^-/Co(II) ratios all signals disappear. The optical titration of this sample has the same qualitative behaviour of that shown in Fig. 4.16. The first addition of cyanide does not change the spectrum, whilst at higher CN^-/Co(II) ratios the d-d bands decrease and a new band was formed at 390 nm. The availability of the cobalt, once substituted at the copper site, to react toward external agents was also demonstrated by reacting the [Zn-Co] protein with H_2O_2. Addition of ten-fold excess of H_2O_2 either to the phosphate or to the "water" form produces a decrease of the E.P.R. signal due to the Co(II) high spin and a parallel appearance of a sharp signal due to a radical in the region $g \simeq 2$. The reaction proceeds slowly with time but after the disappearance of about half the signal the reaction seemed to stop even after addition of further equivalents of H_2O_2. At this point the d-d bands of the optical spectrum had half of their original intensity but no new bands appeared due, for instance, to the oxidized Co(III) (Fig. 4.18). Addition of sodium dithionite does not restore the original spectrum. A similar behaviour was obtained in the optical spectrum of the [Co-Co] protein after reaction with H_2O_2. More interesting results were obtained by following the reaction by E.P.R. Fig. 4.19 shows that in this case, together with the appearance of the sharp signal at $g \simeq 2$, there is also a perturbation of

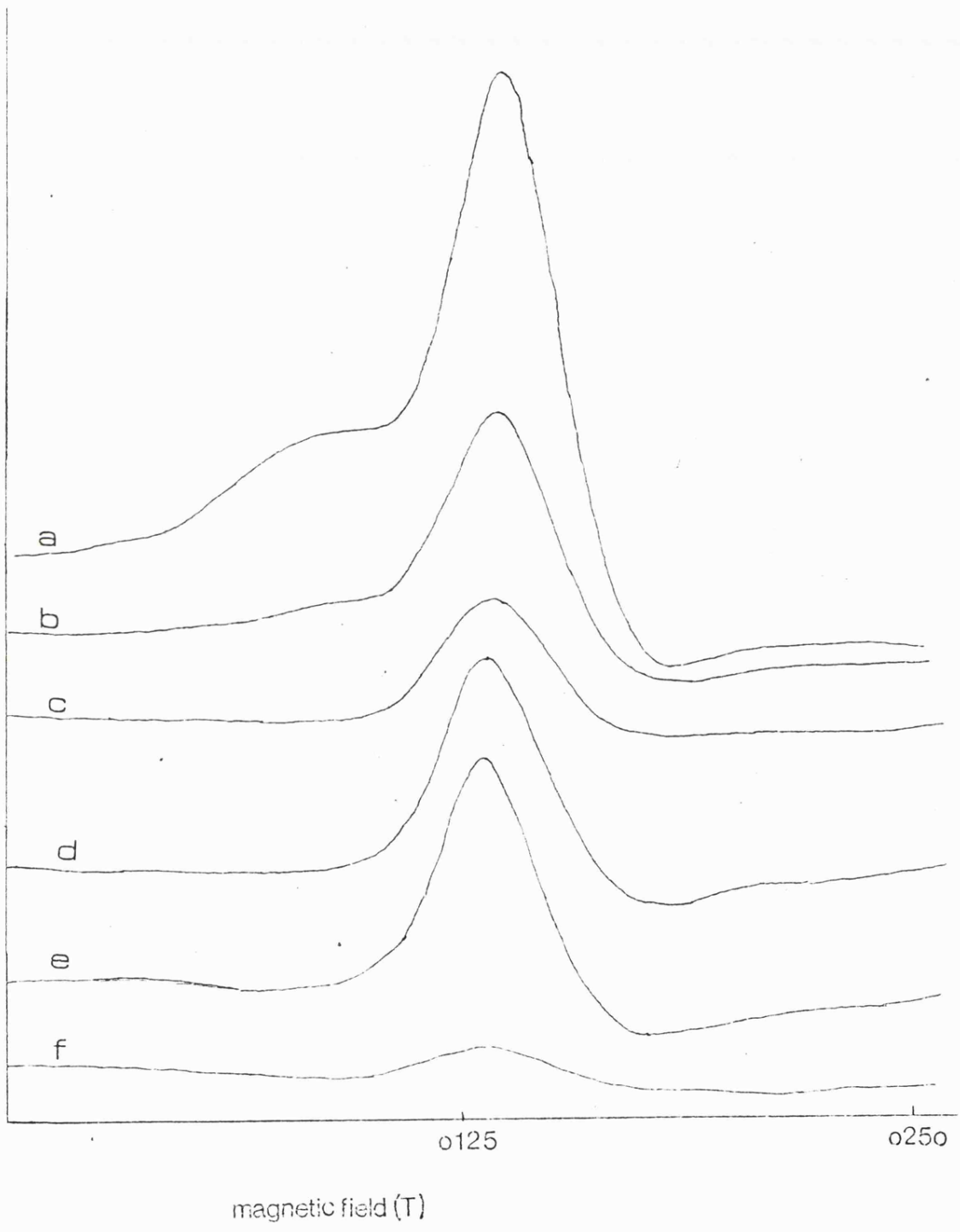

FIG. 4.17 E.P.R. titration of the [Co-Co]SOD with CN^-; protein 10^{-3} M; Co(II) at the zinc site 2×10^{-3} M; Co(II) at the copper site 1.5×10^{-3} M. CN^-:Co ratios (b) 2, (c) 8, (d) 16, (e) 24, (f) 64.

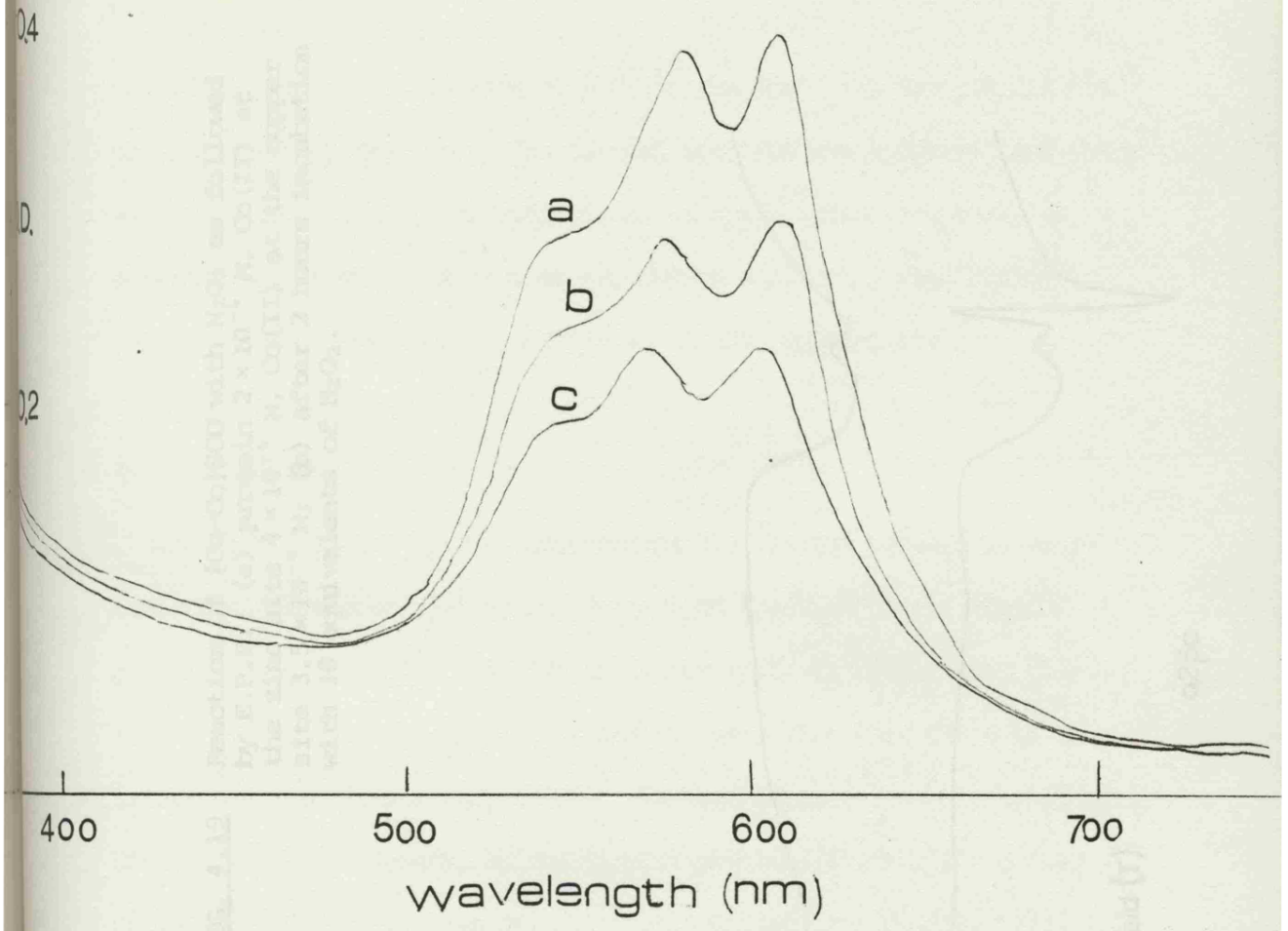

FIG. 4.18 Reaction of [Zn-Co]SOD in 0.1 M phosphate buffer with H_2O_2; (a) protein 0.55×10^{-3}, Co(II) 1.2×10^{-3} M; (b) after addition of 10 equivalents of H_2O_2 and 3 hours incubation; (c) after 6 hours incubation.

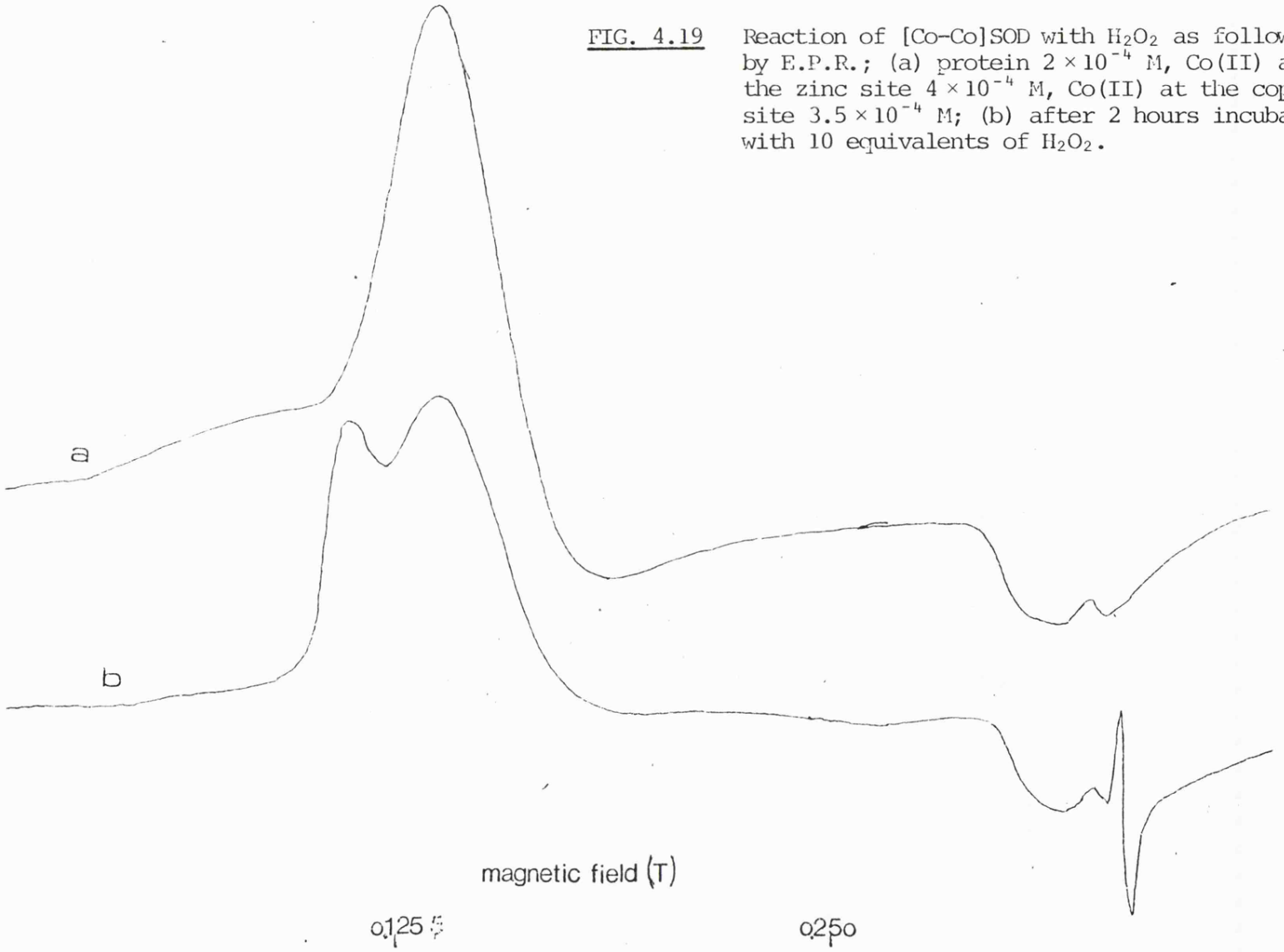

FIG. 4.19 Reaction of [Co-Co]SOD with H_2O_2 as followed by E.P.R.; (a) protein 2×10^{-4} M, Co(II) at the zinc site 4×10^{-4} M, Co(II) at the copper site 3.5×10^{-4} M; (b) after 2 hours incubation with 10 equivalents of H_2O_2.

the signals in the low field region suggesting a different interaction in the Co-Co pair.

Addition of 10 equivalents of H_2O_2 to the [Co - •••] protein did not give rise to any reaction. The optical spectrum was unchanged and there was no evidence for the radical signal at $g \simeq 2$, indicating that its presence in the previous samples was due to a direct participation in the reaction of the cobalt substituted at the copper site.

4. Discussion

The fact that the optical spectrum of the [Zn-Co] protein is very similar to that displayed by the difference spectrum of the [Co-Co] protein, (see Figs. 4.5 and 4.7) indicates that, in both cases, the cobalt is bound in the same place and suggests that this place is the native pentacoordinate copper site. Further support for this hypothesis comes from E.P.R. spectra of the [Co-Co] protein, where all the four native metal binding sites are presumably filled with Co(II). Fig. 4.8 shows that the spectrum of the [Co-Co] derivative (curve c) in spite of having at least twice the cobalt content of the [Co - •••] derivative represented by curves a and b shows a smaller amplitude and a broader signal in the region typical of higher g-values for high spin cobalt. This effect is indicative of some type of magnetic interaction presumably of dipolar origin between the two cobalt centres, such as expected if the two cobalt atoms occupy the zinc and copper sites respectively and then their distance is only 6 Å [8]. Moreover in the [Zn-Co] protein the cobalt ion is suitable for reaction with external agents such as CN^- and H_2O_2 as is the copper in the native enzyme [28]. Further evidence for an exposed location of the new cobalt binding site is the sensitivity of this cobalt derivative to the presence of phosphate, which did not affect

the properties of the cobalt species previously described [1-3]. The dependence of the spectral properties of this cobalt chromophore on the presence of the phosphate buffer is one of the most peculiar characteristics of the [Zn-Co] derivative. In Table 4.5 the absorption maxima of three cobalt derivatives of superoxide dismutase together with those of some anion derivatives of carbonic anhydrase are given. The band intensities and position of the [Zn-Co] "phosphate" form are similar to those of the cyanide derivative of carbonic anhydrase and of the [Co - •••] derivative of superoxide dismutase. These last two proteins have been assigned tetrahedral coordination around the cobalt on the basis of optical [2,5] and magnetic circular dichroism data [29,30]. The intensities of the bands of the "phosphate" form in the visible region and the energy of the near infrared band which is attributable to the spin-allowed ligand field transition $\nu_2[^4A_2 \rightarrow {}^4T_1\ (F)]$ [31] strongly suggest a tetrahedral coordination for this chromophore. Neglecting the spin-orbit coupling, the strength of the ligand field interaction Δt around the cobalt can be calculated by:

$$\Delta t^2 - 0.529\ (\nu_2 + \nu_3)\ \Delta t + 0.29\ \nu_2\ \nu_3 = 0$$

Taking the energy values reported in Table 4.5 for the "phosphate" form the value of $\Delta t = 5{,}400\ cm^{-1}$ is obtained. This value is of the same order of magnitude of that found for the [Co - •••] protein (see Part A of Chapter 4) and of those found for model cobalt complexes having nitrogen ligands mainly from imidazole or benzimidazole groups [7]. The ligand field value of the [Zn-Co] protein is then in agreement with the nitrogen ligands shown by the X-ray structural data of the native enzyme [8] and it is further evidence that the cobalt binds at the native copper site. The coordination of this chromophore reflects a tetrahedral symmetry, probably with some distortion, as suggested by the three components of

TABLE 4.5

Absorption maxima of some cobalt derivatives of SOD and BCA.
[Units are nm and extinction coefficients are given in brackets]

[Zn(II)-Co(II)] SOD water	450 (80)	520 (100)	610 (70)	780 (20)
[Zn(II)-Co(II)] SOD phosphate	540 (225)	580 (330)	605 (330)	1050 (40)
[Co(II)-Cu(I)] SOD	530 (315)	560 (425)	588 (450)	1000 (90)
Co(II)-BCA-CN^-	544 (510)	565 (540)	585 (650)	980 (75)
Co(II)-BCA-Cl^-	495 (160)	552 (220)	591 (270)	720 (4)
Co(II)-BCA-acetate	470 (100)	515 (180)	555 (110)	710 (9)

the ν_3 band in the visible region separated by 1,280 and 715 cm^{-1} respectively, a value too large to be attributed to spin-orbit coupling alone. The E.P.R. spectrum of this form (Fig. 4.6) is consistent with the presence of a rhombic distortion even if it is not possible to carry out any detailed analysis of the spectrum as only one feature at $g \simeq 6.9$ is clearly resolved, the others being too broad to be detected.

The band position and intensity of the [Zn-Co] SOD "water" form are more similar to those shown by the chloride and acetate derivatives of carbonic anhydrase (Table 4.5). Its molar intensity in the visible region is lower than 150 mol^{-1} cm^{-1} and it has a very weak band at 780 nm. This kind of spectrum has been recognized as diagnostic of pentacoordination [5]. It can be concluded that in the case of superoxide dismutase the same cobalt chromophore is able to change its symmetry depending on the phosphate buffer. Further support for this hypothesis comes from the E.P.R. spectra of these forms. The "water" form is, in fact, characterized by a hyperfine splitting $A \simeq 100$ gauss in the region $g \simeq 6$, and such a high value has never been found in tetrahedral compounds [32]. Moreover, the E.P.R. spectrum of the "phosphate" form seems to be characterized by two signals (Fig. 4.6), one of which is similar to that of the "water" species, suggesting an equilibrium between the two forms, which on freezing moves toward the pentacoordinate "water" form due to entropy reasons. This equilibrium is also shown by the presence of the low energy band typical of the "phosphate" form in the near infrared spectrum of the "water" form (Fig. 4.12). The question is how phosphate is able to affect the cobalt site. The fact that the cobalt is pentacoordinate in water and becomes tetrahedral in the presence of phosphate suggests that the buffer anion does not simply replace a metal-bound ligand molecule. Both the "water" and "phosphate" forms can be conformational

isomers stabilized by rather long-range effects. Thus phosphate could just bind to a nearby positively charged side chain. This hypothesis is confirmed by the optical titration experiments shown in Fig. 4.13 where it is shown that the "phosphate" loses its typical spectrum upon an increase in the pH of one unit. The process is reversible and the apparent pK of the titration is about 8.2, a value that could reflect the dissociation constant of the phosphate between the $H_2PO_4^-$ and the HPO_4^{2-} forms. The hypothesis that the phosphate buffer binds to a nearby positively charged side-chain and not directly to the metal comes also by the fact that the "phosphate" form can be simulated by the addition of periodate to the "water" form (Fig. 4.14). Periodate, in fact, has been shown to bind in the phosphate domain of phosphate binding enzymes by interacting with a basic side-chain [27]. The fact that both periodate and phosphate are able to produce the same spectral changes to the "water" form could suggest that this perturbation is obtained by binding to a positively charged side-chain. Further work is needed to completely clarify this point.

Reaction with external agents such as CN^- and H_2O_2 produces the same behaviour in the [Zn-Co] SOD "water" and "phosphate" forms. Addition of CN^- gives rise to a clear low-spin intermediate form only at low temperatures indicating that in these conditions the anion binds more easily to the metal. This behaviour strictly resembles that of the cobalt derivative of carbonic anhydrase [33]. Also in that case, binding of cyanide was temperature dependent but the equilibrium was between the monocyanide and the dicyanide form at room and low temperatures respectively [33,34]. In the case of [Zn-Co] superoxide dismutase there is no evidence for a monocyanide high-spin form at room temperature suggesting that only one CN^- is bound at low temperature to form a distorted square pyramidal structure. The E.P.R.

spectrum has, in fact, a clear rhombic shape and also the departure of the $g_3 = 2.027$ from the spin only value indicates a mixing of d_{z^2} and $d_{x^2-y^2}$ orbitals as the ground state, instead of a pure d_{z^2} as expected for a regular square pyramidal geometry. This distortion accounts also for the lack of binding of O_2 in contrast with that observed with carbonic anhydrase [33]. The ability to bind oxygen is, in fact, typical of most axial low-spin cobalt chelates such as porphyrins where the O_2 molecule binds to the sixth coordination position to form octahedral cobalt complexes [35]. The titration with CN^- of the [Co-Co] derivative gave some interesting results. Addition of a small excess of CN^- did not produce the appearance of the low spin form seen in the [Zn-Co] protein but led to a disappearance of the spectral features related to the [Co-Co] cluster. This behaviour suggests that the CN^- binds to the more external cobalt (i.e. the one substituted for copper) forming the low spin intermediate adduct that is undetectable because it is able to produce a magnetic interaction with the high spin cobalt at the zinc site. In fact, when ~10 equivalents of CN^- are added to the protein and almost all the external high spin cobalt is transformed to low spin, the only signal left is a weak signal at $g \simeq 4$. This signal arises from about 25% of the molecules that have the cobalt substituted into the zinc site and not cobalt substituted into the copper site. Moreover, on addition of further excess of cyanide that produces the depletion of the more external cobalt atom, the high-spin signal at $g \simeq 4$ increases, indicating the release of the magnetic interaction. It is difficult to understand which are the actual electronic levels in this case; surely a strong exchange must occur between the two sites. No similar synthetic model compounds have been studied. In the [Co-Cu] SOD that is completely E.P.R. silent, the magnetic susceptibility studies showed an exchange constant $J \geqslant 300$

cm^{-1} (see Part A). The metal cluster of superoxide dismutase seems then to prefer to couple $S = 3/2$, $S = 1/2$ (i.e. Co^{2+} high spin - Co^{2+} low spin or Co^{2+} high spin - Cu^{2+}) rather than $S = 3/2$, $S = 3/2$ (i.e. Co^{2+} high spin - Co^{2+} high spin). In fact, in this case the magnetic moment measured at room temperature showed a value $\mu = 4.3 \pm 0.3$ indicating that the broadening of the E.P.R. spectra was of dipolar origin.

The reaction of the different cobalt derivatives with H_2O_2 shows again the similar behaviour of [Zn-Co] SOD in both the "phosphate" and the "water" forms in contrast to the corresponding cases of [Co - •••] SOD. In this latter case the metal was inaccessible to H_2O_2 and both the optical and E.P.R. spectra remain unchanged. In the two derivatives of [Zn-Co] SOD the increase in intensity of a radical signal in the E.P.R. spectrum associated with a parallel decrease in intensity of the Co(II) signal implies a direct participation of the cobalt in the reaction with H_2O_2. Hydrogen peroxide is often used in several Co(II) proteins to oxidize the metal to Co(III). In the case of superoxide dismutase the optical spectrum of the Co(III) ion is not observed, and addition of sodium dithionite does not restore the original signal. The external Co(II) must be involved in direct reaction with H_2O_2 as also shown in the E.P.R. spectrum of Fig. 4.19 where some modification of the signals coming from the Co-Co cluster is observed.

Studies are in progress in this field and, in particular, it would be interesting to verify if addition of H_2O_2 to the [Zn-Co] or [Co-Co] protein produces the destruction of some amino acid residue as observed in the native protein [36].

C. K-edge X-ray absorption spectroscopy of Co(II) binding sites of copper- and zinc- containing proteins and of some low molecular weight cobalt complexes

X-ray absorption spectroscopy near the K-edge [XANES] has been recently quite widely used for the investigation of the active sites in metalloproteins. In particular, it has been used to investigate copper [37], zinc [38] and iron [39] containing proteins, but the cobalt derivatives have never been studied. In this work the K-edge of some cobalt compounds of known structure, and the cobalt derivatives of superoxide dismutase, carbonic anhydrase, stellacyanin and alcohol dehydrogenase has been carried out, and the properties of their X-ray absorption spectra are compared.

Two tetrahedral, two distorted trigonal bipyramidal and one octahedral Co(II) complexes were chosen for the low molecular weight model compounds in order to observe differences in the K-absorption edge up on changing the geometry about the cobalt.

The molecular structure of cobalt (imidazole)$_2$(acetate)$_2$(coordination sphere CoN_2O_2) [40], Co(aptsz)$_2I_2$ (coordination sphere S_2I_2) [41], [Co(S_2PPh_2)$_2$].C_9H_7N (coordination sphere S_4N) [42], are shown in Fig. 4.20. No X-ray structure analysis has been done for the Co(atsz)$_2I_2$.$2H_2O$ [41], or for the Co(II) tris bipyridyl perchlorate compound [43] but from the chemical analysis and the properties of the visible absorption spectra a CoN_2S_2O and CoN_6 chromophore can be assigned respectively.

X-ray absorption data were taken at the Synchrotron Radiation Facility P.U.L.S. of the Frascati National Laboratories. Synchrotron radiation emitted by the Adone storage ring, working at 1.5 GeV and about 50 mA, was monochromatized by a Si (220) channel cut single crystal monochromator. The energy resolution at 7.5 KeV was ±0.5 eV. The samples were measured as powder films layered on a kapton tape; their

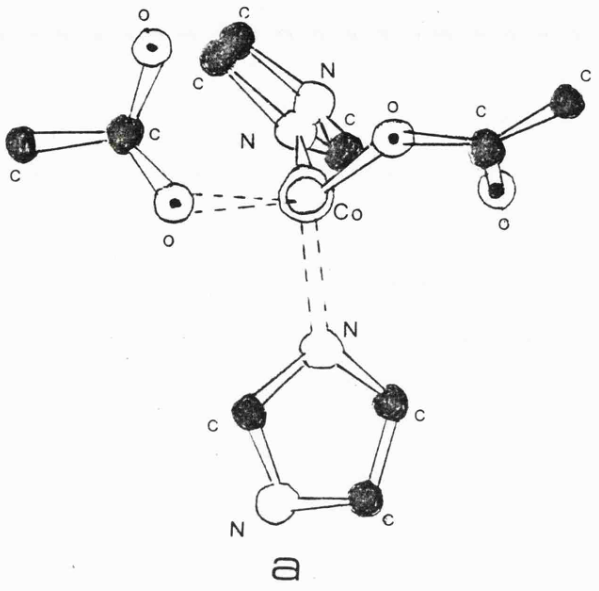

a

FIG. 4.20 Molecular structure of: (a) $Co(imidazole)_2(acetate)_2$; (b) $Co(aptsz)_2I_2$; (c) $Co(S_2PPh_2)_2.C_9H_7N$.

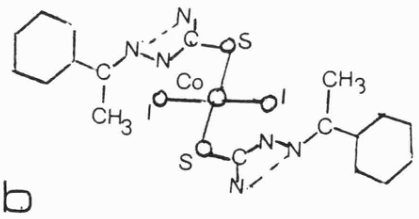

b

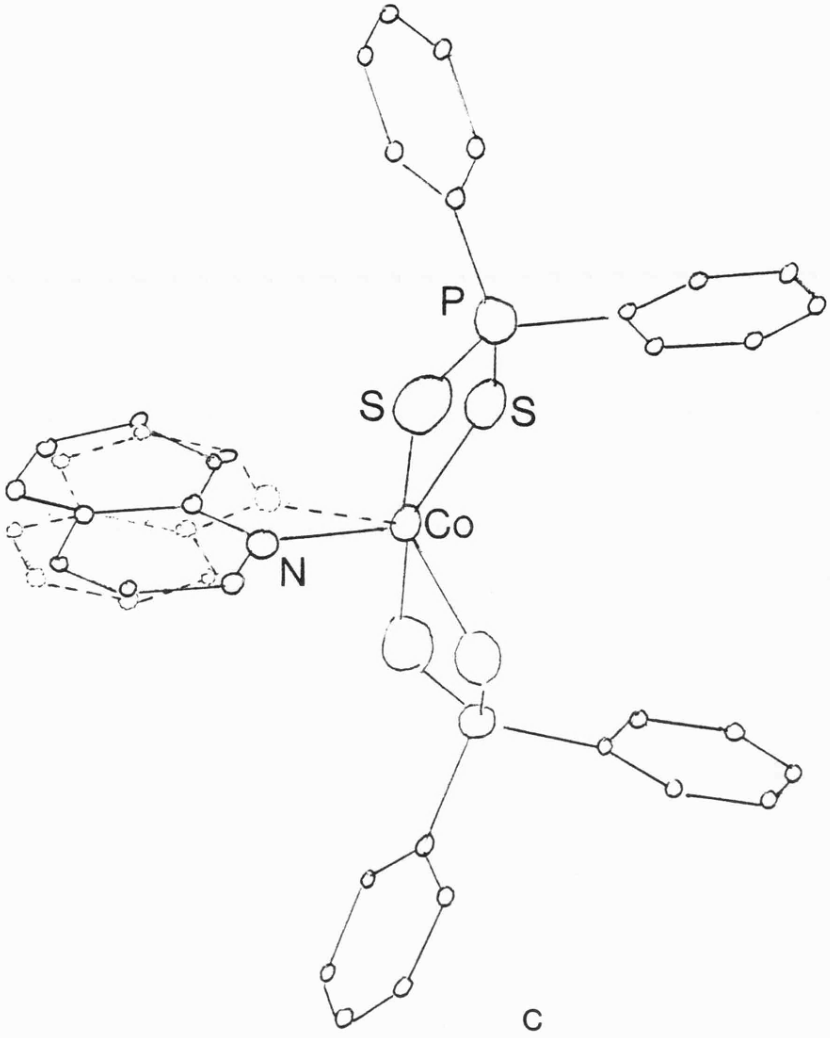

FIG. 4.20 (see caption on previous page)

thickness was chosen so as to obtain the best contrast at the K-edge. Fig. 4.21 shows the XANES spectra of Co(imidazole)$_2$(acetate)$_2$, Co(aptsz)$_2$I$_2$ and Co tris-bipyridyl perchlorate. All the spectra were characterized by an absorption at lower energy (near 7712 eV in our conditions) assigned to the 1s → 3d transition, a second absorption present as a shoulder 8-10 eV higher in energy assigned to the 1s → 4s transition, and an intense absorption, still higher in energy, assigned to the 1s → 4p transition. It is immediately apparent that the intensity of the first transition in the octahedral complex is much less than that for the tetrahedral complexes. In fact, in the first complex this peak is nearly absent whilst it is fairly pronounced in the other two. This is due to the fact that in tetrahedral geometry the p-d orbitals can mix with each other and the forbidden 1s → 3d transition becomes partly allowed. It is interesting to note that also the spectra of the five-coordinate [Co(S$_2$PPh$_2$)$_2$].C$_9$H$_7$N and Co(atsz)$_2$I$_2$.2H$_2$O given in Fig. 4.22 show a quite intense 1s → 3d peak. Complexes with trigonal bipyramidal distorted geometry are also able to display a 1s → 3d transition of comparable intensity to that of tetrahedral complexes. This peak can then only indicate the presence of a distorted geometry but cannot be taken as diagnostic for a pseudo-tetrahedral chromophore. In Table 4.6 the comparison of the energy difference between the first two transitions of all the compounds studied is reported. From the data of Table 4.6 it is immediately clear that the energy difference between the first two peaks decreases as the covalency of the first coordination sphere of the metal increases. It is interesting to note that this trend does not depend on the geometry of the chromophore but only on the covalent character of the ligands.

Once this trend has been obtained for complexes of cobalt on the basis

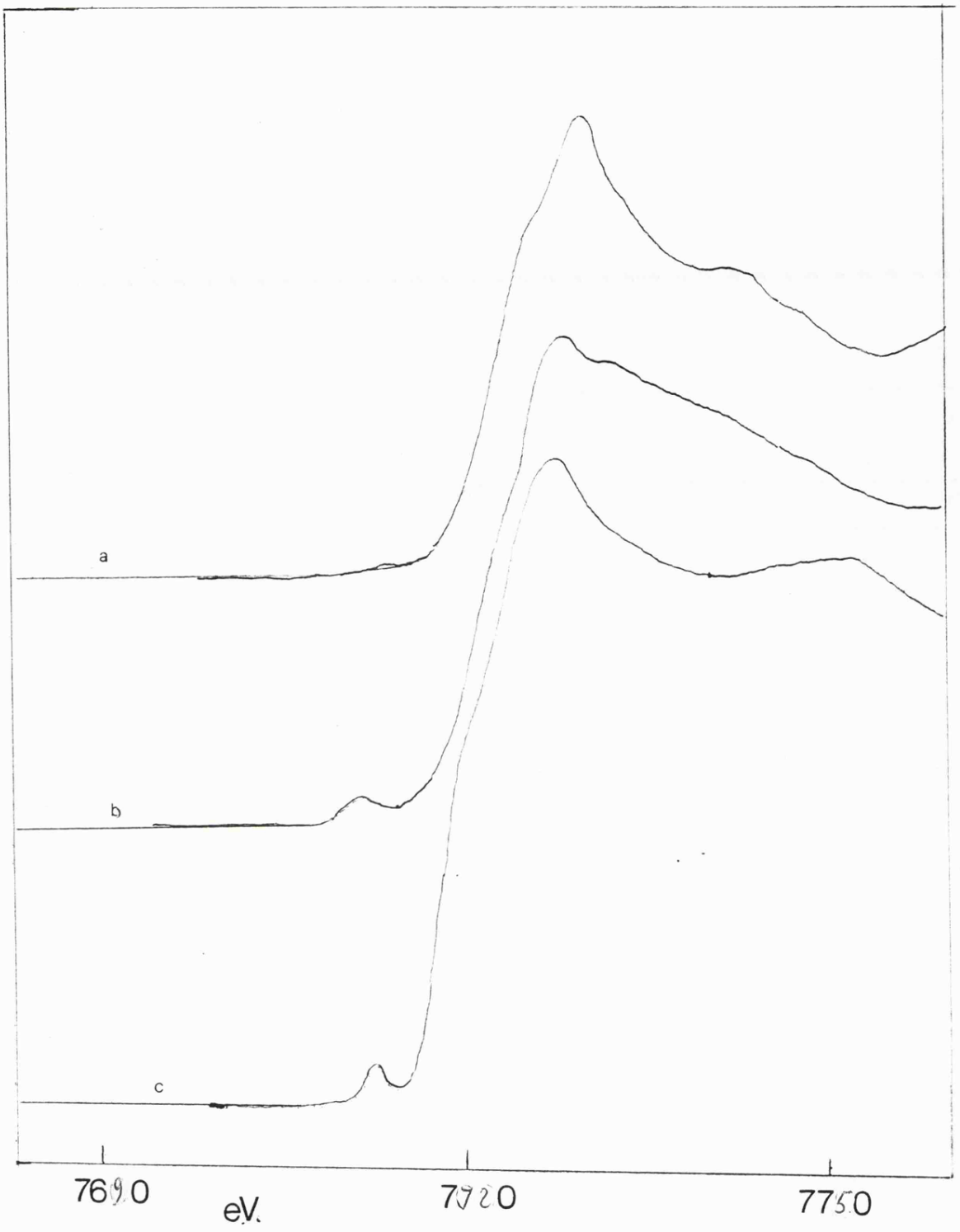

FIG. 4.21 X-ray absorption edge of: (a) octahedral Co(II) tris bipyridyl perchlorate; (b) tetrahedral Co(II) bisimidazole acetate; (c) tetrahedral $Co(aptsz)_2I_2$. [Curves are displaced vertically for clarity.]

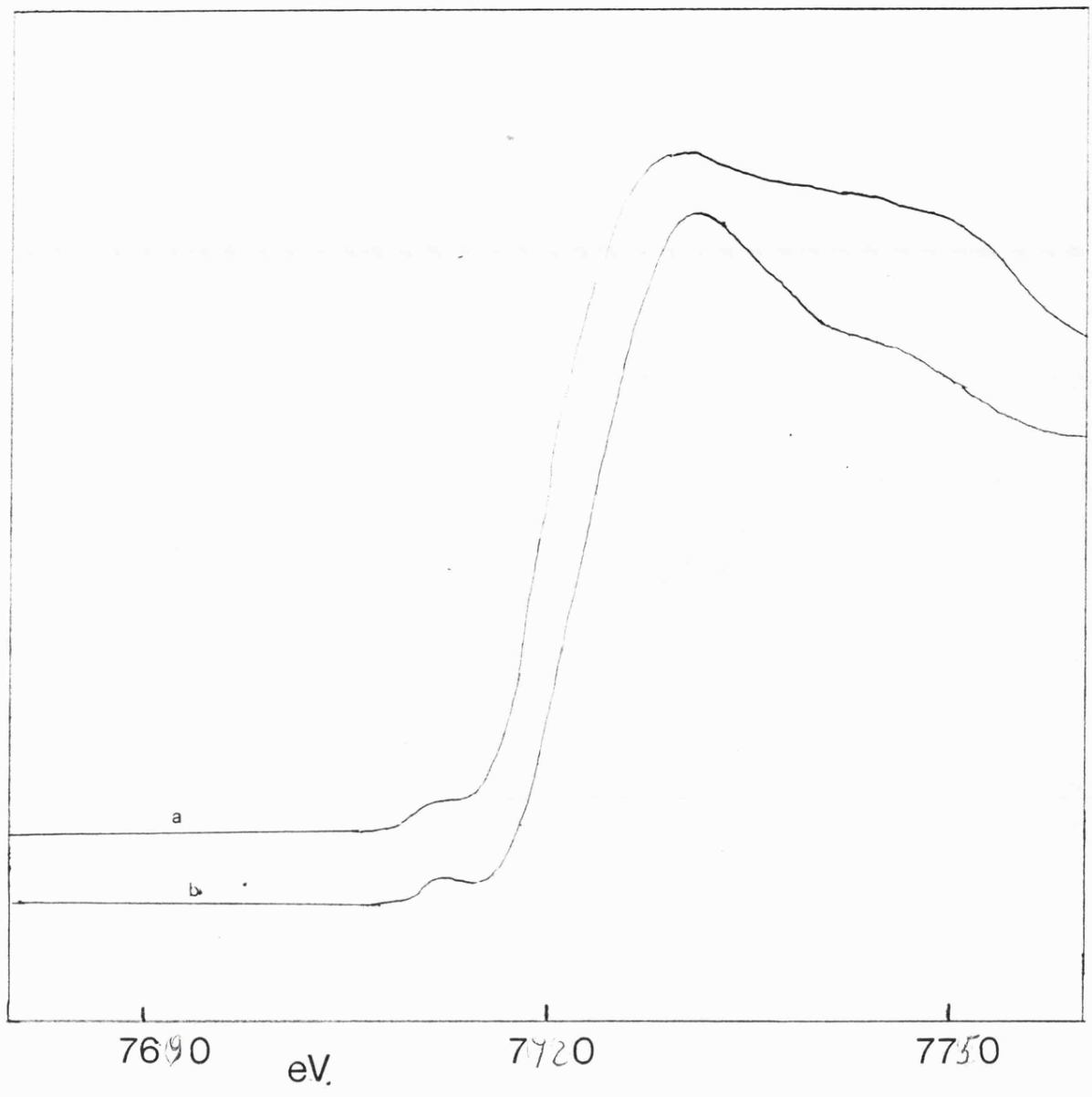

FIG. 4.22 X-ray absorption edge of: (a) $Co(atsz)_2I_2$; (b) $Co(S_2PPh_2)_2$. [Curves are displaced vertically for clarity.]

TABLE 4.6

Energy difference between the 1s → 3d and 1s → 4s transition

	Co(II) Compounds	Coordination Sphere	ΔE/eV
INCREASING COVALENCY ↓	Co tris bipyridyl	CoN_6	9.6
	$Co(imidazole)_2(acetate)_2$	CoN_2O_2	8.7
	$Co(atsz)_2I_2$	CoN_2S_2O	8.0
	$[Co(S_2PPh_2)_2]C_9H_7N$	CoS_4N	7.1
	$Co(aptsz)_2I_2$	CoS_2I_2	4.0

of a study of compounds of known structure, it is possible to begin a study of the cobalt derivatives of some metalloproteins. In particular, three cobalt derivatives of superoxide dismutase were studied, namely [Co(II)-Cu(II)], [Co(II)-Cu(I)] and [Co(II) - •••]. In all these derivatives the cobalt has been substituted into the native zinc, having the copper in the oxidized state, in the reduced state, or completely absent. The interest in this work is in observing if there is some differences in the coordination of the cobalt in the three different copper situations, and in particular in obtaining additional information on the structure of the cobalt site in the Cu(II)-protein, which is not observable by E.P.R. [2]. The samples were studied as a film of lyophilized protein layered on a kapton tape; their thickness was chosen so as to obtain the best contrast at the K-edge. The protein powders were always monitored by E.P.R. before the experiment to verify that their spectra were identical to those of solutions. After the experiment, optical spectra of the dissolved powders were recorded to detect any possible damage occurring during the radiation treatment.

In Fig. 4.23 the XANES spectra for cobalt bovine superoxide dismutase

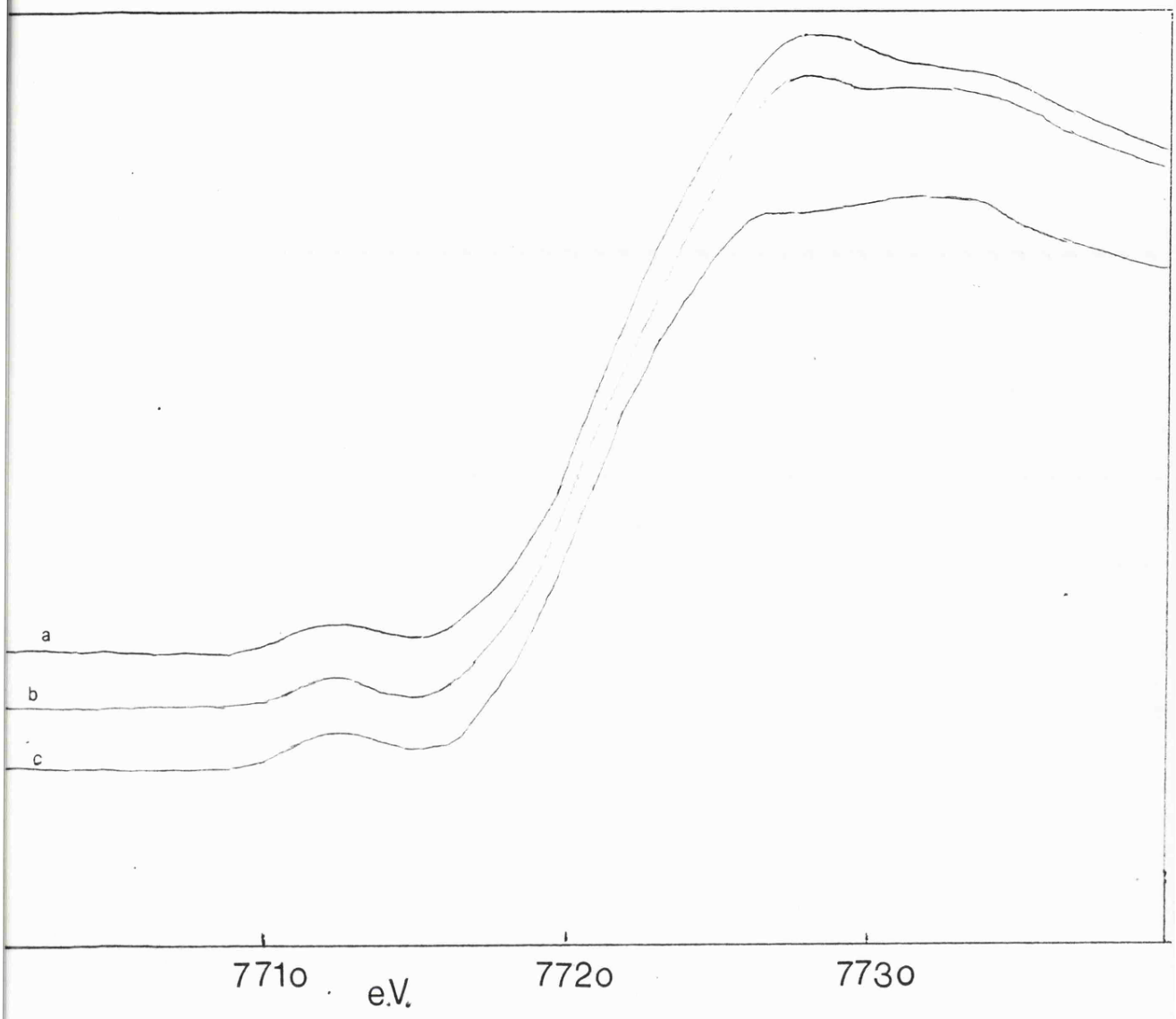

FIG. 4.23 X-ray absorption edge of cobalt superoxide dismutase: (a) [Co(II)-···]SOD; (b) [Co(II)-Cu(I)]SOD; (c) [Co(II)-Cu(II)]SOD. [Curves are displaced vertically for clarity.]

in the Cu-free, the Cu(I) and the Cu(II) derivatives are reported. The spectra are again characterized by three main absorptions, one the $1s \rightarrow 3d$ transition at lower energy, the second a shoulder $\simeq 8.5$ eV higher in energy assigned to the $1s \rightarrow 4s$ transition, and the third an intense $1s \rightarrow 4p$ transition still higher in energy. A common feature of the three spectra is the relatively high intensity of the $1s \rightarrow 3d$ transition, diagnostic of a distorted pentacoordinate or tetrahedral structure at the cobalt site. A tetrahedral coordination has been already inferred from optical and E.P.R. spectra in the case of [Co(II)-Cu(I)] and [Co(II)- $\cdots$] superoxide dismutase as shown in the Part A of the Chapter 4 of this thesis, and so a tetrahedral coordination is preferred for the cobalt site. Moreover, the K-edge spectra of the cobalt ion in the Cu(I) and Cu-free proteins are completely superimposable and confirm the previous suggestion that reduction of the copper leads to the release of Cu(I) from the bridging imidazole [2,3]. The XANES spectrum of the [Co(II)-Cu(II)] protein shows some difference in the high energy region around the intense $1s \rightarrow 4p$ absorption. Changes in this region involve the higher electronic states of the cobalt ion and may be related to slight conformational changes and/or to the different charge of the bridging imidazole, depending on the state of the copper. From the similarity of the spectrum of the three different derivatives in the lower energy region and from the same intensity of the first absorption, it may be concluded that the cobalt maintains the same structure independently of the presence of the oxidation state of the copper. In particular, the $1s \rightarrow 4s$ transition is only slightly shifted suggesting that the cobalt always sees the same charge in the three derivatives, as already reported for the zinc [44].

In Fig. 4.24 the XANES spectra of the cobalt derivatives of stella-

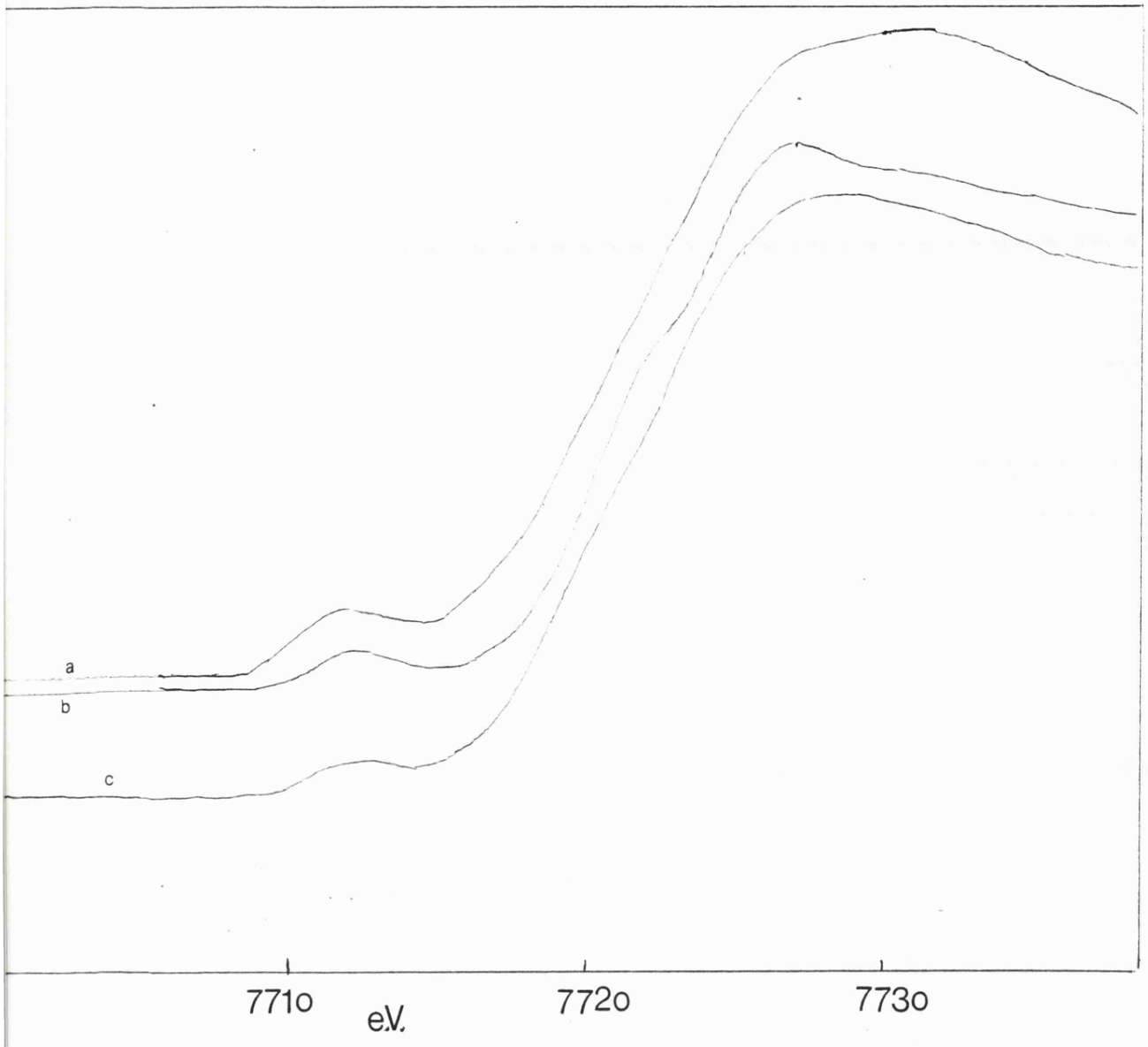

FIG. 4.24 X-ray absorption edge of: (a) Co(II)-stellacyanin; (b) Co(II)-bovine carbonic anhydrase; (c) Co(II)-horse liver alcohol dehydrogenase. [Curves are displaced vertically for clarity.]

cyanin, horse liver alcohol dehydrogenase and bovine carbonic anhydrase are reported. Also these spectra are characterized by an intense $1s \rightarrow 3d$ transition. In particular, that of stellacyanin is twice as high as that of others. In the absence of other information it is difficult to discriminate between distorted tetrahedral and pentacoordinate structures; tetrahedral coordination is perhaps more likely on the basis of previous results [23,25,29]. The comparison of the energy difference between the first two peaks for all the Co(II) proteins studied is reported in Table 4.7 and appears to be more informative.

TABLE 4.7

Energy difference between the $1s \rightarrow 3d$ and $1s \rightarrow 4s$ transitions in Co(II) substituted proteins

	Co(II)-protein	ΔE/eV
INCREASING COVALENCY ↓	Co(II)-carbonic anhydrase	8.6
	[Co(II)- •••]-superoxide dismutase	8.6
	[Co(II)-Cu(I)]-superoxide dismutase	8.6
	[Co(II)-Cu(II)]-superoxide dismutase	8.2
	Co(II)-stellacyanin	6.8
	Co(II)-alcohol dehydrogenase	6.7

In Co(II)-carbonic anhydrase and Co(II)-superoxide dismutase this difference is almost the same and about 1.5 eV greater than in Co(II)-stellacyanin and Co(II)-alcohol dehydrogenase. In the previous study of cobalt model compounds it was found that the $1s \rightarrow 4s$ transition moves to lower energy as the covalency of the ligands increases. This can explain the data of Table 4.7 because the ligand coordination sphere of native

superoxide dismutase is known to be N_3O [8], that of carbonic anhydrase is N_3O [45] and that of horse liver alcohol dehydrogenase is NOS_2 [46]. The shift observed for stellacyanin is similar to that of alcohol dehydrogenase and is in line with the expectation that sulphur ligands are present in the first coordination sphere of the stellacyanin copper [47], as already shown by the X-ray diffraction analysis of azurin [48] and plastocyanin [49].

This work shows that XANES can give additional and complementary information on metal binding sites of proteins, even in cases already subjected to a great deal of spectroscopic observations. In particular, from the investigation of several Co(II)-substituted proteins and cobalt model compounds the following conclusions can be drawn:

(1) The K-edge XANES can identify a geometry lacking a centre of symmetry by the intensity of the $1s \rightarrow 3d$ transition. It is, however, not able to identify subtler differences like those existing between distorted tetrahedral and five-coordinate structures.

(2) The ΔE between the $1s \rightarrow 3d$ and $1s \rightarrow 4s$ transition reflects the degree of covalency of the complex and may be related to the type of ligands. In particular, comparison with horse liver alcohol dehydrogenase indicates that stellacyanin may have two sulphur ligands.

(3) The $1s \rightarrow 4p$ transition and the adjacent region at higher energy are most sensitive to minimal differences of geometry in Co(II) complexes. In the case of superoxide dismutase derivatives, it confirms that [Co(II)-$\cdots$] SOD and [Co(II)-Cu(I)] SOD have identical Co(II) coordination, which is in turn distinct from that of the [Co(II)-Cu(II)] SOD. This is fundamental to the

studies of the mechanism of the enzyme, as this argument has been used, on the basis of optical absorption spectra to infer that Cu(I) is released during catalysis from the imidazolate bridging copper and zinc [50].

REFERENCES

1. L. Calabrese, G. Rotilio and B. Mondovi, Biochim. Biophys. Acta 263, 827 (1972).

2. G. Rotilio, L. Calabrese, B. Mondovi and W. E. Blumberg, J. Biol. Chem. 249, 3157 (1974).

3. L. Calabrese, D. Cocco, L. Morpurgo, B. Mondovi and G. Rotilio, Eur. J. Biochem. 64, 465 (1976).

4. M. Goodgame and F. A. Cotton, J. Amer. Chem. Soc. 84, 1543 (1962).

5. I. Bertini, G. Canti, C. Luchinat and A. Scozzafava, J. Amer. Chem. Soc. 100, 4873 (1978).

6. L. Sacconi, I. Bertini and F. Mani, Inorg. Chem. 6, 262 (1967).

7. R. C. Rosenberg, C. A. Root and H. B. Gray, J. Amer. Chem. Soc. 97, 21 (1975).

8. J. Richardson, K. A. Thomas, B. H. Rubin and D. C. Richardson, Proc. Nat. Acad. Sci. USA 72, 1349 (1975).

9. T. H. Moss and J. A. Fee, Biochem. Biophys. Res. Com. 66, 799 (1975).

10. A. Rigo, M. Terenzi, C. Franconi, B. Mondovi, L. Calabrese and G. Rotilio, FEBS Lett. 39, 154 (1974).

11. M. Cerdonio, F. Mogno, G. L. Romani, C. Messana and C. Gramaccioni, Rev. Sci. Instrum. 48, 300 (1977).

12. R. L. Carlin in 'Transition Metal Chemistry' (ed. by R. L. Carlin) Marcel Dekker Inc., New York, Vol. 1, p.1 (1965).

13. M. D. Sturge, F. R. Merrit, J. C. Hensel and J. P. Remeika, Phys. Rev. 180, 402 (1969).

14. L. J. Guggenberg, C. T. Prewitt, P. Meakin, S. Trofimenko and J. P. Jesson, Inorg. Chem. 12, 508 (1973).

15. M. C. Chen and J. O. Artman, Phys. Rev. 187, 723 (1969).

16. G. Kolks, C. R. Frihart, H. N. Rabinowitz and S. J. Lippard, J. Amer. Chem. Soc. 98, 5720 (1976).

17. G. Kolks and S. J. Lippard, J. Amer. Chem. Soc. 99, 5804 (1977).

18. M. S. Haddad and D. N. Hendrickson, Inorg. Chem. 17, 2622 (1978).

19. J. A. Fee, J. Biol. Chem. 248, 4229 (1973).

20. G. Rotilio and L. Calabrese in 'Superoxide Dismutases' (ed. by A. M. Michelson, J. M. McCord and I. Fridovich) Academic Press, London, p.193 (1977).

21. J. E. Coleman, Biochemistry 4, 2644 (1965).

22. B. L. Vallee, J. A. Rupley, J. L. Coombs and H. Neurath, J. Amer. Chem. Soc. 80, 4750 (1958).

23. W. Maret, I. Anderson, H. Dietrich, H. Schneider-Bernlohr, R. Einarsson and M. Zeppezauer, Eur. J. Biochem. 98, 501 (1979).

24. S. W. May and T. J. Kuo, Biochemistry 78, 3333 (1978).

25. E. I. Solomon, J. Rawlings, D. R. McMillin, P. J. Stephens and H. B. Gray, J. Amer. Chem. Soc. 98, 8046 (1976).

26. G. Rotilio, A. Rigo and L. Calabrese in 'Frontiers in Physico-Chemical Biology' (ed. by B. Pullman) Academic Press, New York, p.357 (1978).

27. M. Rippa, M. Signorini, T. Bellini and F. Dallocchio, Arch. Biochem. Biophys. 189, 506 (1978).

28. G. Rotilio, L. Morpurgo, C. Giovagnoli, L. Calabrese and B. Mondovi, Biochemistry 11, 2187 (1972).

29. J. E. Coleman and R. V. Coleman, J. Biol. Chem. 248, 4718 (1972).

30. G. Rotilio, L. Calabrese and J. E. Coleman, J. Biol. Chem. 248, 3855 (1973).

31. A. B. P. Lever 'Inorganic Electronic Spectroscopy', Elsevier, Amsterdam, Chapter 9 (1968).

32. J. R. Pilbrow, J. Magn. Res. 31, 479 (1978).

33. S. A. Cockle, Biochem. J. 137, 587 (1974).

34. J. S. Taylor and J. E. Coleman, J. Biol. Chem. 246, 7058 (1971).

35. B. M. Hoffmann and D. M. Petering, Proc. Natl. Acad. Sci. USA 67, 637 (1970).

36. R. C. Bray, S. A. Cockle, E. M. Fielden, P. B. Roberts, G. Rotilio and L. Calabrese, Biochem. J. 139, 43 (1974).

37. L. Powers, W. E. Blumberg, B. Chance, C. H. Barlow, J. S. Leigh, J. Smith, F. Yonetani, S. Vik and J. Peisach, Biochim. Biophys. Acta 546, 520 (1979).

38. G. S. Brown, G. Navon and R. G. Shulman, Proc. Natl. Acad. Sci. USA 74, 1794 (1977).

39. R. G. Shulman, Y. Yafet, P. Eisenberger and W. E. Blumberg, Proc. Natl. Acad. Sci. USA 73, 1384 (1976).

40. M. A. Gadet, C.R. Acad. Sci. Paris 272, 1299 (1971).

41. C. Bellitto, A. A. G. Tomlinson, C. Furlani and G. De Munno, Inorg. Chim. Acta 27, 269 (1974).

42. A. Chiesi Villa, C. Guastini, P. Porta and A. A. G. Tomlinson, J. Chem. Soc. Dalton 956 (1978).

43. F. H. Burstall and R. S. Nyholm, J. Chem. Soc. 3571 (1952).

44. W. E. Blumberg, J. Peisach, P. Eisenberger and J. A. Fee, Biochemistry 17, 1842 (1978).

45. S. Lindskog, L. S. Henderson, K. K. Kannan, A. Liljas, P. O. Nyman and B. Stranberg in 'The Enzymes' Academic Press, New York 5, 587 (1971).

46. H. Eklund and C. I. Branden, J. Biol. Chem. 254, 3458 (1979).

47. L. Morpurgo, A. Finazzi-Agro, G. Rotilio and B. Mondovi, Biochim. Biophys. Acta 271, 292 (1972).

48. P. M. Colman, H. C. Freeman, J. M. Guss, M. Murata, V. A. Worris, J. A. M. Ramshaw and M. P. Venkatappa, Nature (London) 272, 319 (1978).

49. E. T. Adman, R. E. Stenkamp, L. C. Sieker and L. H. Jensen, J. Mol. Biol. 123, 35 (1978).

50. M. E. McAdam, E. M. Fielden, F. Lavelle, L. Calabrese, D. Cocco and G. Rotilio, Biochem. J. 167, 271 (1977).

CHAPTER 5

STUDY OF SOME COBALT AND COPPER DERIVATIVES OF BOVINE CARBONIC ANHYDRASE

A. An E.P.R. Study of some Co(II) High Spin Model Complexes and some High Spin Forms of Co(II) Bovine Carbonic Anhydrase

The technique of substitution of Co(II) ion in place of the native metal in Zn or other metalloproteins to provide a "paramagnetic marker" is becoming a very common and useful practice [1]. However, using E.P.R. spectroscopy it has not yet been found possible to distinguish between the relatively low symmetry sites encountered. The main reasons for this is the paucity of data available due to the need to work at liquid helium temperature [2]. In order to distinguish between pseudo-tetrahedral and trigonal-bipyramidal five-coordinate geometries, the most usual and most ambiguous in the field of metallo-proteins, an E.P.R. study of some low molecular weight model complexes and some cobalt derivatives of bovine carbonic anhydrase has been undertaken.

The free Co(II) ion has a ^4F ground state that, in the presence of a tetrahedral or trigonal bipyramidal crystal field, is split into the levels shown in Fig. 3.1. In both cases the $^4A_2$ and the $^4A_2'$ ground state can mix via spin orbit coupling with the excited levels forming the two Kramers doublets $m_s = \pm \frac{1}{2}$ and $m_s = \pm \frac{3}{2}$ separated by the energy $\delta = 2(D^2 + 3E^2)^{\frac{1}{2}}$ (the zero field splitting).

The appropriate spin Hamiltonian is:

$$\mathcal{H} = \beta(g_x H_x S_x + g_y H_y S_y + g_z H_z S_z) + D[S_z^2 - \tfrac{1}{3}S(S+1)] + E[S_x^2 - S_y^2],$$

which can be divided into two parts:

(a) $\mathcal{H}_1 = \beta(g_x H_x S_x + g_y H_y S_y + g_z H_z S_z)$

due to the Zeeman term and

(b) $\mathcal{H}_2 = D[S_z^2 - \frac{1}{3}S(S+1)] + E[S_x^2 - S_y^2]$

due to the crystalline electric field term. D and E represent respectively the axial and rhombic distortion.

The appearance of the spectra is strongly dependent on the relative order of magnitude of $h\nu$ and the zero field splitting. In the case when the zero field splitting is small compared to $h\nu$, three $\Delta M_s = \pm 1$ transitions will be recorded for every principal direction of g. When, on the contrary, the zero field splitting is larger than $h\nu$, the two Kramers doublets constituting the $S = 3/2$ manifold will be separated in energy by $2(D^2 + 3E^2)^{\frac{1}{2}}$ and only transitions within each of them will be obtained. In the case of Co(II), the spin orbit coupling effects are significant [3] so that the energy of the zero field is larger compared to $h\nu$. In this situation we can, to a good approximation, initially neglect H_1 and first solve the eigenvalue problem for H_2. Since we are dealing with the multiplets of a spin quartet, the wave function basis set will be the four $|S_z>$ substates of the quartet. The matrix representation of H_2 with respect to the basis set $|S_z>$ is shown in Table 5.1.

TABLE 5.1

The spin Hamiltonian matrix for $S = 3/2$ spin system in the absence of a magnetic field

$\|S_z>$	$\|3/2>$	$\|1/2>$	$\|-1/2>$	$\|-3/2>$
$\|3/2>$	D	0	$3^{\frac{1}{2}}E$	0
$\|1/2>$	0	-D	0	$3^{\frac{1}{2}}E$
$\|-1/2>$	$3^{\frac{1}{2}}E$	0	-D	0
$\|-3/2>$	0	$3^{\frac{1}{2}}E$	0	D

The eigenfunction of H_2, corresponding to ground and excited Kramers doublets, can be written:

$$\psi_1 = \alpha|3/2> + \beta|-1/2>$$
$$\psi_2 = \alpha|-3/2> + \beta|1/2> \quad \ldots\ (1)$$

due to the mixing of the spin states $m_s = \pm 1/2$ with the states $m_s = \pm 3/2$ via the D and E terms in the spin Hamiltonian.

Solution to the eigenvalue problem, by first diagonalizing the $S = 3/2$ determinant of Table 5.1, yields:

$$\alpha = \{3E^2/[2D^2 + 6E^2 + 2D\ (D^2 + 3E^2)^{\frac{1}{2}}]\}^{\frac{1}{2}} \quad \ldots\ (2)$$

$$\beta = \{[2D^2 + 3E^2 + 2D\ (D^2 + 3E^2)^{\frac{1}{2}}]/[2D^2 + 6E^2 + 2D\ (D^2 + 3E^2)^{\frac{1}{2}}]\}^{\frac{1}{2}} \quad \ldots\ (3)$$

Introducing the parameter $\gamma = E/D$, the ratio between the rhombic and axial component of the crystal field, equations 2 and 3 can be written:

$$\beta^2 = [2 + 3\gamma^2 + 2\sqrt{(1 + 3\gamma^2)}]/[2 + 6\gamma^2 + 2\sqrt{(1 + 3\gamma^2)}] \quad \ldots\ (4)$$

$$\alpha^2 + \beta^2 = 1 \quad \ldots\ (5)$$

On introducing the electronic Zeeman interaction as a perturbation upon the eigenfunction of the crystal field ψ_1 and ψ_2, the following relationships between g_x, g_y, g_z, in the $S = 3/2$ approximation [using the wavefunction in equation (1)], and the principal values g'_x, g'_y, g'_z, in the effective spin $S' = 1/2$ scheme, may be derived.

$$g'_z = g_z\ (\beta^2 - 3\alpha^2)$$
$$g'_x = 2g_x\ (\beta^2 + \sqrt{3}\,\beta\alpha)$$
$$g'_y = 2g_y\ (\beta^2 - \sqrt{3}\,\beta\alpha) \quad \ldots\ (6)$$

Equations 6 can be solved to find the value of β if it is assumed that $g_x = g_y$; γ can then be obtained from equation 4.

This approximation does not introduce any significant error in calculating γ as the difference between g'_x and g'_y is due to the mixing

of the spin states whilst that between g_x and g_y is mainly due to a different orbital contribution. The evaluation of γ gives the degree of magnitude of the rhombic component of the crystal field. Using now the relation $\gamma = E/D$ and the relation obtained from first order perturbation theory (equation 7)

$$D = \tfrac{1}{2}\lambda' [g_z - \tfrac{1}{2}(g_x + g_y)] \quad \ldots\ (7)$$

the value of δ can be evaluated. In equation (7) λ' is the spin orbit coupling constant which is smaller than that of the free ion (-179 cm^{-1}) due to covalent contributions to the bonding. The lowest likely value for λ' is -135 cm^{-1} and so the D and δ values were evaluated by taking λ' between -179 cm^{-1} and -135 cm^{-1}. It is then possible to obtain for every compound the two parameters γ and δ that give information respectively on the degree of the distortion and on the magnitude of the zero field splitting. In particular, the evaluation of δ can be useful in the determination of the symmetry of the compound as one would expect a greater value for pentacoordinated systems than for the tetrahedral ones due to the closer proximity of the ground and excited states. To test this hypothesis, a series of cobalt compounds of known structure have been studied and their δ values have been compared with those of some cobalt derivatives of carbonic anhydrase. Two pentacoordinated compounds, four tetrahedral compounds and one pseudo-tetrahedral compound with two long-bonded ligands were chosen as the low molecular weight models.

The two pentacoordinated compounds were, namely, $[Co(atsz)_2Cl]Cl.H_2O$ and $[Co(atsz)_2H_2O]I_2.H_2O$ where atsz = acetonethiosemicarbazone, $[NH_2C(S)NHN{=}C(CH_3)_2]$. For the chloro complex the crystal structure is available [4] and showed a (N_2S_2Cl) coordination sphere with the chlorine atom and two sulphur atoms lying approximately in a plane, the two

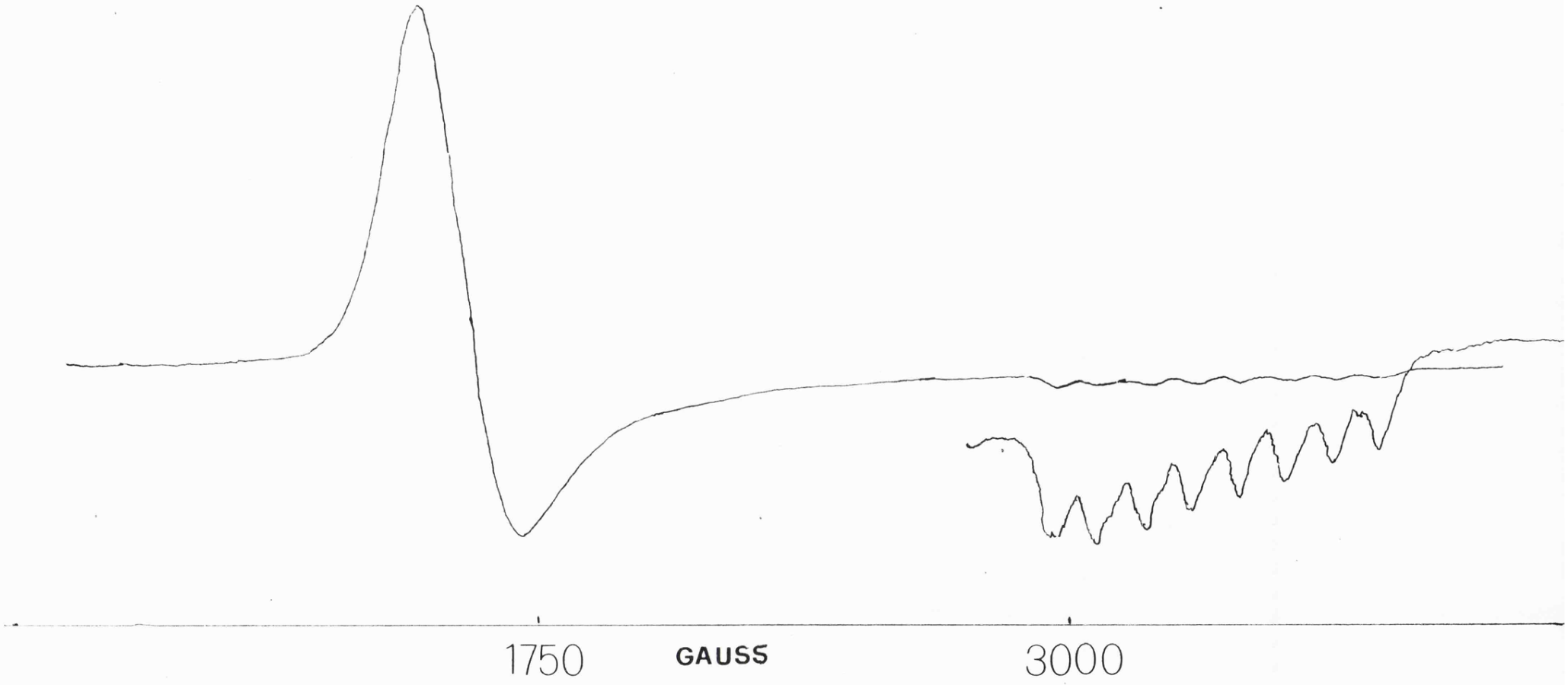

FIG. 5.1 X-Band E.P.R. spectrum of $[Co(atsz)_2Cl]Cl.H_2O$ dissolved in ethanol. Temperature 10 K, power 5 mW.

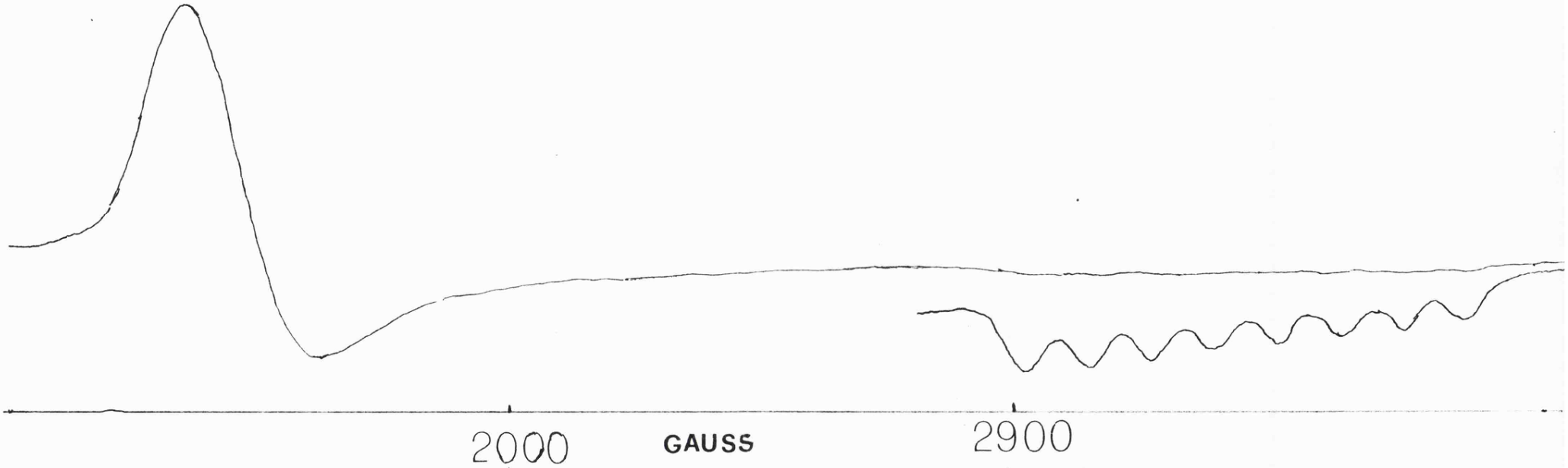

FIG. 5.2 X-Band E.P.R. spectrum of $[Co(atsz)_2H_2O]I_2.H_2O$ dissolved in acetone. Temperature 10 K, power 5 mW.

nitrogen atoms being in an apical position to form a trigonal bipyramidal structure. For the iodo complex, a similar geometry with a N_2S_2O coordination sphere was suggested from optical and analytical data [5]. The tetrahedral compounds were, namely, $[Co(Im)_2(CH_3CO_2)_2]$ where Im = imidazole, $[Co(\gamma\text{-pic})_2Br_2]$ where γ-pic = γ-picoline, $[Co(aptsz)_2I_2]$ where aptsz = acetophenonethiosemicarbazone $[NH_2C(S)NHN=C(CH_3)(C_6H_5)]$, $[Co(atsz)Cl_2]$ where atsz = acetonethiosemicarbazone.

The crystal structure data of the tetrahedral compounds are available [5-8] from which the following first coordination spheres can be respectively assigned: N_2O_2, N_2Br_2, S_2I_2, $NSCl_2$.

Particularly interesting is the structure of the $[Co(etu)_2(CH_3CO_2)_2]$ [9] that shows the cobalt to be in pseudo-tetrahedral (S_2O_2) geometry with two further long-bonded ligands from the two oxygen atoms of the acetate groups. All the E.P.R. spectra were run with a Varian E-9 spectrometer equipped with an Air Products and Chemical CT-3-110 liquid transfer Cryo-Tip refrigerator to reach temperatures near that of liquid helium. When possible the complexes were doped into the relative Zn matrix, the doped complexes being obtained by co-crystallization from the appropriate solvents. Nominal concentration of 0.5 to 2% Co^{++} were used. As no suitable diamagnetic hosts for $[Co(Im)_2(CH_3CO_2)_2]$, $[Co(atsz)_2Cl]Cl.H_2O$, $[Co(atsz)_2H_2O]I_2.H_2O$ and $[Co(aptsz)_2I_2]$ were available, the spectra were recorded on frozen glasses.

In Figs. 5.1 and 5.2 the E.P.R. spectra of $[Co(atsz)_2Cl]Cl.H_2O$ and $[Co(atsz)_2H_2O]I_2.H_2O$ are reported. Both spectra are axial and have a strikingly identical ^{59}Co hyperfine structure on the $g_{//}$ region ($A_{//}$ = 108 G). Some difference is only observed in the g-values (see Table 5.2) probably due to the different covalency rather than to a difference in geometry. Both spectra were recorded as frozen glasses, the first being

FIG. 5.3 X-Band E.P.R. spectrum of $[Co(aptsz)_2I_2]$ dissolved in acetone. Temperature 10 K, power 5 mW.

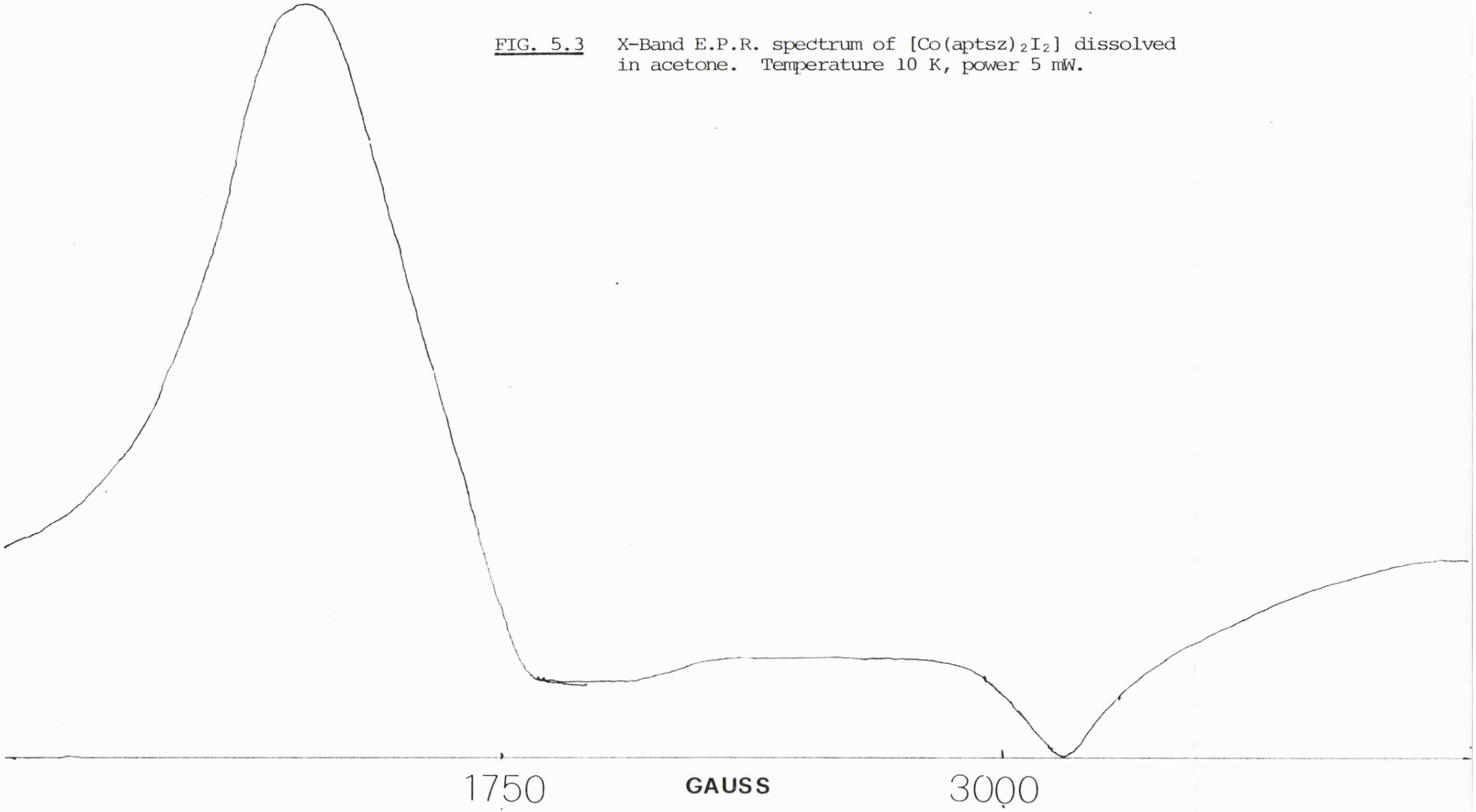

FIG. 5.4 X-Band E.P.R. spectrum of $[Co(Im)_2(CH_3CO_2)_2]$ dissolved in water. Temperature 10 K, power 5 mW.

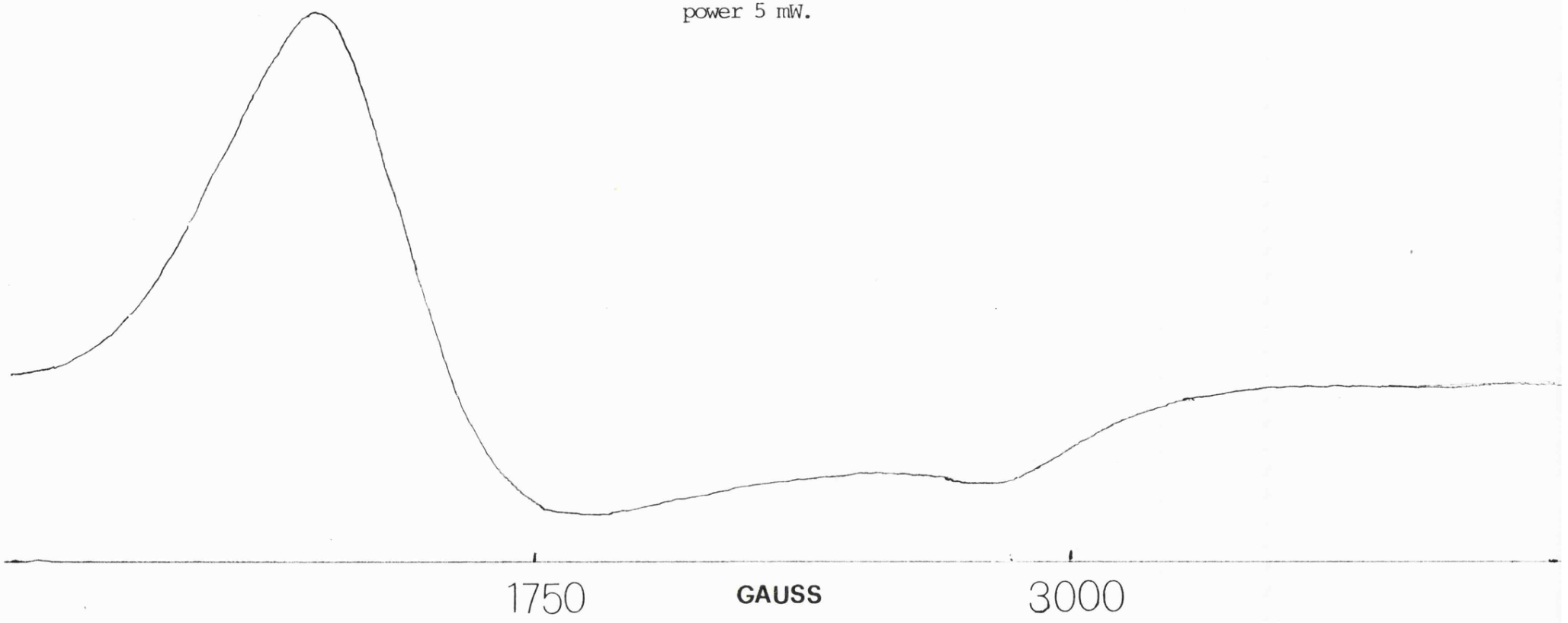

dissolved in EtOH and the second in acetone. It is interesting to notice that $[Co(atsz)_2Cl]Cl.H_2O$ changed colour (blue → violet) on freezing, presumably due to a displacement of the Cl^- by an EtOH, the coordination remaining the same.

The frozen solution spectra of the tetrahedral $[Co(aptsz)_2I_2]$ dissolved in acetone also gives a virtually axial spectrum (Fig. 5.3) but without any evidence of hyperfine structure. The strong C_2 distortion present in this complex in the solid state seems not to be reflected in the E.P.R. spectrum; this may be an indication that the structure is more regular in solution. Similarly, $[Co(Im)_2(CH_3CO_2)_2]$ with a pseudo-tetrahedral CoN_2O_2 stereochemistry, dissolved in water gives a virtually axial spectrum without any evidence of hyperfine structure (Fig. 5.4). By way of contrast $[Co(\gamma\text{-pic})_2Br_2]$, again pseudo-tetrahedral in structure, has a clearly rhombic spectrum but no evidence of hyperfine structure (Fig. 5.5). A δ value of 6-8 cm^{-1} (see Table 5.2) is obtained for this sample using the procedure previously described.

These differences which may, in part, be due to "relaxation" of the variously distorted structures between the solid state and solution suggest that either the local symmetry about the Co(II) changes on going down to low temperature or that there are more subtle stereochemical changes due to activity of the low-energy states close to the ground state, giving rise to spectral differences even between closely related pseudo-tetrahedral structures.

The spectrum of $[Co(etu)_2(CH_3CO_2)_2]$ (Fig. 5.6) was recorded because it is one of the few Co(II) complexes with a pseudo-tetrahedral structure but having, in addition, two long-bonded ligands (i.e. two oxygen atoms of the acetate groups) and which is already known to exert a significant influence on the optical spectrum [9]. Its E.P.R. spectrum is rhombic

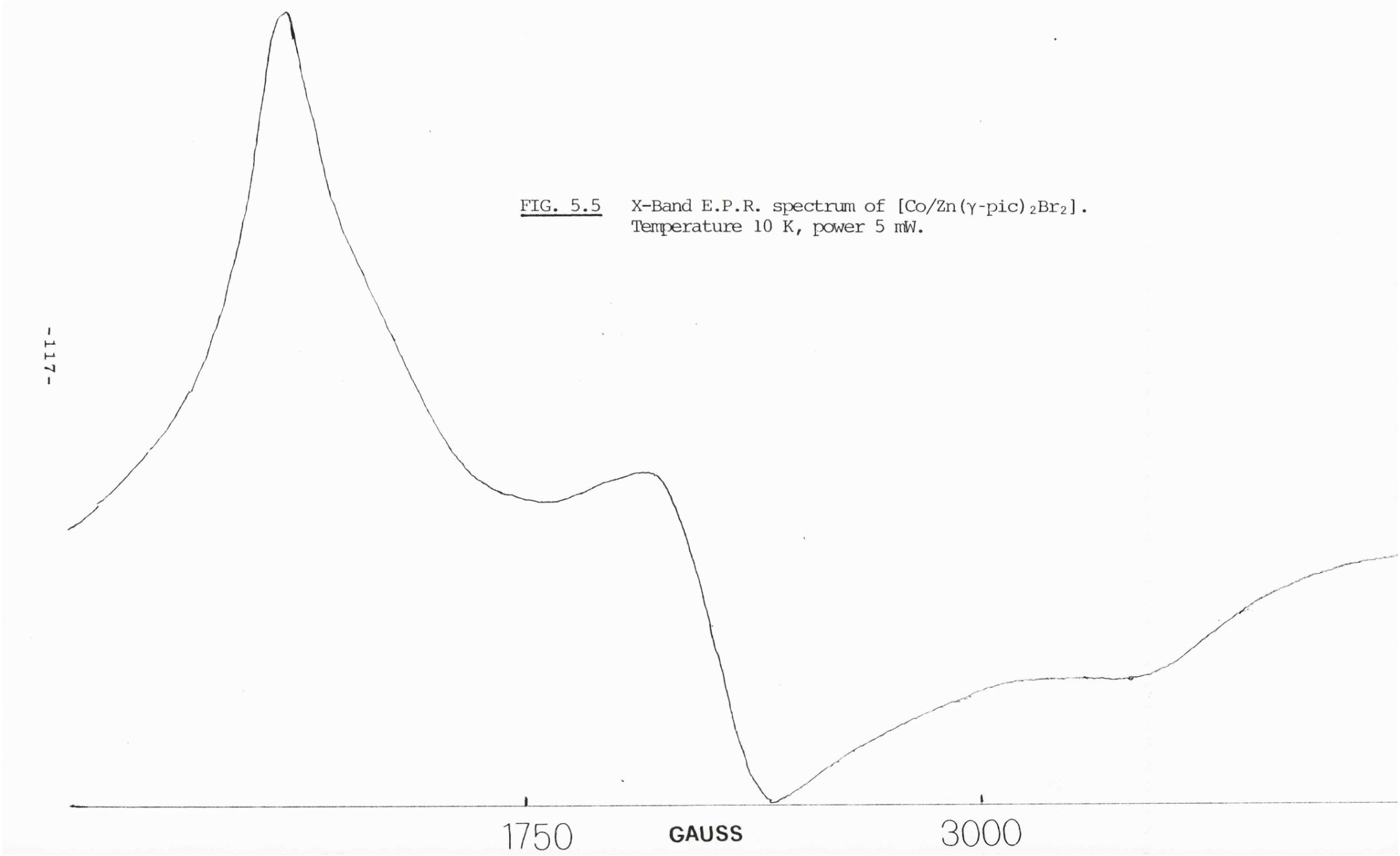

FIG. 5.5 X-Band E.P.R. spectrum of [Co/Zn(γ-pic)$_2$Br$_2$]. Temperature 10 K, power 5 mW.

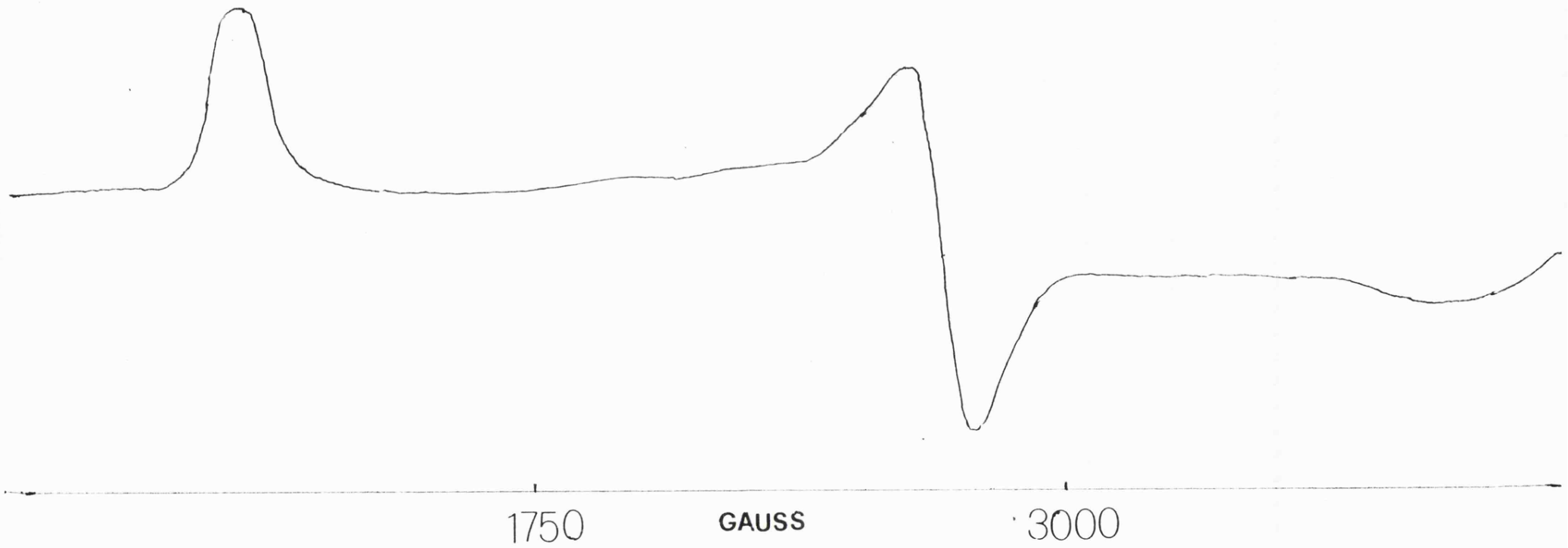

FIG. 5.6 X-Band E.P.R. spectrum of $[Co/Zn(etu)_2(CH_3CO_2)_2]$. Temperature 10 K, power 5 mW.

and by application of the above mentioned calculation, leads to a δ value of 32-42 cm^{-1} (Table 5.2).

The spectrum of $[Co(atsz)Cl_2]$, a low symmetry complex with a $CoNSCl_2$ chromophore, is more complicated. At ca. 10 K there is evidence for the presence of at least two species (Fig. 5.7) whose g-values are assigned as: $g'_x = 5.88$, $g'_y = 2.61$, $g'_z = 1.70$ (A) and $g'_x = 4.43$, $g'_y = 3.39$, $g'_z = 1.91$ (B). Other assignments are possible but would lead to very low g-values (<1.9) in the $S = \frac{3}{2}$ notation. Both centres show clear ^{59}Co hyperfine structure. With increase in temperature, there was little obvious difference in intensity between the two signals, both becoming very indistinct at 15 K. Nevertheless a simple phase change would be expected to give rise to a single site on going to low temperature, which does not appear to occur.

The Figs. 5.1 to 5.7 show that the E.P.R. spectra of Co(II) high spin complexes are difficult to interpretate as subtle stereochemical changes can produce big differences in the shape of the spectra. Nevertheless, looking at Table 5.2, where the $g_{//}$ and $g_{\perp}$ in the $S = \frac{3}{2}$ scheme and the γ and δ values calculated using equations 4-6 are reported, it is possible to observe some differences in the E.P.R. spectra of tetrahedral and pentacoordinated compounds. In Table 5.2 the E.P.R. parameters of other cobalt complexes recorded by other authors [10-12] but which were analyzed by the procedure previously described, are given.

Firstly the difference of δ values is immediately apparent, low values up to 17 cm^{-1} being associated with tetracoordinated species, whilst higher values of 50-80 cm^{-1} are associated with pentacoordination. Moreover pentacoordinated species are characterized by the presence of quite high values of ^{59}Co hyperfine coupling but which seems to be completely absent for the tetrahedral environments. The $[Co(atsz)Cl_2]$ complex, which is known to have a distorted tetrahedral geometry from

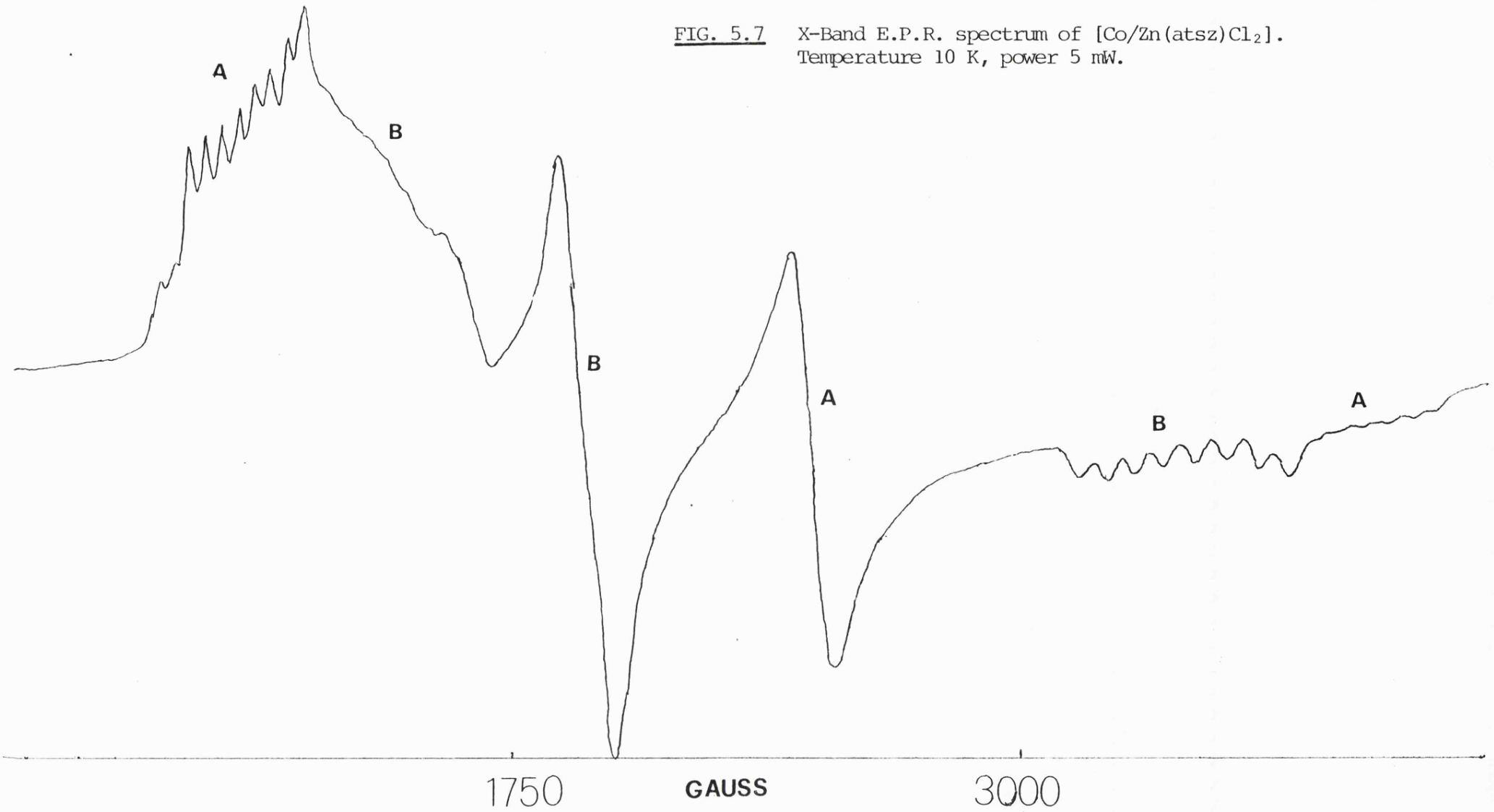

FIG. 5.7 X-Band E.P.R. spectrum of [Co/Zn(atsz)Cl_2].
Temperature 10 K, power 5 mW.

TABLE 5.2

Experimental and Calculated E.P.R. Parameters of High Spin Co(II) Complexes

COMPLEX [a]	g'_x	g'_y	g'_z	A'_x (cm^{-1})	A'_y (cm^{-1})	A'_z (cm^{-1})	$g_{//}$	$g_\perp$	β^2	γ	δ [b] (cm^{-1})	Ref.
PENTACOORDINATE												
$[Co(Et_4dien)Cl_2]$	7.08	2.53	1.59	0.030	0.006	0.009	2.19	2.58	0.931	0.357	81-62	10
$[Co(terpy)Cl_2]$	5.93	3.53	1.88	0.014	0.004	0.009	2.05	2.41	0.979	0.171	67-50	10
$[Co(atsz)_2Cl]Cl.H_2O$	4.04	4.04	1.94	0.010								This work
$[Co(atsz)H_2O]I_2.H_2O$	4.21	4.21	1.99	0.010								" "
TETRACOORDINATE												
$[Co(aptsz)_2I_2]$	3.86	3.86	2.07									" "
$[Co(\gamma\text{-pic})_2Br_2]$	5.88	2.95	1.93				2.29	2.25	0.965	0.228	8-5	" "
$[Co(Im)_2(CH_3CO_2)_2]$	4.18	4.18	2.29									" "
$[Co(m\text{-}OMeA)_2Cl_2]$	5.67	3.17	2.00				2.24	2.27	0.974	0.194	6-4	11
$[Co(p\text{-}OMeA)_2Br_2]$	5.25	3.81	2.15				2.23	2.28	0.991	0.107	9-7	11
$[Co\,py_2\,Cl_2]$	6.08	2.68	1.79				2.21	2.30	0.952	0.260	17-13	12
$[Co(2,4\text{-}lu)_2Br_2]$	6.79	1.65	1.29				2.30	2.37	0.890	0.450	16-12	12
$[Co(atsz)Cl_2]$ (A)	5.88	2.61	1.70	0.004	0.006	-	2.11	2.23	0.952	0.260	24-17	This work
(B)	4.43	3.39	1.91	0.005	-	0.007	1.96	1.97	0.994	0.090	1-0.8	" "
INTERMEDIATE												
$[Co(etu)_2(CH_3CO_2)_2]$	6.17	2.58	1.66	-	-	-	2.10	2.31	0.947	0.306	42-32	" "

[a] Abbreviations used: Et_4dien = N,N,N',N'-tetraethylenetriamine; terpy = terpyridyl; m-OMeA = m-methoxyaniline; p-MeA = p-methylaniline; py = pyridine; 2,4-lu = 2,4-lutidine.

[b] For $\lambda' = -179$ and -135 cm^{-1} respectively.

room temperature crystal structure data [8], seems to escape from this classification. The sample gives rise to two species both having a quite large hyperfine coupling, one of them showing the largest δ value for any of the tetrahedral complexes in Table 5.2. It is difficult to explain these data, but the presence of two different E.P.R. signals in a sample that has a clear and definite structure at room temperature, indicates some change in geometry and probably also in the Co(II) ligand environment at 10 K thus rendering impossible any correlation between structure and E.P.R. parameters.

Particularly interesting are the results obtained for $[Co(etu)_2(CH_3CO_2)_2]$, a complex having pseudo-tetrahedral geometry, but with two long-bonded ligands. The spectrum is rhombic and the calculated zero-field splitting δ lies between those found for the tetracoordinate and the pentacoordinate compounds.

At this point, having obtained an empirical correlation (Table 5.2) between the magnitude of the δ value and the geometry of the cobalt chromophore, it is possible to analyze the E.P.R. spectra of some cobalt derivatives of metalloproteins so as to have further information on their structure. In this way, the iodo derivative and the low and high pH forms of Co(II)BCA were investigated. Many physical and spectroscopic measurements have been previously carried out at the metal site of CoBCA in order to elucidate the bonding and the stereochemistry at the metal site. This has led to the hypothesis that Co(II) has pseudotetrahedral or pentacoordinate structure [13,14]. In a M.C.D. study, a change from tetrahedral to a pentacoordinate geometry has been hypothesised for the Co(II)BCA on passing from acid to alkaline pH [15]. On the other hand, based on optical spectra, a substantially tetrahedral structure for both the low and high pH forms was assigned and a temperature dependent equilibrium between tetra- and penta- coordination was suggested for the

iodo derivative [16]. To gain more information about these suggestions, an E.P.R. investigation seemed very useful.

In Figs. 5.8-10 the E.P.R. spectra at 10 K of Co(II)BCA at pH 6 and 9.5 and in the presence of 0.1 M NaI at pH 6.0 are shown. The spectrum of the low pH form shows axial symmetry with $g_{\perp}$ ca. 4 and $g_{//}$ ca. 2. In this case the δ parameter cannot be measured, but the axial shape of the spectrum, without any evidence of hyperfine structure, is consistent with a pseudotetrahedral geometry. On the other hand, the spectra of the iodo derivative and of the high pH form both show rhombic distortion. The spectrum of the iodo derivative exhibits also a clear hyperfine structure of about 92 gauss on the low field component, due to the cobalt nuclear spin $I = 7/2$. The γ and δ values of these two samples together with the other E.P.R. parameters are reported in Table 5.3. Their δ value ranges between those found for tetracoordinate and pentacoordinate compounds reported in Table 5.2, and is very similar to that found for $[Co(etu)_2(CH_3CO_2)_2]$, a complex with pseudo-tetrahedral geometry but with long-bonded ligands. A similar value of δ has been measured by magnetic susceptibility for the acetazolamide complex of Co(II)BCA [17] and it was considered to be indicative of pentacoordination. Other evidence favouring pentacoordination is the presence of hyperfine structure in the iodide derivative which seems to be absent in tetracoordinate compounds (see Table 5.2 and ref. 10). All these indications suggest a pentacoordinate structure for the two cobalt carbonic anhydrase derivatives probably with a fifth ligand far removed as suggested by the similarity of the δ value found with the $[Co(etu)_2(CH_3CO_2)_2]$ model compound. This assignment is in agreement with the hypothesis of an intermediate pentacoordinate form in the enzymic reaction of carbonic anhydrase [18].

These results provide some evidence that the zero-field splitting

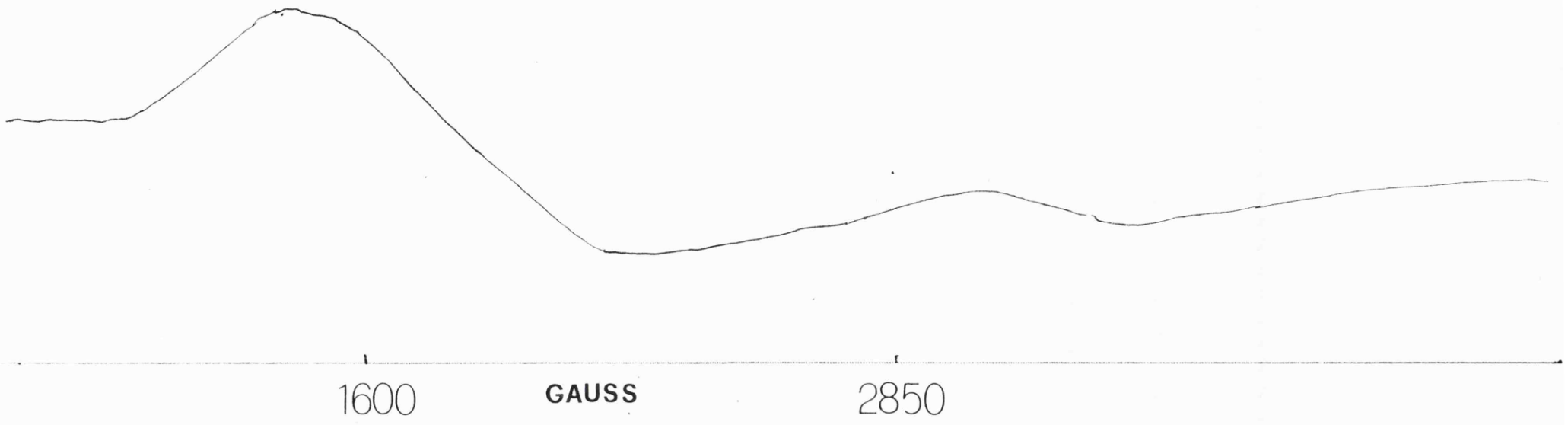

FIG. 5.8 X-Band E.P.R. spectrum of 0.9 mM Co(II)BCA in water at pH 6.0. Temperature 10 K, power 5 mW.

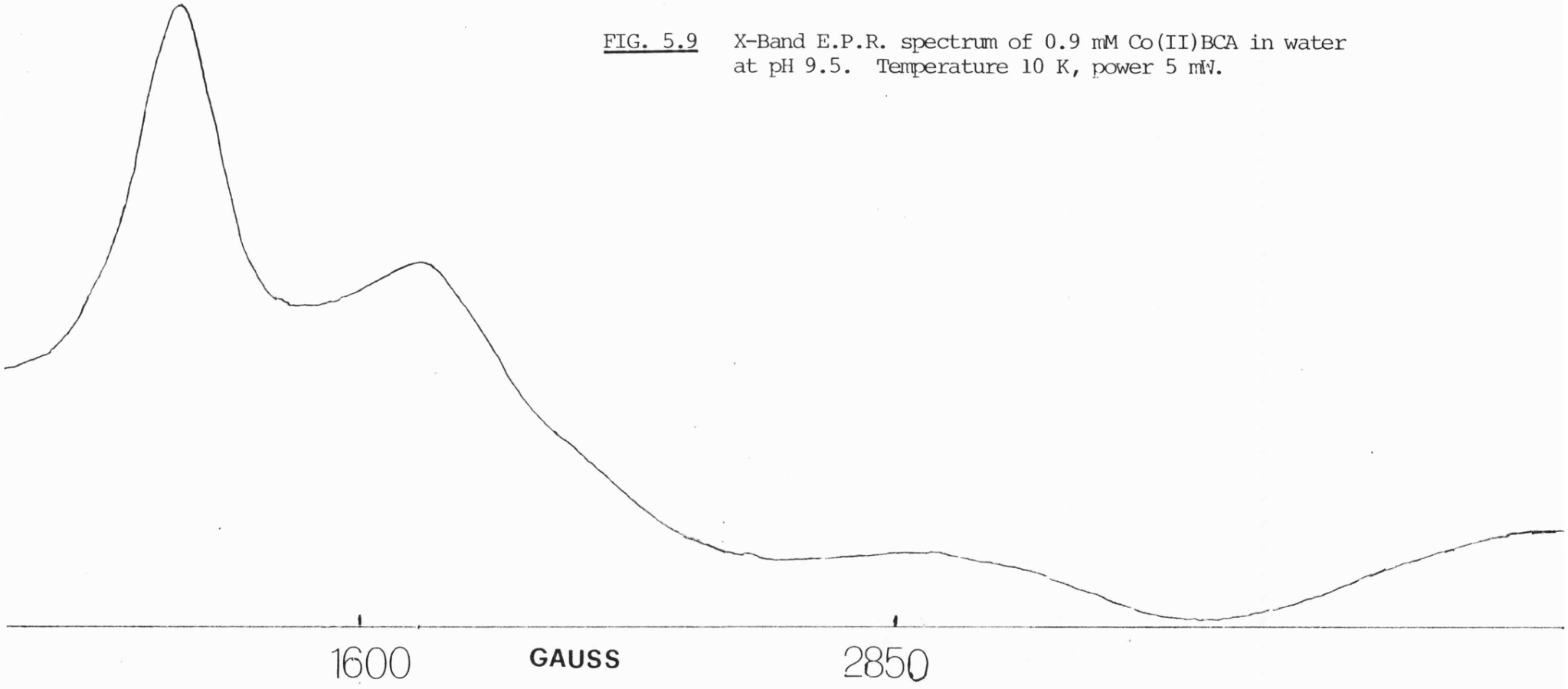

FIG. 5.9 X-Band E.P.R. spectrum of 0.9 mM Co(II)BCA in water at pH 9.5. Temperature 10 K, power 5 mW.

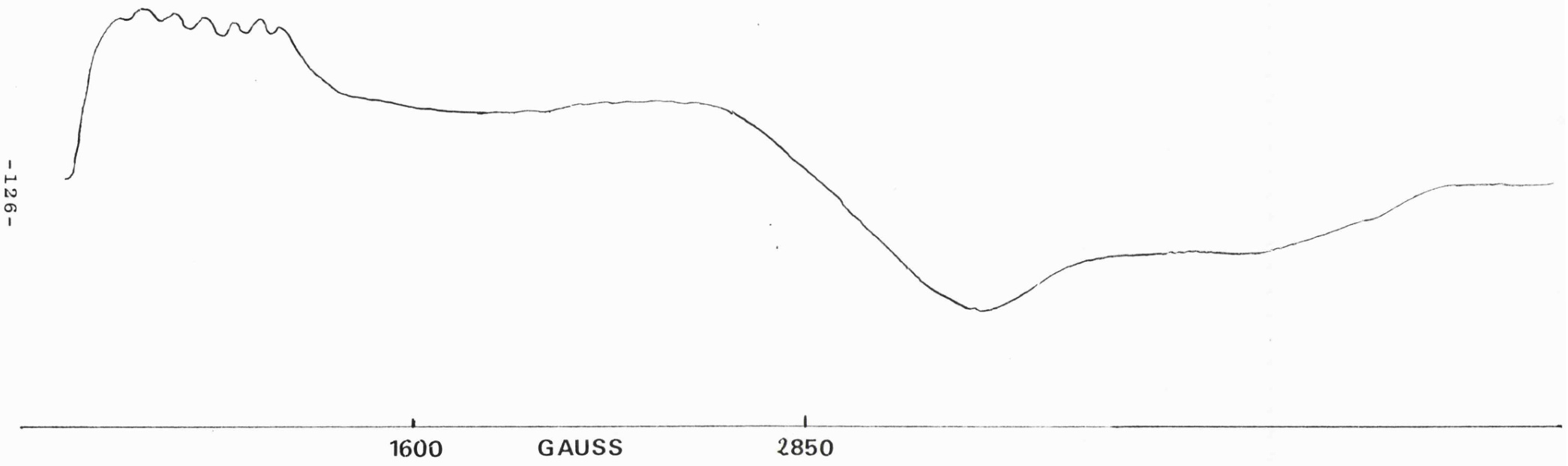

FIG. 5.10 X-Band E.P.R. spectrum of 0.9 mM Co(II)BCA at pH 6.0 in presence of 0.1 M NaI. Temperature 10 K, power 5 mW.

TABLE 5.3

Experimental and Calculated E.P.R. Parameters of High Spin Co(II) Carbonic Anhydrase Derivatives

COMPOUND	g'_x	g'_y	g'_z	A'_x (cm^{-1})	A'_y (cm^{-1})	A'_z (cm^{-1})	$g_{//}$	$g_\perp$	β^2	γ	δ[a]
Co BCA-I	6.82	2.26	1.56	0.009	-	-	2.25	2.46	0.923	0.362	44-33
Co BCA-OH	5.60	3.20	1.85	-	-	-	2.04	2.25	0.976	0.190	39-30

[a] For $\lambda' = -179$ and -135 cm^{-1}.

value can be used diagnostically for the assignment of the geometry, but some caution must be used when E.P.R. spectroscopy alone is used, mainly because of the possible structural changes that might take place at low temperature. This is clearly shown by the behaviour of the $[Co(atsz)Cl_2]$ complex where the temperature induces some geometrical changes.

B. Reaction of Native Bovine Carbonic Anhydrase and of the Cu(II) and Co(II) Derivatives with Diethyldithiocarbamate

The interest in the reaction of sodium diethyldithiocarbamate (DDC hereafter), a well-known metal chelating agent, with metallo-enzymes has recently increased, since it was shown to inhibit *in vivo* [19] the enzyme superoxide dismutase and to react with its copper ions [20]. The latter reaction was described as a biphasic process, consisting of the formation of an active enzyme-DDC complex with particular spectral properties, followed by abstraction of copper from the enzyme by DDC and loss of the catalytic activity. Such conclusions were not entirely confirmed by further experimental work [21], in particular, the formation of the enzyme-DDC adduct in significant amounts was excluded. In connection with these results, a more general approach to the reactions of enzyme-bound metals with DDC and to the spectral properties of DDC complexes of copper proteins seemed worthwhile. As a first step, the behaviour of carbonic anhydrase, a Zn(II)-containing enzyme, and of its derivatives containing Co(II) or Cu(II) substituted at the Zn site in the presence of DDC was investigated in order to gain a better understanding of the mechanism of the *in vivo* inhibition by DDC of Zn- and Cu-enzymes [22].

The p-nitrophenylacetate hydrolase activity of bovine carbonic anhydrase was inhibited by DDC and an inhibition constant K_i = [Enzyme.DDC]/[Enzyme]-[DDC] = 1.7×10^3 M^{-1} was measured in 0.05 M tris-sulphate buffer pH 7.6 at 30°C (Fig. 5.11). A mM solution of the enzyme, dialyzed against 10^{-2} M DDC at pH 6.0 in phosphate buffer and at pH 9.0 in borate buffer for 24 hours at 5°C showed no decrease of activity after removal of DDC by subsequent dialysis against the same buffer. This indicated that the process of DDC binding to the enzyme is completely reversible and does not produce any loss of Zn.

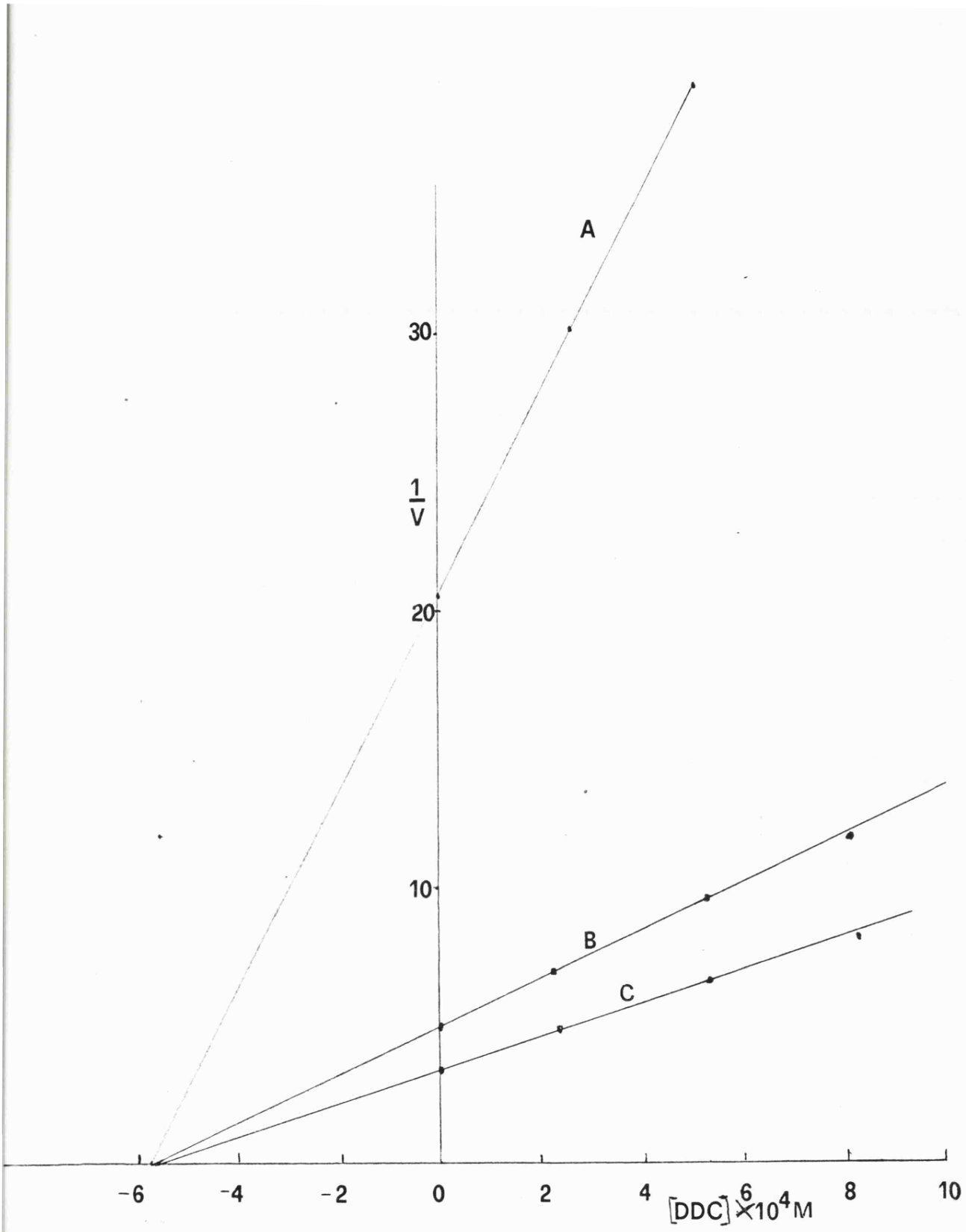

FIG. 5.11 Plot of the reciprocal velocity of the enzymatic activity toward p-nitrophenylacetate against the concentration of the inhibitor. Protein 3×10^{-7} M pH 7.6; p-nitrophenylacetate 0.18×10^{-3} M. curve a, 0.55×10^{-3} M. curve b, 1.1×10^{-3} M. curve c.

The p-nitrophenylacetate hydrolase activity of the Co(II)-bovine carbonic anhydrase was also inhibited by DDC and a DDC concentration one order of magnitude lower than for the native Zn enzyme was required to obtain a comparable effect. However, a precise value for the inhibition constant could not be obtained in 0.05 M tris-sulphate buffer pH 7.6 since the dependence of the reciprocal velocity on the DDC concentration was not linear, which was interpreted as due to the occurrence of concomitant reactions. In fact, addition of DDC to the Co(II)-enzyme in unbuffered aqueous solution (pH 6.2) produced a large change of the electronic visible spectrum, followed by the almost immediate formation of a green precipitate, likely to be a Co-DDC complex. The reaction was not studied in detail, but higher than stoichiometric molar DDC excesses over the metal ion brought about substantial metal removal from the protein.

When DDC was added to the Co(II)-enzyme in an unbuffered aqueous solution brought to pH 9.5 by addition of 0.2 M NaOH, no precipitate was formed, even on addition of a 40-fold molar DDC excess. Fig. 5.12 shows a spectrophotometric titration of the Co(II)-enzyme with DDC at approximately pH 10. The presence of isosbestic points at 600 and 675 nm indicates that a single new species was formed. Its spectrum was characterized by two absorption bands with maximum absorbance at 510 and 570 nm ($\varepsilon = 175$ and 210 M^{-1} cm^{-1} respectively) and by a weaker absorption band at 700 nm ($\varepsilon = 35$ M^{-1} cm^{-1}, Fig. 5.12 insert). From the decrease of absorption at 640 nm a binding constant $K_{app} = 9 \times 10^2$ M^{-1} was calculated. This value was lower than expected from the inhibition experiments, but the difference is due to the well-known pH dependence of anion binding reactions of Co(II)-carbonic anhydrase [23]. On the other hand in the pH region where the DDC adduct of the Co(II)-enzyme is stable, the rate of

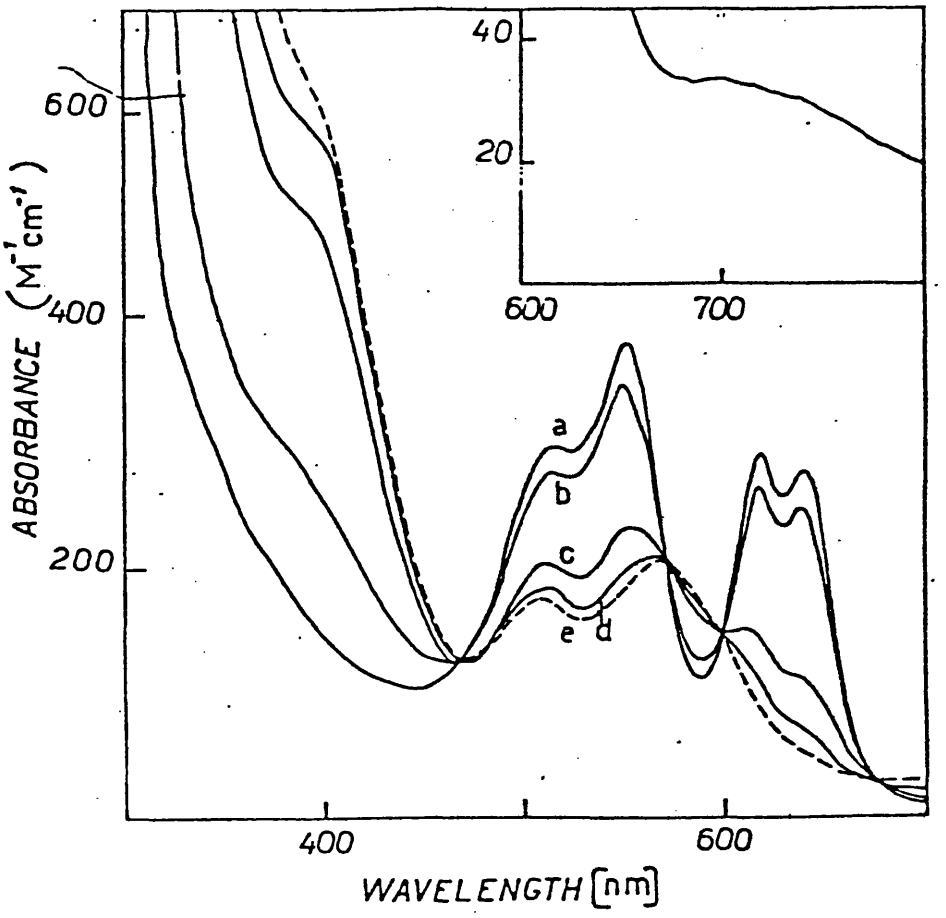

FIG. 5.12 Optical absorption spectra of DDC-treated Co(II)-bovine carbonic anhydrase. 1.0 mM enzyme in unbuffered aqueous solution pH 9.5 (a) and at the following mM DDC concentrations: 0.25 (b), 1.5 (c), 2.8 (d), 3.2 (e). Insert: a detail of spectrum (e).

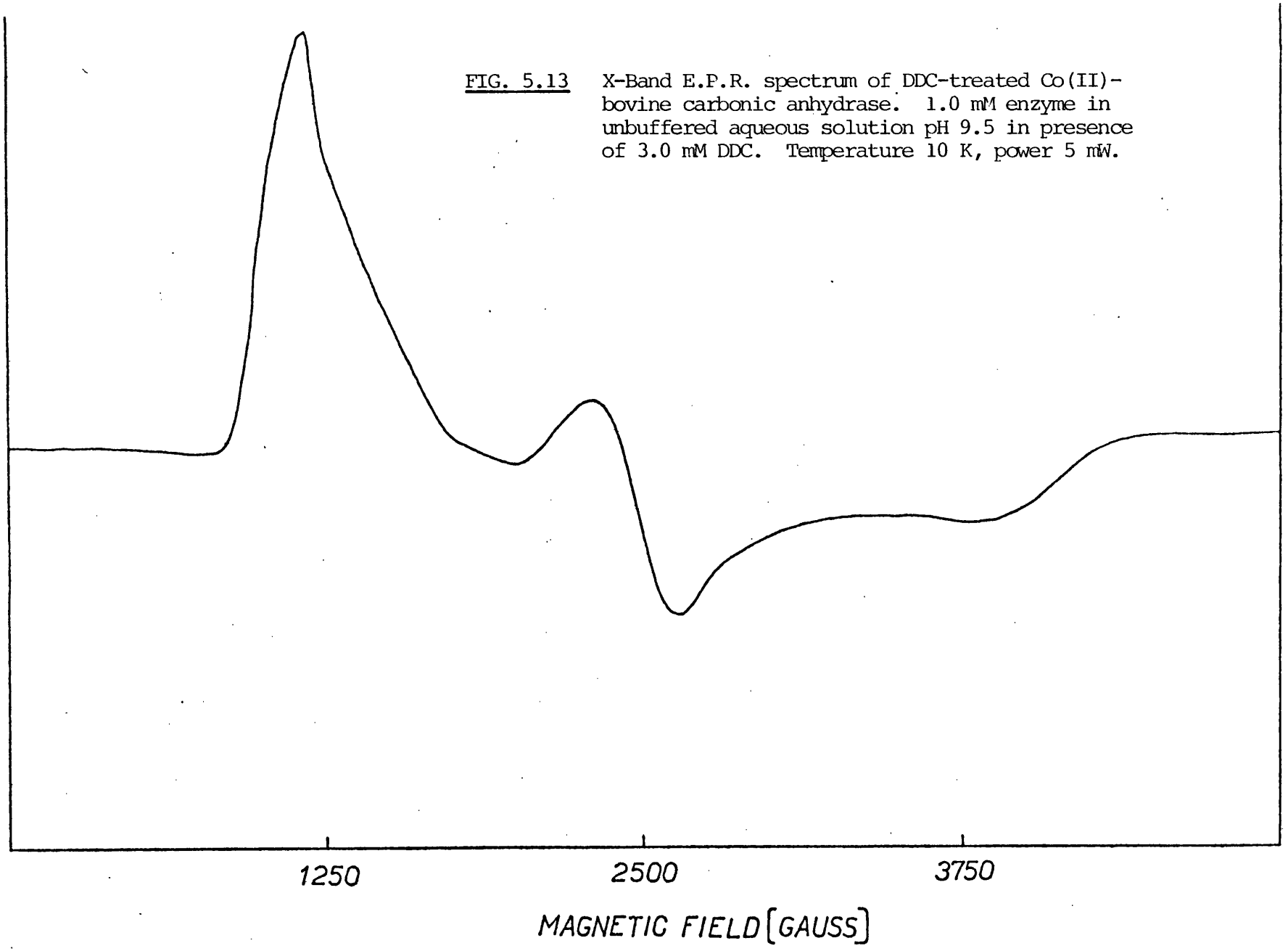

FIG. 5.13 X-Band E.P.R. spectrum of DDC-treated Co(II)-bovine carbonic anhydrase. 1.0 mM enzyme in unbuffered aqueous solution pH 9.5 in presence of 3.0 mM DDC. Temperature 10 K, power 5 mW.

spontaneous hydrolysis of the p-nitrophenyl acetate is high, which makes measurements of the inhibition constant difficult. The E.P.R. spectrum (at 10 K) (Fig. 5.13) of 2.2 mM Co(II)-enzyme reacted with 5 mM DDC at pH 9.5 confirms that a single species characterized by a rhombic line shape is formed. Its E.P.R. parameters are reported in Table 5.4.

Nuclear magnetic relaxation experiments carried out by Rigo at Venice on a 2.2 mM aqueous enzyme solution at pH 9.5, showed a decrease of water proton relaxivity from $R = 1000\ s^{-1}\ M^{-1}$ to $R = 230\ s^{-1}\ M^{-1}$, on binding of one DDC molecule per Co(II).

Fig. 5.14 shows the optical spectra of the Cu(II)-enzyme reacted with increasing amounts of DDC in an unbuffered aqueous solution, at approximately pH 6.0. On addition of less than stoichiometric DDC an intense absorption band developed at 390 nm ($\varepsilon = 4300\ M^{-1}\ cm^{-1}$), apparently asymmetrical on the higher wavelength side. Concomitantly, the maximum of the Cu(II) d-d absorption band at 780 nm ($\varepsilon_{max} = 130\ M^{-1}\ cm^{-1}$) was shifted to lower wavelength and its intensity increased ($\lambda_{max} = 675$ nm, $\varepsilon_{max} = 350\ M^{-1}\ cm^{-1}$). At higher DDC concentrations a second, more intense band appeared at 440 nm and a dark-brown precipitate formed on standing. Centrifugation of the precipitate in conditions where both absorption bands were present caused the disappearance of only the 440 nm component. The E.P.R. spectra of stoichiometric DDC-protein mixtures in unbuffered aqueous solution, pH 6.0 (Fig. 5.15 and Table 5.5) showed that at least two species were always present, their relative weights depending on the different experimental conditions. While approximately equal amounts of the two species were present at room temperature (curve c), one was predominant in the frozen state (curve b) and the other in the lyophilized state (curve d). Changes of pH, from 6.0 to pH 10, were ineffective in this respect. In any case the spectra showed a superhyperfine multiplet

FIG. 5.14 Optical absorption spectra of DDC-treated Cu(II)-bovine carbonic anhydrase. 0.8 mM enzyme in unbuffered aqueous solution pH 6.0 (a) and at the following mM DDC concentrations: 0.4 (b), 0.8 (c), 1.2 (d), 3.6 (e). [The central scale refers to the absorbance of the dashed curve.]

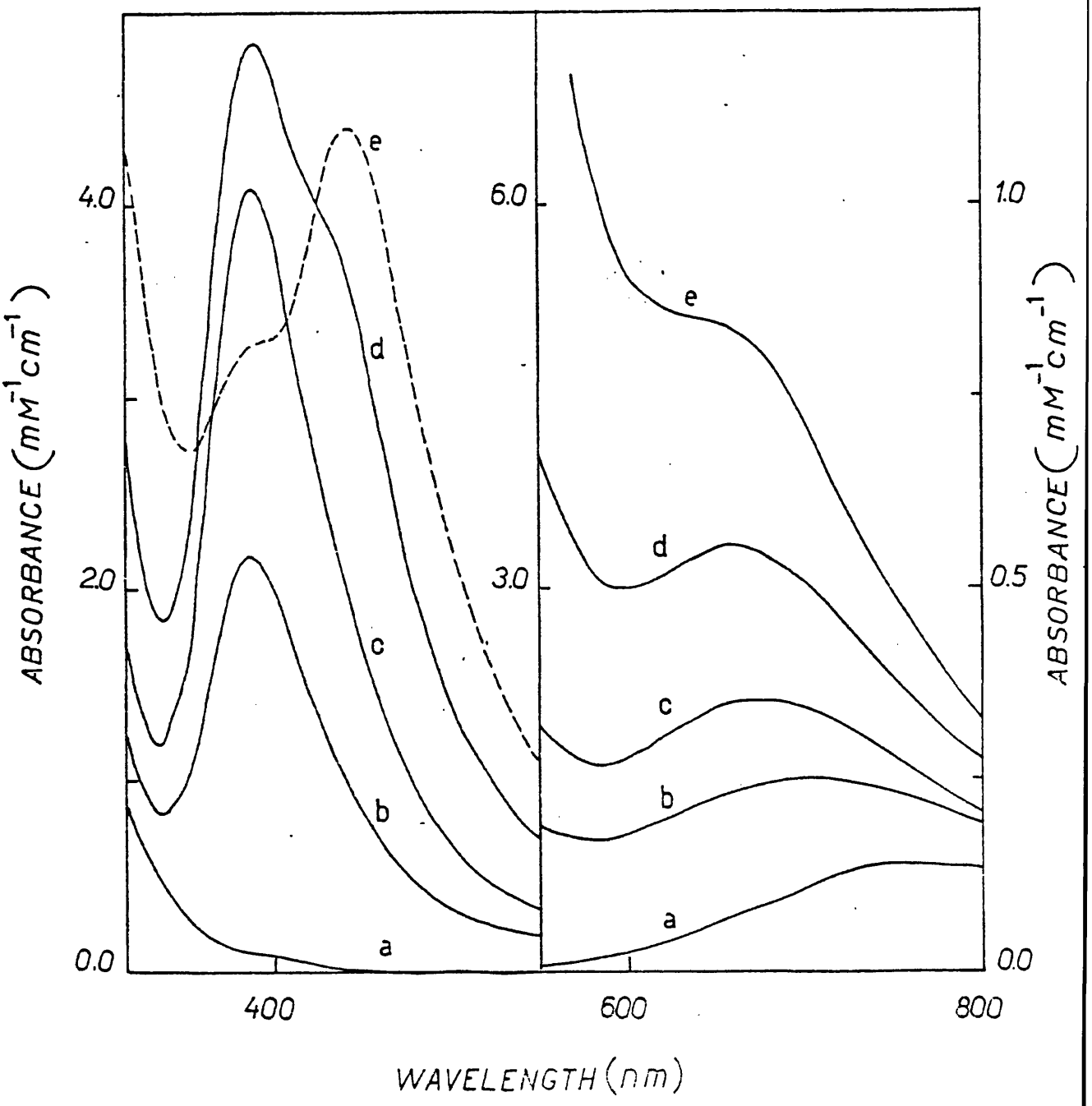

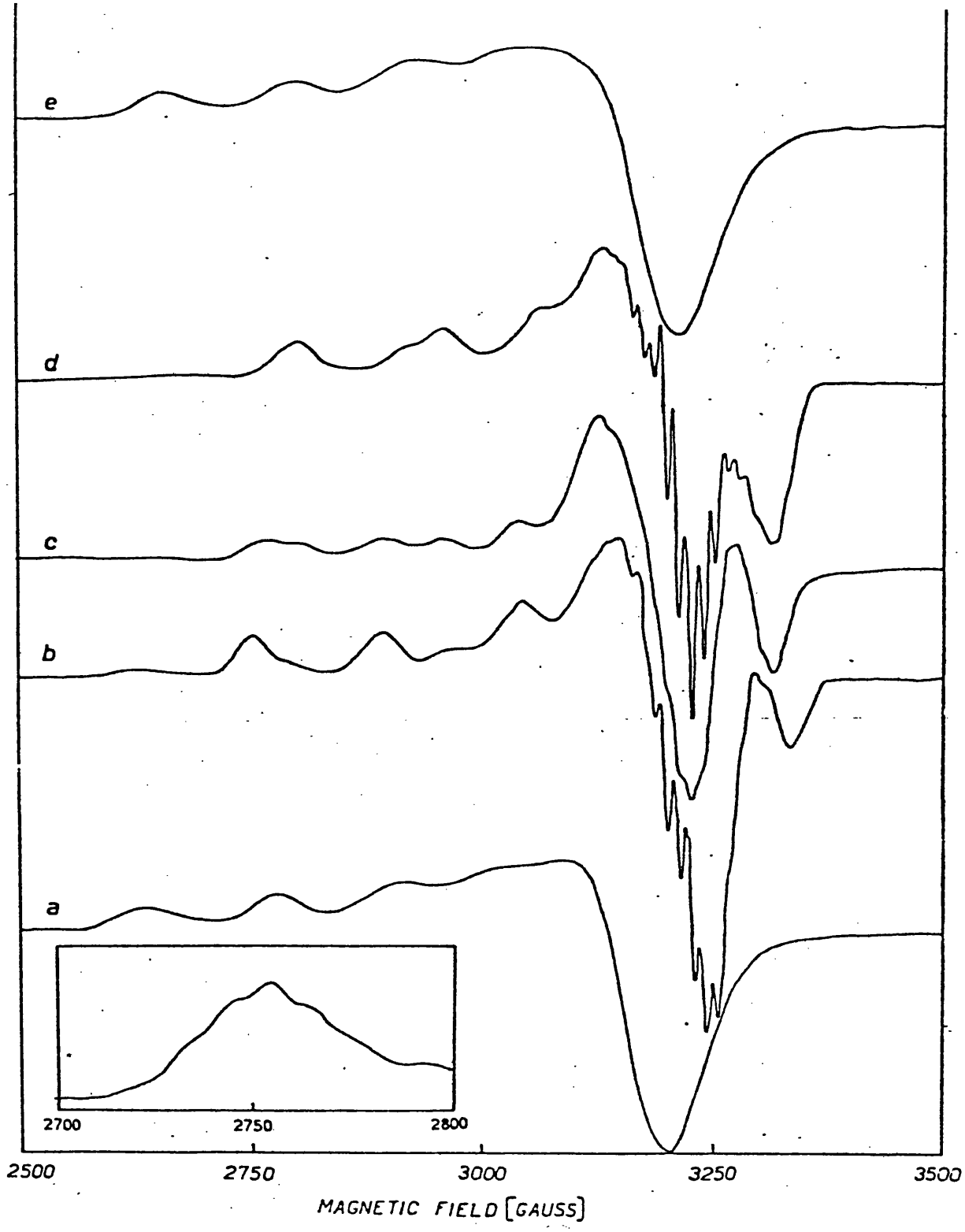

FIG. 5.15 ESR spectra of $^{63}Cu(II)$-bovine carbonic anhydrase and of DDC derivatives. 2.5 mM aqueous enzyme pH 6.0 measured at 77°K (a); plus 2.7 mM DDC measured at 77°K (b); same solution as in (b) measured at 25°C (c); same solution as in (b) lyophilized and measured at 25°C (d); same solution as in (a) lyophilized and measured at 25°C (e). 9.15 GHz frequency, 20 mwatts power, 10 Gauss modulation amplitude. Insert: first hyperfine line of spectrum (b) at higher instrument gain.

TABLE 5.4

E.P.R. parameters[a] of Co(II) carbonic anhydrase at pH 9.5

	g_x'	g_y'	g_z'	δ[b] (cm^{-1})
free enzyme	5.60	3.20	1.85	39-30
DDC adduct	5.61	2.69	1.71	27-20

[a] Determined graphically: g_z' on the high field minimum; g_y' on the central cross-over point; g_x' on the low field maximum.

[b] For $\lambda' = -179$ and -135 cm^{-1} respectively.

TABLE 5.5

E.P.R. parameters of ^{63}Cu(II) bovine carbonic anhydrase and of its DDC derivatives

Sample	$g_{//}$	$A_{//}$ (Gauss)
Free enzyme at 77°K	2.29	143
DDC-treated enzyme at 77°K	2.20	147
" " " at 25°C	2.19	142
" " " at 25°C	2.15	158
" " " lyophilized	2.15	158
Free enzyme lyophilized	2.28	139

structure on the $g_{\perp}$ line, with a 14 Gauss splitting typical of nitrogen coordination. A five lines superhyperfine pattern could be detected on the hyperfine line at lowest field of frozen samples (Fig. 5.15 insert), as expected for copper coordination to two in-plane magnetically equivalent nitrogen atoms. At higher [DDC]/[protein] ratio an isotropic E.P.R. signal at $g \simeq 2$ was progressively formed. This signal has already been shown [21] to be typical of the free Cu(II)-DDC chelate and, therefore, to indicate removal of the metal from the protein.

In unbuffered aqueous solution at pH 10, the formation of the free Cu(II)-DDC complex was slower and required a higher [DDC]/[protein] ratio than at lower pH. Less than 20% of the copper was in the form absorbing at 440 nm after one hour at [DDC]/[protein] = 3. Nuclear magnetic relaxation rate titrations at pH 10 have showed a decrease of water proton relaxivity from $R = 6350\ s^{-1}\ M^{-1}$ to $R = 1700\ s^{-1}\ M^{-1}$, on addition of DDC in slight excess over the stoichiometric concentration. The residual relaxivity was not affected by further titration with DDC up to a ratio [DDC]/[protein] = 4.

The results reported above show that DDC has a greater inhibition power toward the Co(II) than the native Zn(II)-enzyme. The Cu(II)-enzyme, which is inactive, reacts with DDC in a stoichiometric ratio. Cu(II) is easily extracted from the enzyme, whilst Co(II) is removed with some difficulty and Zn(II), the metal present in the native protein, is unaffected by DDC in any condition. This behaviour conforms to a general trend already observed with metallo-proteins as DDC was successfully employed in removing Cu from several copper enzymes such as ceruloplasmin [24], amine oxidase [25], and superoxide dismutase [21], whilst protein-bound Zn is rather inert toward ligand substitution by metal chelating agents in the case of carbonic anhydrase [26]. This depends on many

factors such as the stability constants of metal-ligand, enzyme-metal-ligand and enzyme-metal complexes. The apo-carbonic anhydrase binding constant for Zn(II) is approximately 10^3 larger than that for Co(II) [27]. Kinetic factors must also be considered [26]. Therefore, the inhibition of copper and zinc enzymes, observed to occur in vivo [19,22], in the case of copper may be actually due to removal of the metal from the enzymes [21], but in the case of zinc may also be due to formation of ternary complexes. In the latter case reactivation by metal re-addition is not a reconstitution effect, but a displacement of DDC from the ternary complex with protein bound zinc.

In the Co(II) carbonic anhydrase the metal is bound, as in the native enzymes, to three hystidyl residues and to one water molecule [28]. Due to the presence of water, or OH^- at alkaline pH, in the metal coordination sphere, the enzyme enhances the nuclear magnetic relaxation rate of water solutions [29,30]. On addition of DDC, such an effect is nearly abolished, indicating that, in the conditions used in the present work, water or OH^- is displaced by incoming DDC. Since DDC is a bidentate chelate ligand, it seems obvious that the Co(II) is pentacoordinate in the DDC adduct. This is confirmed by some features of the optical spectrum (Fig. 5.12), such as its relatively low intensity ($\varepsilon_{max} = 200\ M^{-1}\ cm^{-1}$) and the presence of a very weak absorption band at 700 nm [30]. The latter can be identified as an ^4F-^4F transition that occurs at such high energy as in the present case only in pentacoordinate Co(II) complexes [30]. The E.P.R. spectrum (Fig. 5.13) does not conflict with this assignment. The zero-field splitting value of 20-27 cm^{-1} (Table 5.4), is compatible with a pentacoordinate structure, although it cannot exclude a pseudo-tetrahedral or other distorted structures (see Part A).

In the Cu(II)-DDC derivative the formation of a ternary enzyme-Cu(II)-

DDC adduct on addition of stoichiometric ligand is supported by the appearance of a charge transfer band at 390 nm (Fig. 5.14). At higher [DDC]/[Cu(II)] ratios a band at 440 nm is formed, which is typical of the free Cu(II)-DDC complex [20,21]. Also the E.P.R. spectra unequivocally show the formation of the ternary adduct at stoichiometric [DDC]/[Cu(II)] ratio. In fact, the superhyperfine pattern on the $g_{\perp}$ line indicates the presence of nitrogen ligands, provided by the protein histidyl residues, in the metal coordination sphere. Furthermore, the lowest field hyperfine line of the frozen sample shows a distinct five-line pattern which is diagnostic of coordination by two in-plane magnetically equivalent nitrogen atoms. The same pattern was observed with the $(CN)_2$-Cu(II)-carbonic anhydrase complex, for which a five-coordinate structure was suggested, where two in-plane nitrogens are provided by the protein histidines and the other two in-plane ligands by CN^- [31]. In the DDC complex the other two in-plane positions are occupied by the bidentate sulphur ligand, as shown by the shift of $g_{//}$ and $A_{//}$, respectively to a smaller and larger value than in the unreacted enzyme. Such shifts are theoretically related to the binding of electron-rich sulphur ligands [32,33]. In this context a crucial question is why two different adducts are formed and what is the difference between them. Cu(II)-carbonic anhydrase is known to bind monovalent anions without loss of coordinated water, whilst bidentate ligands, such as oxalate cause a decrease of the enzyme contribution to water relaxivity [34]. On addition of DDC to Cu(II)-enzyme solutions, the decrease of relaxivity peculiar to bidentate ligands is observed, but a large residual relaxivity is left, even in the presence of excess DDC. This may indicate that a fraction of enzyme molecules retain coordinated water, as also reported to occur in Co(II) carbonic anhydrase adducts with some monovalent anions [30]. In the

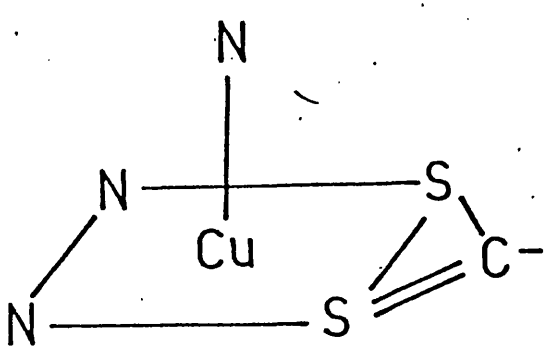

STRUCTURE 1

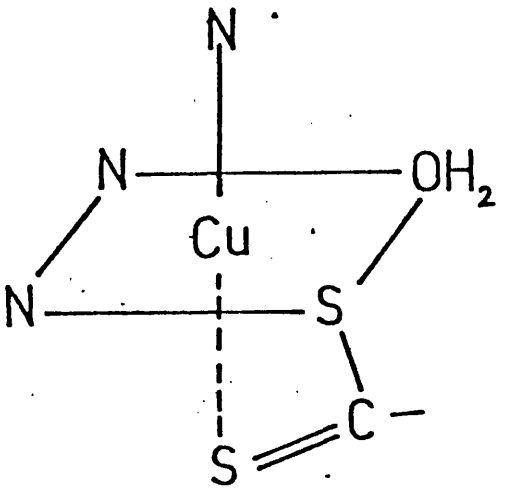

STRUCTURE 2

FIG. 5.16 Proposed schematized structures for the DDC-Cu(II)-enzyme in the lyophilized state (structure 1) and in the frozen state (structure 2).

present case, the equilibrium between water-free and water-bound molecules appears to be shifted by freezing in favour of the latter and by lyophilization in favour of the former ones. Since the shift of E.P.R. parameters is larger in lyophilized than in frozen samples (Table 5.5), it may be assumed that both sulphur atoms from DDC are bound in the Cu(II) equatorial plane in the absence of coordinated water, and only one of them when coordination of water is retained. In the latter case, the second sulphur atom could be accommodated in an apical position, where it does not appreciably affect the E.P.R. parameters [33]. By also taking into account the superhyperfine structure from two in-plane nitrogens on the lowest field hyperfine line of the frozen sample spectrum (Fig. 5.15 insert) and its similarity to that of the dicyanide adduct [31], structures 1 and 2 can be tentatively assigned to the two species (Fig. 5.16). At higher [DDC]/[Cu(II)] ratio, removal of copper takes place as the Cu(II)-DDC complex and the corresponding optical and E.P.R. spectra are identical to those observed in the case of superoxide dismutase [20,21]. Thus the reaction with DDC of Cu(II)-carbonic anhydrase shows a distinct pattern which is not observed with the copper of superoxide dismutase [21] where no enzyme-bound DDC complex could be spectroscopically identified. The presence of diagnostic E.P.R. and optical spectra of ternary complexes makes Cu(II)-carbonic anhydrase a useful model for investigating the mechanism of reaction and inactivation of copper-containing enzymes with DDC.

REFERENCES

1. S. Lindskog, Structure and Bonding, 8, 153 (1970).

2. A. Abragam and B. Bleaney, 'The Electron Spin Resonance Spectra of Transition Metal Ions', O.U.P. (1970).

3. A. D. Liehr, J. Phys. Chem. 67, 1314 (1963).

4. M. Bonamico, G. Dessy, V. Fares and L. Scaramuzza, Cryst. Struct. Commun. 5, 605 (1976).

5. C. Bellitto, A. A. G. Tomlinson, C. Furlani and G. De Munno, Inorg. Chim. Acta 27, 269 (1978).

6. A. Gadet, C. R. Acad. Sci. (Paris) C272, 1299 (1971).

7. C. Fanfani, A. Nunzi and P. F. Zanazzi, Acta Cryst. (B) 28, 323 (1972).

8. M. Mathew and G. J. Palenik, Inorg. Chim. Acta 5, 349 (1971).

9. E. M. Holt, S. L. Holt and K. J. Watson, J. Am. Chem. Soc. 92, 2721 (1970).

10. F. S. Kennedy, H. A. O. Hill, T. A. Kaden and B. L. Vallee, Biochem. Biophys. Res. Comm. 48, 889 (1972).

11. V. K. Voronkova, M. M. Zaripov, Yu. V. Yablokov, A. V. Ablov and M. A. Ablova, Dokl. Akad. Nauk. SSSR 214, 377 (1974).

12. Yu. V. Yablokov, V. K. Voronkova, V. F. Shiskhov, A. V. Ablov and Zh. Yu. Vaisbein, Sov. Phys. Solid State 13, 831 (1971).

13. S. Lindskog and B. G. Malmstrom, J. Biol. Chem. 237, 1129 (1962).

14. A. E. Dennard and R. J. P. Williams, Trans. Metal Chem. 2, 115 (1966).

15. B. Holmquist, Biochemistry 16, 4591 (1977).

16. I. Bertini, C. Luchinat and A. Scozzafava, Inorg. Chim. Acta 22, 223 (1977).

17. R. Aasa, M. Hanson and S. Lindskog, Biochim. Biophys. Acta 453, 211 (1976).

18. K. K. Kannan, M. Petef, K. Fridborg, H. Cid-Dresdner and S. Lovgren, FEBS Letters 73, 115 (1977).

19. R. E. Heikkila, F. S. Cabbat and G. Cohen, J. Biol. Chem. 251, 2182 (1976).

20. H. P. Misra, J. Biol. Chem. 254, 11623 (1978).

21. D. Cocco, L. Calabrese, A. Rigo, F. Argese and G. Rotilio, J. Biol. Chem. (1981) in press.

22. D. A. Rigas, C. Eginitis-Rigas and C. Head, Biochem. Biophys. Res. Commun. 88, 373 (1970).

23. L. Morpurgo, G. Rotilio, A. Finazzi-Agro and B. Mondovi, Arch. Biochem. Biophys. 170, 360 (1975).

24. A. G. Morrell and I. H. Scheinberg, Science 127, 588 (1958).

25. B. Mondovi, G. Rotilio, M. T. Costa, A. Finazzi-Agro, E. Chiancone, P. E. Hansen and H. Beinhart, J. Biol. Chem. 242, 1160 (1967).

26. J. Hirose and Y. Kidani, Chem. Pharm. Bull. 26, 1768 (1978).

27. S. Lindskog and P. O. Nyman, Biochem. Biophys. Acta 85, 462 (1964).

28. S. Lindskog, L. E. Enderson, K. K. Kannan, A. Liljas, P. O. Nyman and B. Strandberg, Enzymes, 3rd. Ed. 5, 587 (1971).

29. M. E. Fabry, S. H. Koenig and W. E. Shillinger, J. Biol. Chem. 245, 4256 (1970).

30. I. Bertini, G. Canti, C. Luchinat and A. Scozzafava, J. Am. Chem. Soc. 100, 4873 (1978).

31. P. H. Haffner and J. E. Coleman, J. Biol. Chem. 250, 996 (1975).

32. W. E. Blumberg and J. Peisach, J. Chem. Phys. 49, 1793 (1968).

33. U. Sakuguchi and A. W. Addison, J.C.S. Dalton 600 (1979).

34. I. Bertini, G. Canti, C. Luchinat and A. Scozzafava, J.C.S. Dalton 1269 (1978).

CHAPTER 6

A γ-IRRADIATION INVESTIGATION OF NATIVE CARBONIC ANHYDRASE AND SUPEROXIDE DISMUTASE

The effect of high energy radiation upon simple metal complexes is usually to add an electron and thus reduce the charge on the metal. This is known to occur in, for example, γ-irradiated $K_2Zn(CN)_4$, $K_2Cd(SCN)_4$ and $K_2Cd(CN)_4$ [1,2] where a large and nearly isotropic hyperfine coupling to the metal atoms is found. A value of g of ca. 2 is readily observed in the electron spin resonance spectrum (e.s.r.) and shows that the unpaired electron is largely in an s orbital on the metal. In favourable cases, information may be obtained about the coordinating atoms and the stereochemistry of the ligands about the metal.

This technique has been applied to some metalloproteins, namely bovine carbonic anhydrase (BCA) and superoxide dismutase (SOD). These proteins are particularly interesting in that they are zinc proteins. The BCA has one zinc atom coordinated roughly tetrahedrally to three imidazolate bases and another group which is probably water [3]. SOD has one zinc and one copper atom joined by an imidazole bridge in a tetrahedral and distorted pentacoordinate structure respectively [4] (see also Chapter 1). Beside the native Superoxide Dismutase also the [Zn-•••]SOD and the complete apo-protein, where both the metals have been removed, have been irradiated. In this way it was possible to check any difference in the E.P.R. signal of the Zn^+ between the [Zn-Cu] and the [Zn-•••]SOD, and to detect any signal coming from the proteic part looking at the contribution of the γ-irradiated apo-protein. The enzymes were prepared as described in Chapter 2, and were irradiated in the lyophilized state and in aqueous solution at 77 K in a Vickrad ^{60}Co γ-ray source. The radiation dose was about 0.6 Mrad. After irradiation, care was taken not to warm up the sample while transferring it to the E.P.R. finger dewar.

The e.s.r. spectra of the pure solid enzymes before irradiation were free of signals except for native SOD which exhibited its typical Cu^{2+}

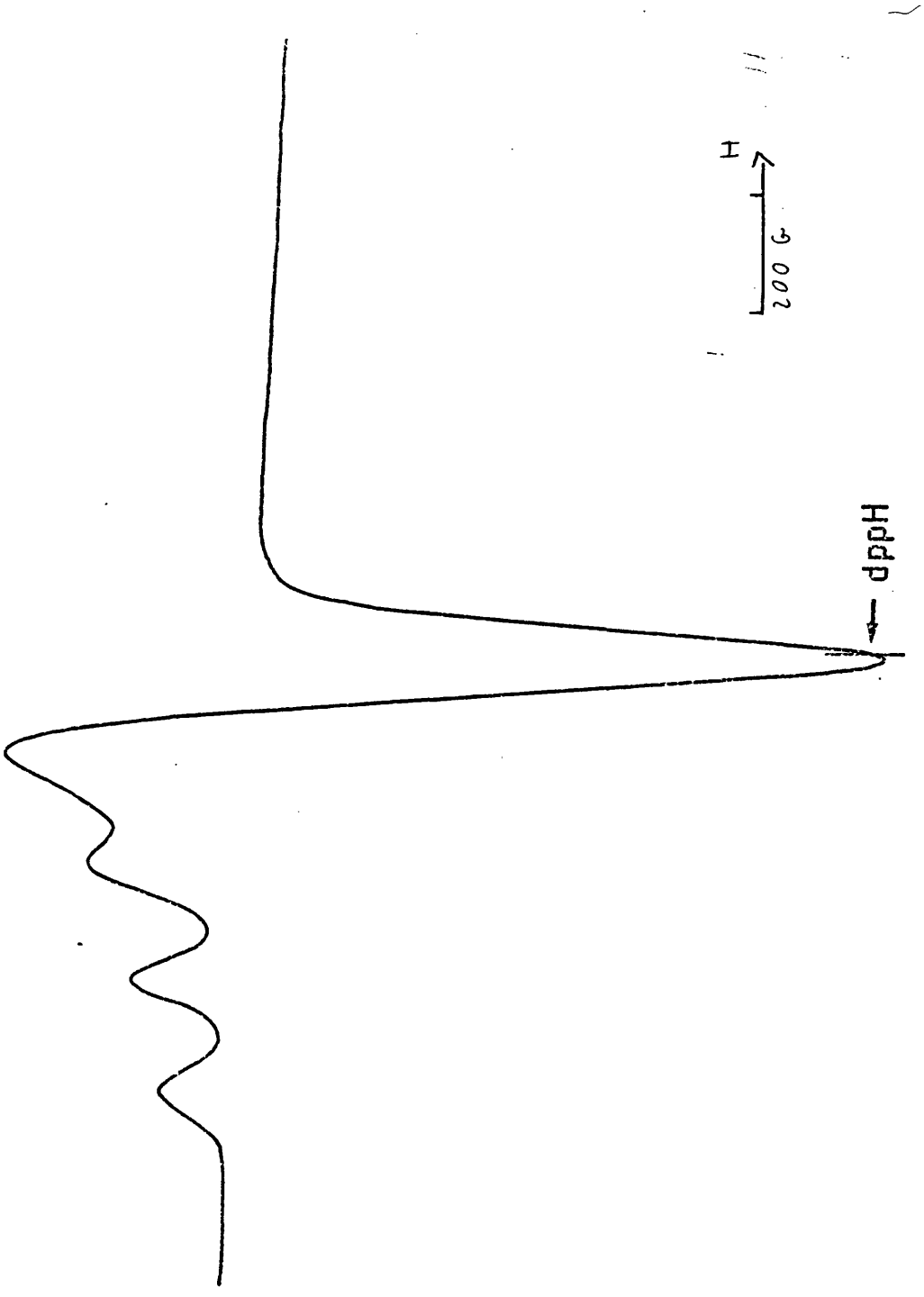

FIG. 6.1 E.P.R. spectrum at 77 K of native superoxide dismutase before irradiation.

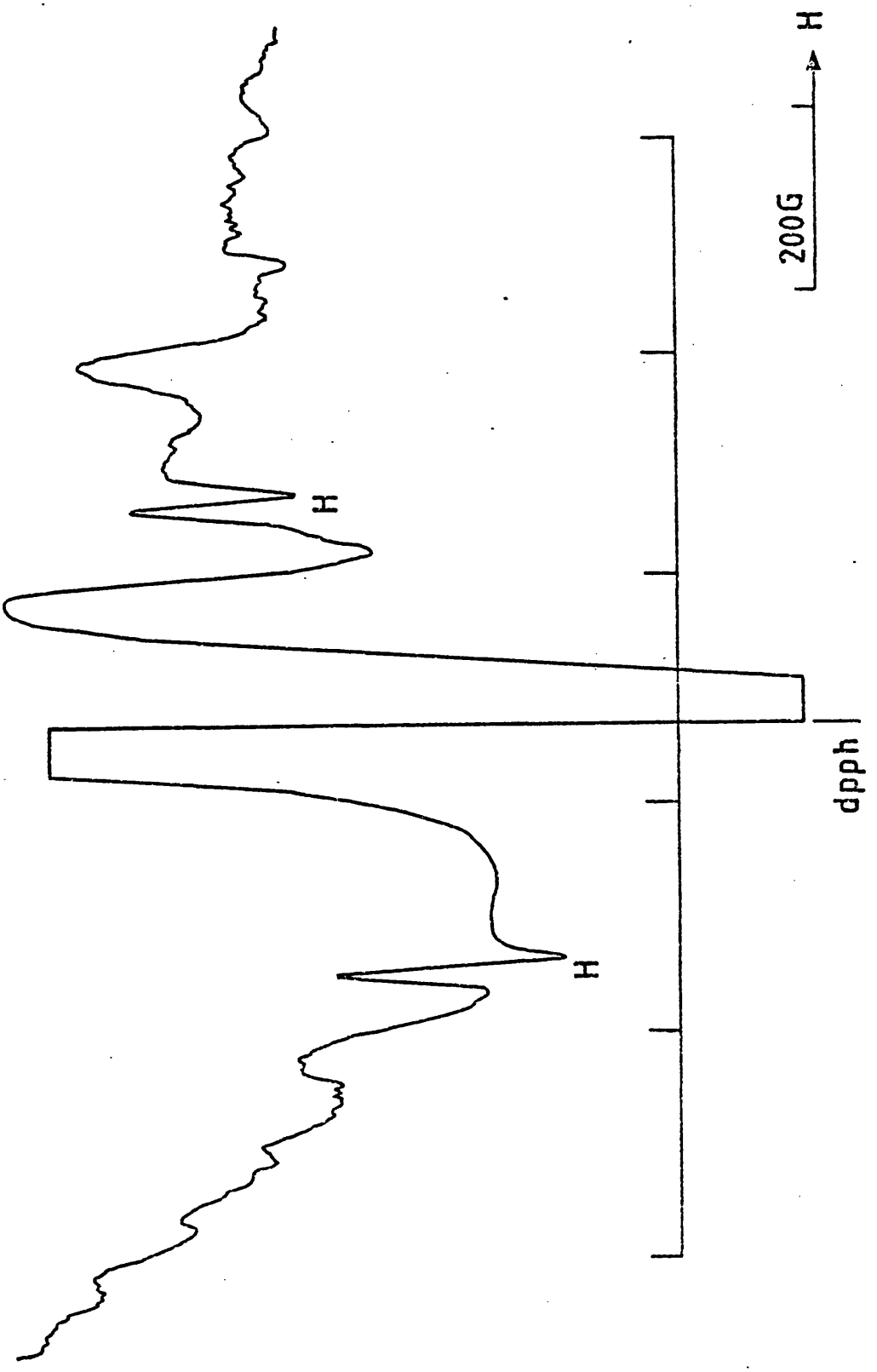

FIG. 6.2 E.P.R. spectrum at 77 K of native bovine carbonic anhydrase after irradiation. The two proton lines are indicated H. The six lines due to ^{67}Zn are also indicated.

spectrum [5] (Fig. 6.1). After irradiation, the spectra of the pure solid enzymes all exhibited a very intense symmetrical line at g = 2.002, under high gain several weak but fairly well-resolved lines on either side of the strong central line could be seen. These were centred on g = 1.97 and were attributed to isotropic hyperfine coupling to ^{67}Zn ($I = 5/2$, 4.11%) with a coupling of ca. 250 G. In addition, a pair of weak lines with a separation of about 505 G is attributed to ^{1}H. The ^{67}Zn lines exhibited considerable linewidth variation. The $M_I = +\frac{1}{2}$ line was seen only as a broadening of the strong central line. The outer $\pm 5/2$ lines could only be seen as very broad features after signal accumulation. Irradiated [Zn]BCA and [Zn $\cdots$]SOD yielded the best resolved ^{67}Zn spectra (Fig. 6.2). In the case of irradiated [Zn-Cu]SOD, the spectrum was dominated by the Cu^{2+} signal which was identical in intensity and form to the spectrum before irradiation (Fig. 6.3). In addition, on the high field side, the $M_I = -1/2$ and $-3/2$ lines of ^{67}Zn could be seen at high gain. No signal in the g = 4 region could be seen.

The effect of high energy radiation on these enzymes is to generate a number of radicals by breaking bonds with the liberation of free protons and electrons. These protons and electrons readily move through the lattice, and may recombine or react with other molecules. The equilibrium yield of free protons is very low compared with the protein radical centred on g = 2. Contributing to this protein radical signal is the signal due to the Zn isotopes (I = 0). The most interesting feature of the spectrum are the hyperfine lines due to ^{67}Zn. The large hyperfine coupling and value of $g < 2$ show it to arise from Zn^{+} ions with configuration $3d^{10}$, $4s^{1}$. Taking the value of A_{iso} for 100% 4s electron on Zn as 454 G [6], the hyperfine coupling shows the spin density in the 4s orbital as ca. 55%.

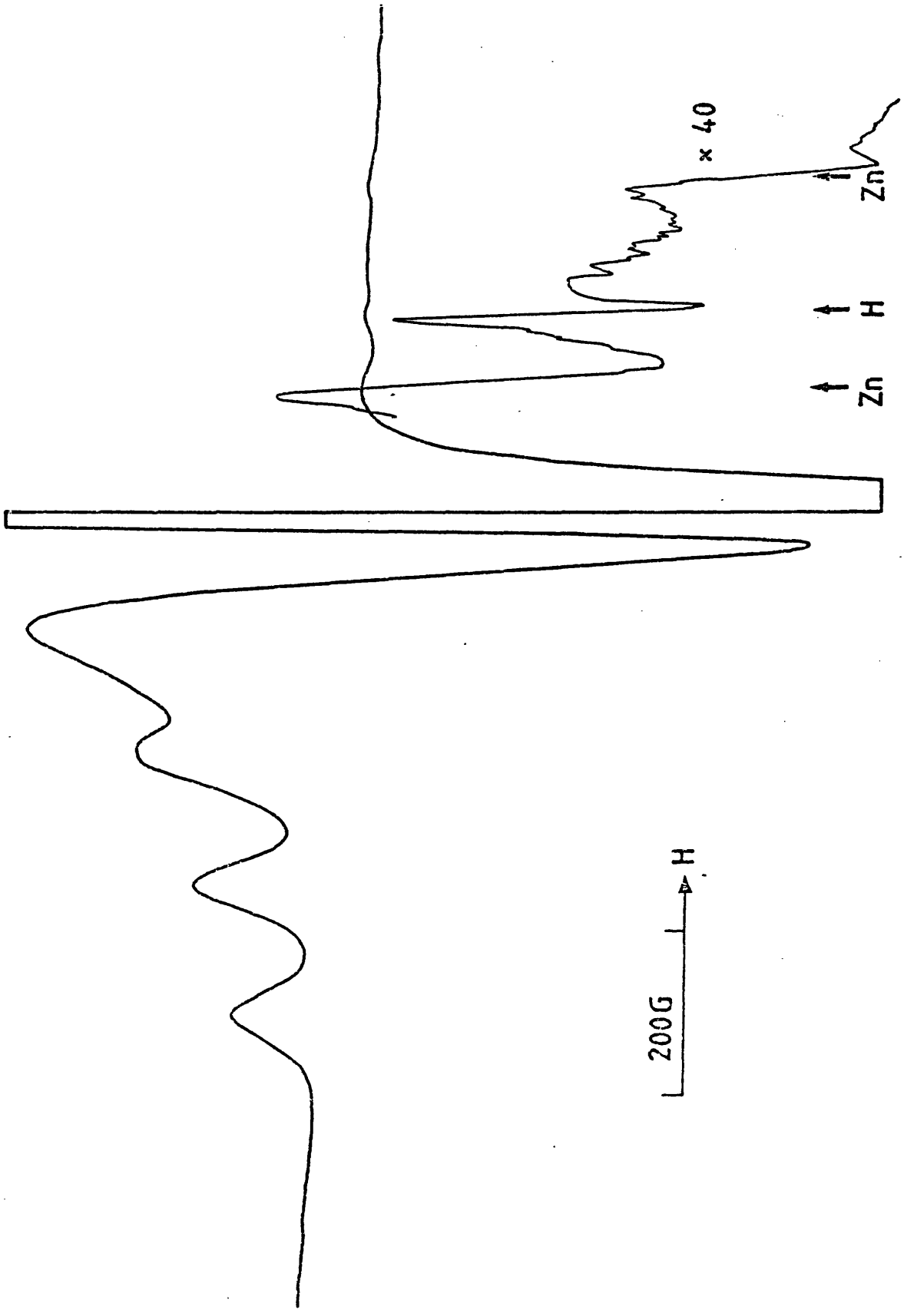

FIG. 6.3 E.P.R. spectrum at 77 K of native Superoxide Dismutase after irradiation.

If the remaining 45% of the unpaired electron were delocalised to that extent, hyperfine coupling to the adjacent imidazole nitrogen atoms would have been seen on the Zn (I = 0) line. The linewidth of the strong central line is about 20 G and would only hide hyperfine coupling equivalent to a few per cent spin density in a nitrogen 2s orbital. The other possibility is that the remaining spin density is in the Zn 4p orbital. Taking 65 G as the value of 100% spin density in a ^{67}Zn 4p orbital [6], and considering the equations:

$$6.1 \quad \ldots \quad A_{/\!/} = A_s + A_p$$

$$A_{\perp} = A_s - \frac{A_p}{2}$$

then the maximum values of $A_{/\!/}$ and $A_{\perp}$ would be 278 and 236 G respectively. This small anisotropy might well account for the considerable broadening of the observed hyperfine lines at high and low field. These results may be compared [1,2] with the radical in γ-irradiated $K_2[Zn(CN)_4]$ where $g_{/\!/} = 2.000$, $g_{\perp} = 1.999$, $A_{/\!/} = 131$ G and $A_{\perp} = 110$ G which yield spin densities of 25% in 4s and 60% in the 4p orbitals. The unpaired electron is thus in an approximately sp hybrid orbital on Zn which must not be interacting with any ligand. To accommodate this, two structural possibilities exist, either there is a distortion toward trigonal bipyramid with the electron constrained in a largely non-bonding orbital (I) or there is loss of a ligand, to give structure (II).

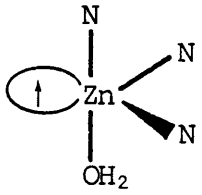

(I)

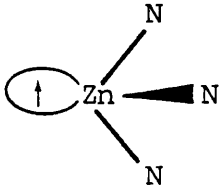

(II)

Because the known coordination and stereochemistry about the zinc atom in the enzymes is approximately tetrahedral [3,4], structure (II) is the more probable.

In the case of Carbonic Anhydrase the ligand lost can be the water molecule, whilst for the Superoxide Dismutase it must be a proteic ligand. The identity of the Cu^{++} E.P.R. spectrum of the [Zn-Cu]SOD sample before and after irradiation excludes that the ligand released is the bridging imidazole, as in this case the Cu^{++} is known to change its spectrum which become more axial and increases its hyperfine constant value in the parallel region [7].

It is interesting that both the [Zn-Cu] and [Zn-•••]SOD samples shows the same E.P.R. Zn^{+} signal after irradiation. Moreover no new signal in the $g = 4$ region nor change in the Cu^{++} spectrum in the irradiated [Zn-Cu]SOD was detected. This implies that there is no magnetic interaction between the Cu^{++} and the Zn^{+} metal ions, contrary to what is observed in the [Co-Cu] and [Co-Co]SOD derivatives (see Chapter 4). This supports the suggestion that the unpaired electron is in a non-bonding orbital which would be of the wrong symmetry to couple with the unpaired electron on Cu^{2+}. This is because the unpaired electron on the Cu^{2+} is in a $d_{x^2-y^2}$ orbital which interacts through the π electron system of the imidazole [8]. If the zinc electron is in an sp (σ) hybrid, then this is of the wrong symmetry to interact with π-electrons.

In irradiated aqueous solution, the spectrum from the free protons was very intense and originated from the solvent. The ^{67}Zn signals were the same as before, only weaker because of the lower concentration. The protein signal showed extra features on the low field side typical of irradiated free proteins.

REFERENCES

1. J. I. Isoya and S. Fujiwara, Bull. Chem. Soc. Japan 45, 2182 (1972).

2. M. C. R. Symons, D. X. West and J. G. Wilkinson, J.C.S. Dalton Trans. 1565 (1976).

3. K. K. Kannan, B. Notstrand, K. Fridborg, S. Lovgren, A. Ohlsson and M. Peter, Proc. Nat. Acad. Sci. USA 72, 51 (1975).

4. J. S. Richardson, K. A. Thomas, B. H. Rubin and D. C. Richardson, Proc. Nat. Acad. Sci. USA 72, 1349 (1975).

5. G. Rotilio, L. Morpurgo, C. Giovagnoli, L. Calabrese and B. Mondovi, Biochemistry 11, 2187 (1972).

6. B. A. Goodman and J. B. Raynor, Adv. Inorg. Chem. and Radiochem. 13, 136 (1970).

7. L. Calabrese, D. Cocco, L. Morpurgo, B. Mondovi and G. Rotilio, FEBS Letters 59, 29 (1975).

8. Chin-Lin O'Young, J. C. Dewan, H. R. Lilienthal and S. J. Lippard, J. Am. Chem. Soc. 100, 7291 (1978).

SPECTROSCOPIC STUDY OF COBALT II SUBSTITUTED IN SOME COPPER AND ZINC ENZYMES

by A. DESIDERI

ABSTRACT

The substitution of the cobalt atom into the active site of zinc metalloenzymes is becoming a useful and common practice. The zinc atom, in fact, is magnetically and optically silent, whilst the cobalt has a characteristic optical and E.P.R. spectrum, so that it can be followed spectroscopically to obtain structural and functional information on the enzyme.

In this thesis a spectroscopic study of the cobalt substituted into two metalloenzymes, namely copper-zinc-Superoxide Dismutase and Zinc-Carbonic Anhydrase, and of some low molecular weight cobalt complexes has been performed.

In Superoxide Dismutase the cobalt has been selectively substituted either into the zinc or into the copper site, so that all the possible derivatives [Co-Cu], [Co-•••], [Co-Co] and [Zn-Co], have been investigated.

The [Co-•••]SOD derivative is characterized by an axial E.P.R. spectrum and by an absorption spectrum in the visible region of intermediate intensity $\varepsilon_{530}=315$, $\varepsilon_{560}=425$, $\varepsilon_{588}=450$ and a near infrared band at 1000 nm ($\varepsilon=90$), indicating a tetrahedral coordination with a quite strong crystal field around the Co(II) centre. The [Co-Cu]SOD derivative does not show any E.P.R. signal and a magnetic susceptibility study, carried out between 30-210 K indicates that this is due to the strong antiferromagnetic coupling ($2J \geqslant 600$ cm^{-1}) occurring between the two metal centres. The [Zn-Co]SOD derivative shows an interesting phosphate buffer spectral dependence. In particular, the electronic spectrum, carried out in the presence of phosphate buffer, has three quite intense bands in the visible region ($\varepsilon_{540}=225$, $\varepsilon_{580}=330$, $\varepsilon_{605}=330$) and a band in the near infrared at 1050 nm ($\varepsilon=40$). When the same spectrum is carried out in the absence of phosphate buffer the bands in the visible region are much less intense and the near infrared band is shifted toward lower wavelengths. This behaviour indicates a change in symmetry around the Co(II) centre, from tetrahedral to pentacoordinate in the presence and in the absence of phosphate respectively. The E.P.R. spectra also support this hypothesis.

The reaction of cyanide and H_2O_2 with the [Zn-Co] and [Co-Co]SOD derivatives have also been investigated. The binding of CN^- to the cobalt is temperature or freezing dependent. The E.P.R. spectra carried out at

77 K shows, in fact, that the CN^- easily binds to the cobalt which is transformed into a low spin form, whilst the electronic room temperature spectra show that a very large CN^-:Co ratio is needed to decrease the d-d bands of the unreacted high spin cobalt. The E.P.R. spectrum is rhombic with $g_z = 2.027$ and $A_z = 115 \times 10^{-4} cm^{-1}$, suggesting a distorted pentacoordinate structure around the metal. The reaction with H_2O_2 shows a decrease of the electronic absorption spectrum of the cobalt and the appearance of a radical at $g \simeq 2$ in the E.P.R. spectrum. Oxidation of the Co(II) to Co(III) can probably be excluded because addition of sodium dithionite does not restore back the original spectrum.

A comparative study of the K-absorption edge of several cobalt derivatives has allowed several structural correlations to be done. In particular, the [Co(II)-•••] and the [Co(II)-Cu(I)]SOD derivatives have a completely identical K-edge spectrum, which is slightly different from that of the [Co(II)-Cu(II)] derivative, indicating that a conformational change and/or a different charge on the imidazole bridging the two metal sites occurs coincidentally with the change of copper valence.

An E.P.R. study on low molecular weight model compounds suggests that the zero field splitting value δ between the two Kramers doublets in a high spin cobalt(II) ion can be used diagnostically to assign the geometry around the metal centre. The zero field splitting value is, in fact, greater in the pentacoordinate case than in the tetrahedral one. By comparison with the model compounds a pentacoordinate structure is assigned to the high pH and the iodide form of the cobalt carbonic anhydrase derivative.

The study of the reaction of the native and the copper and cobalt substituted Carbonic Anhydrase shows that Cu(II) is easily extracted from the enzyme, Co(II) with some difficulty and Zn(II) is unaffected in any condition. Before the depletion, a stable pentacoordinate species and two stable and different intermediates in the case of cobalt and copper respectively are observed.

A γ-irradiation investigation of the native Carbonic Anhydrase and Superoxide Dismutase has allowed detection of the E.P.R. signal of the Zn^+ ion with a configuration $3d^{10}\,4s^1$. In both cases, the electron seems to be in an approximately sp hybrid orbital so explaining the lack of magnetic interaction in the native SOD. In fact, the σ hybrid orbital of the zinc is in a wrong symmetry to couple with the π electron system of the imidazole and with the ground state of the copper.